Draft version August 12, 2019
Typeset using LaTeX **preprint** style in AASTeX62

A 'constant Lagrangian' RMW-RSS quantified fit of the galaxy rotation curves of the complete SPARC database of 175 LTG galaxies.

E.P.J. de Haas[1]

[1]*Nijmegen, The Netherlands*

(Dated: May 18, 2018)

ABSTRACT

In this paper I categorize and analyze the 'constant Lagrangian' model fits I made of the complete SPARC database of 175 LTG galaxies. The difference with the previous papers is the application of the RMWRSS (Root Mean Weighted Residual Sum of Squares) method to quantify the quality of the fit, using a continuous curve. Of the 175 galaxies, 77 allowed a single fit rotation curve, so about 44 percent. Another 18 galaxies could almost be plotted on a single fit. Then 13 galaxies could be fitted really nice on crossing dual curves. The reason for the appearance of this dual curve, in its two versions, could be given and related to the galactic constitution and dynamics. From then on, the fitting got more and more complex. So I got a 44 percent positive rate for a direct fit of the measured rotation curves on the prime model. This result rules out stochastic coincidence as an explanation of those fits.

Keywords: Galaxies: kinematics and dynamics, Galactic rotation curves, Dark Matter, MOND, Schwarzschild

1. INTRODUCTION

In a recent draft (posted on the scientific amateur's preprint website Vixra) I introduced a 'constant Lagrangian' model for galactic dynamics (**?**). In a few sequential drafts I went from a qualitative attempt at fitting real rotational velocity curves using the proposed model, see (de Haas 2018c,b), towards a quantitative analysis by including the error bars of the measured velocity, (de Haas 2018d,a). In that last preprint I presented the analysis of the full set of 175 galaxies at the SPARC database, as provided by (Lelli et al. 2016) in the file Rotmod-LTG.zip. That rotation curve fitting result was presented in a non-categorized order, it just followed the order of the alphabetic-numerical list. I subsequently categorizes the fitting curves according to the fitting result.

In this paper, after repeating the presentation of the 'constant Lagrangian' model, I present a more quantified fit of the 175 galaxy rotation curves of the SPARC database. For every single fit and almost single fit galaxy curve I added a mean weighted quantification of every measurement relative to the fitting curve and then give a Root Mean Weighted Residual Sum of Squares value (RMWRSS) to quantify the quality of the fitting curve relative to the measured rotation curve. See Fig.(1).The

haas2u@gmail.com

RMWRSS method lead to an additional parameter, the offset velocity V_0. With these new tools, 77 of the 175 galaxies, so 44%, allowed for a single fit within the margins of errors.

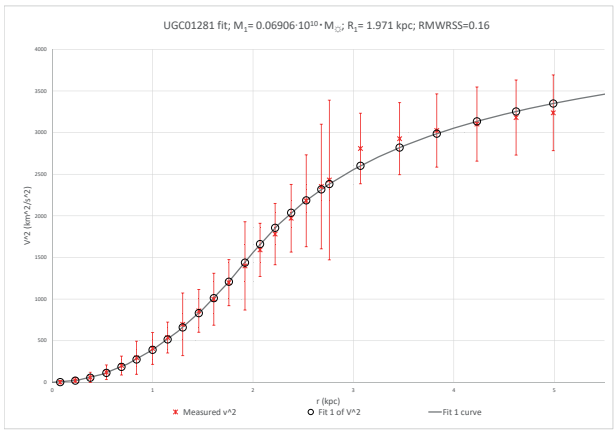

UGC01281

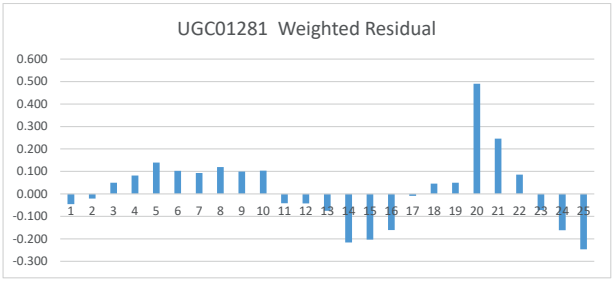

UGC01281 WR; RMWRSS = 0.16

Figure 1. The weighted residual graph and the RMWRSS value quantify the quality of the fitting curve.

The automated fitting process, a programmed iteration towards a minimum RMWRSS, also lead to a surprising outcome for some galaxies, with a fitting curve that didn't have a constant Lagrangian but a Newtonian like progress towards a final, non-zero velocity at the outer regions of the galaxies involved. See Fig.(2).

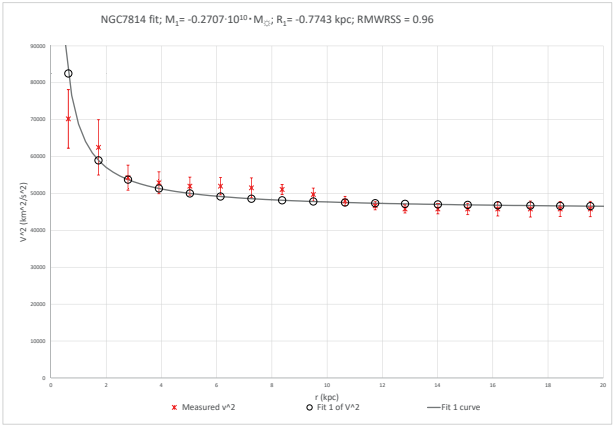

NGC7814

Figure 2. Galaxy with an semi-Newtonian regime.

This iteration solution wasn't deliberate, but popped up as a surprise of the automated fitting process towards a minimum RMWRSS value. I subsequently recognized such partial curves in the rotation curves of more complicated galaxies, galaxies that needed more than one fitting curve in order to model the measurements. See Fig.(3).

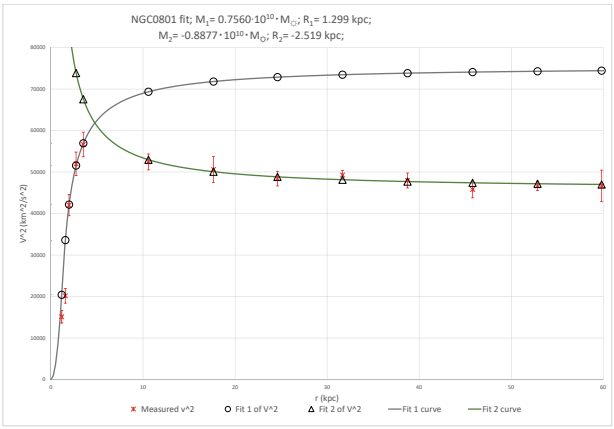

NGC0801

Figure 3. Galaxy with a transition from a constant Lagrangian to an semi-Newtonian regime.

More complicated combinations of fitting curves were necessary for more chaotic galaxies, with in the end a selection of galaxies for which the fitting process became to random and subjective to allow for a quantification other than 'unsuccessful'. See Fig.(4).

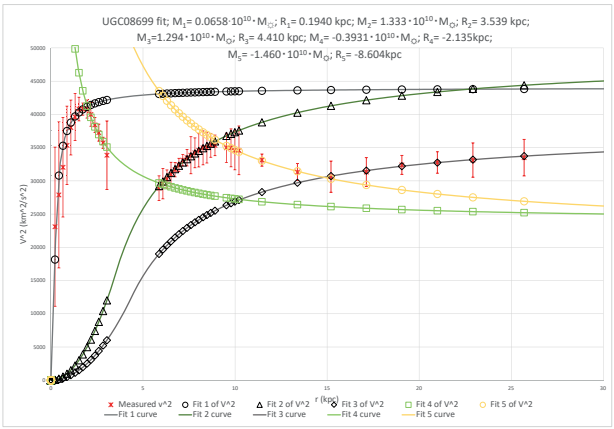

UGC08699

Figure 4. Galaxy with multiple transitions from a constant Lagrangian to an semi-Newtonian regime and vice versa.

In the following part I first repeat the theory behind the model, before presenting the 175 fits of the full SPARC database using my model.

2. THE VIRIAL THEOREM IN TROUBLE ON THE GALACTIC SCALE.

In 1932 the Dutch astronomer Oort observed that the stars in the galactic vicinity of the Sun are moving peculiarly fast, almost 8 times as fast as could be inferred from the calculated Newtonian acceleration. Oort assumed that dark matter would be the cause of this apparent difference, with 'dark' referring to ordinary matter not seen by us due to various reasons (Oort 1932).

In 1933 Dark Matter was mentioned as "dunkle Materie" in a paper by Zwicky. Fritz Zwicky was studying the Coma Cluster of galaxies and found that his calculations for orbital acceleration and stellar mass within it was off by a large factor. He concluded that there should be a much greater density of dark matter within the cluster than there was luminous matter. Zwicky concluded that this constituted an unsolved problem (Zwicky 1933). In 1937 Zwicky regarded his study on the Coma Cluster a test of Newton's law of gravity on the largest cosmological scale possible, by applying the virial theorem on a cluster of galaxies. He also mentioned in his 1937 paper the possibility to test the virial theorem by applying it to the rotational velocities of the individual stars in the separate galaxies. But he concluded that this was technologically out of reach (Zwicky 1937).

The breakthrough research of Rubin and Ford around 1970-1975 established beyond doubt the outer rotational velocity curves of individual galaxies, which turned out to be flat (Rubin et al. 1978). This was in conflict with velocity curves that resulted from the application of the virial theorem to the luminous mass of these galaxies. Rubin and Ford cited colleagues who suggested the existence of a large galactic halo of dark matter. In a 1980 paper presenting further research they concluded that the form of the rotation curves implied that significant non-luminous mass should be located at large distances beyond the optical galaxy. The total mass of a galaxy should, for large distances, increase at least as fast as the distance from the center (Rubin et al. 1980).

The third major evidence for Dark Matter was the gravitational lensing effect of clusters of galaxies. The mass of stars and hot gas in clusters who collectively act as a gravitational lens is too small to bend the light from the background galaxies as much as they actually do. A large density of dark matter in the center of these cluster is needed to explain the strength of the observed lensing effect (Koopmans et al. 2009).

In the course of decades it has become more and more clear that ordinary matter can't be the cause of those observed phenomena. That realization caused the term 'dark matter' to evolve into 'Dark Matter', with the capital letters indicating its elusive character. Today it has been predominantly, but not unanimously, been accepted that non-baryonic particles must exist in the calculated densities. A range of different astrophysical observations point in this direction (The ATLAS Collaboration 2018).

3. MOND

One of the few non-particle approaches to the problem of Dark Matter is MOND or MOdified Newtonian Dynamics. MOND started in 1983 with two seminal paper of Milgrom. I quote from his papers:

> *All determinations of dynamical mass within galaxies and galaxy systems make use of a virial relation of the form* $V^2 = MGr^{-1}$ *where* V *is some typical velocity of particles in the system,* r *is of the order of the size of the system,* M *is the mass to be determined, and* G *is the gravitational constant. [...] It must have occurred to many that there may, in fact, not be much hidden mass in the universe and that the dynamical masses determined*

on the basis of the above virial relation are gross overestimates of the true gravitational masses.(Milgrom 1983b)

Instead of assuming the Newtonian theory to remain valid in and around galaxies, Milgrom modified Newtons second law by making inertia a function of acceleration (Milgrom 1983b). Milgrom replaced $m_g\mathbf{a} = \mathbf{F}$ by

$$m_g\mu\left(\frac{a}{a_0}\right)\mathbf{a} = \mathbf{F}. \tag{1}$$

With such a deviation only reveals itself for accelerations with $a \approx a_0$. When $a \gg a_0$, $\mu \approx 1$ and the Newtonian regime reasserts itself. This resulted in the capacity to reasonably fit most of the galaxy rotation curves and it lead to an intrinsic connection to the baryonic Tully-Fisher relation as $V_\infty^4 = a_0 GM$ (Milgrom 1983a).

The original Tully-Fisher relation is a relation between the luminosity of a spiral galaxy and its, maximum, rotation velocity (Tully & Fisher 1977). The physical basis of the Tully-Fisher relation is the relation between a galaxy's total baryonic mass and the velocity at the flat end of the rotation curve, the final velocity. According to McGaugh both stellar and gas mass of galaxies have to be taken into account in the relation that is referred to as the Baryonic Tully-Fisher (BTF) relation. In 2005 McGaugh determined the baryonic version of the LT relation as $M_d = 50v_f^4$, see (McGaugh 2005). In this form, M_d is expressed in solar mass $M_\odot = 1,99 \cdot 10^{30}\ kg$ units and the final velocity of the galactic rotation velocity curve v_f is expressed in km/s. If we express the galactic mass in kg and the velocity in m/s we get the total baryonic mass, final velocity relations in SI unit values as $M_b = 1,0 \cdot 10^{20} v_f^4$.

In 1983, Milgrom interpreted the BTF relation as indicative of his proposed deviation from Newtonian gravity, justifying his modification of Newtonian dynamics or MOND (Milgrom 1983b). Using McGaug's 2005 values in SI units, Milgrom's presentation of the BTF relation can be cast in the form $v_f^4 = 1,0 \cdot 10^{-20} M_b = G a_0 M_b$, resulting in an acceleration $a_0 = 1,5 \cdot 10^{-10}\ m/s^2$ in McGaug's values. Milgrom hypothesized that this relation should hold exactly, thus interpreting it as an inductively found law of nature, instead of looking at it as just a coincidental empirical relation (Milgrom 1983a). The resulting acceleration can be written as $5 \cdot a_0 \approx cH_0$, with the velocity of light c and the Hubble constant H_0. According to Milgrom, the deeper significance of this relation between this special galactic acceleration and the Hubble acceleration should be revealed by future cosmological insights (Milgrom 1983b).

4. CLASSICAL LAGRANGIAN DYNAMICS

One problem with Milgrom's MOND is that is rather asynchronous to modify gravity by returning to Newton instead of starting by Einstein's General Relativity. But in the standard cosmological General Relativity approach towards the galaxy rotation curve problem the existence of Dark Matter is presumed from the beginning. The 'constant Lagrangian' model can be seen as an intermediate approach: it uses General Relativity concepts without presuming from the start the existence of Dark Matter. This intermediate approach starts with Lagrangian mechanics.

The classical Lagrangian equation of motion reads

$$\frac{d}{dt}\left(\frac{\partial L}{\partial \dot{q}}\right) - \frac{\partial L}{\partial q} = 0. \tag{2}$$

In classical gravitational dynamics I assume circular orbits with $\dot{q} = v$ and $q = r$. The Lagrangian itself is then given by $L = K - V$, with V the Newtonian potential gravitational energy and K the kinetic energy. One then gets

$$\frac{d}{dt}\left(\frac{\partial L}{\partial \dot{q}}\right) = \frac{dp}{dt} = F. \tag{3}$$

The other part gives

$$\frac{\partial L}{\partial q} = -\frac{dV}{dr}, \tag{4}$$

so one gets Newton's equation of motion in a central field of gravity

$$F_g = -\frac{dV}{dr}. \tag{5}$$

Further analysis of the context results in the identification of the Hamiltonian of the system, $H = K+V$, as being a constant of the orbital motion and the virial theorem as describing a relation between K and V in one single orbit but also between different orbits, given by the relation $2K + V = 0$.

The classical virial theorem has two main interpretations. The first one states that in circular orbits, the centripetal force equals the gravitational force. This leads directly to the scalar relation $2K = -V$. The second one states that masses in collapsing orbits have to dissipate half of the potential energy in order to resume a stable lower orbit because in such a collapse from a higher stable orbit to a lower stable orbit, only half of the freed potential energy can be transformed into kinetic energy.

On the galactic scale it is assumed that velocities are so low and gravitational fields are so weak, that Newtonian mechanics suffices and not much of relativity is needed. The problem with the rotational velocities of stars in galaxies and galaxies in cluster of galaxies is thus supposed to be a Newtonian physics issue that can be dealt with in the dynamics described above. The Dark Matter solution to the too fast rotational galactic velocities has two faces. On the one hand one tries to describe the density distribution of Dark Matter, needed in order to match the measurements with classical dynamics, specifically the virial theorem. On the other hand one tries to identify the Dark Matter constituents, usually seen as an out-of-the-box extension of the known Standard Model of particle physics.

5. A GEODETIC APPROACH OF GRAVITATIONAL ORBITS

If one tries to apply the concepts of General Relativity to the galaxy rotation problem and related virial theorem, the notion of geodetic motion in General Relativity must be central. The analysis can start in a semi-relativistic approach, by applying the classical Lagrangian equation of motion to geodetic orbits. The most important aspect of geodetic motion in GR is that it requires no force to move on a geodetic. This has important implications for the Lagrangian equation of motion, because $F_g = 0$ on a geodetic. One gets

$$\frac{d}{dt}\left(\frac{\partial L}{\partial \dot{q}}\right) = F_g = 0 \tag{6}$$

and as a consequence also

$$\frac{\partial L}{\partial q} = -\frac{dL}{dr} = 0. \tag{7}$$

As a result, one has

$$L = K - V = constant \tag{8}$$

on geodetic orbits. This is the theoretical core of the 'constant Lagrangian' model for galactic dynamics. The difference between the classical approach and this paper, the additional choice so to speak, is that I assume a model in which the Lagrangian is a constant for all orbits of my model galaxy. That's all. The effort in presenting this model is in the sequence of introduction, interpretation, application and implication of this core ad-hoc assumption of a constant L for all r on a model galaxy rotation curve.

The first observation is that I do not use the Einstein Equations but the classical Lagrangian equations on geodetic orbits. This choice has to be interpreted as an in between approximation. Newton's law of gravity follows from the Einstein Equations in case of a weak field: Newton is the weak field limit of Einstein. But in Einstein's time, the planetary solar system was already assumed to be a weak gravitational field. More essentially is the observation that an axiomatic theory of gravity that states that in geodetic motion, no forces of gravity exist, only local curvature of space-time, will not magically transform into an axiomatic theory that is all about forces of gravity in orbits around central masses, just by slowly weakening the potential. The use of the classical Lagrangian has to be interpreted as an in between these two conflicting axiomatic systems. I use Lagrange as the diplomatic mediator between Newton and Einstein. The theoretical core of my model is breathtakingly simple. The rest, it's introduction, interpretation, application and implication, isn't simple at all.

Although the requirement that the force of gravity is zero on a geodetic orbit seems obvious from a GR perspective, there is still dispute among the experts relative to this issue. Relative to the geodetic precession or the de Sitter precession, discussion and opposite views remain as to the role of the force of gravity in this effect. Some claim that the force of gravity cannot have any role in it, others describe the geodetic precession as the sum of a time-like Thomas precession due to the force of gravity and a Schouten precession due to the curvature of three dimensional space (de Haas 2014). Given this paradoxical situation relative to a well established effect of General Relativity, it is by no means settled how to handle the requirement of having no gravitational force on a geodetic motion relative to satellites orbiting the earth. So let alone relative to galactic orbits, where General Relativity too had to presume the existence of Dark Matter.

The Lagrangian of the system as being the constant of the geodetic motion is used on a daily basis by many of us because it is applied by GNSS systems for the relativistic correction of atomic clocks in satellites. Let's elaborate this a bit further. In General Relativity, the proper time-rate $d\tau$ is defined through the metric distance ds as $ds \equiv cd\tau$. The square metric distance is defined through

$$ds^2 \equiv g_{\mu\nu} dx^\mu dx^\nu. \tag{9}$$

Given coordinate world time-rate dt, which is the time-rate of a standard clock at a position where $d\tau = dt$ (in GR-Schwarzschild this implies a clock at rest at infinity), we get the general

$$\frac{ds^2}{dt^2} = \frac{c^2 d\tau^2}{dt^2} = g_{\mu\nu} \frac{dx^\mu}{dt} \frac{dx^\nu}{dt} = g_{\mu\nu} V^\mu V^\nu, \tag{10}$$

with the geodesic four-vector velocity V^μ. In this equation, $d\tau$ stands for the local proper clock-rate of a clock in a geodetic orbit in a field of gravity and dt is the universal clock-rate. Because of this interpretation of dt, the velocity V^μ is the velocity as seen from a position where $d\tau = dt$. See for

example (Singer 1956), (Weinberg 1972, p. 79), (Misner et al. 1973, p. 1054-1055), (Straumann 1984, p. 97), (Ohanian & Ruffini 2013, p. 119).

In case of the Schwarzschild metric in polar coordinates, we have (Ruggiero et al. 2008)

$$ds^2 = \left(1 + \frac{2\Phi}{c^2}\right) c^2 dt^2 - \left(1 + \frac{2\Phi}{c^2}\right)^{-1} dr^2 - r^2 d\theta^2 - r^2 sin^2\theta d\phi^2. \tag{11}$$

In case of a clock on a circular geodesic on the equator of a central non-rotating mass M we have $\frac{dr}{dt} = 0$, $\frac{d\theta}{dt} = 0$, $sin\theta = 1$ and $\frac{d\phi}{dt} = \omega$. We thus get

$$\frac{ds^2}{dt^2} = \frac{c^2 d\tau^2}{dt^2} = \left(1 + \frac{2\Phi}{c^2}\right) c^2 - r^2\omega^2 \tag{12}$$

and

$$\frac{d\tau^2}{dt^2} = 1 + \frac{2\Phi}{c^2} - \frac{r^2\omega^2}{c^2}. \tag{13}$$

With $v_{orbit} = r\omega$ we have

$$\frac{d\tau^2}{dt^2} = 1 + \frac{2\Phi}{c^2} - \frac{v_{orbit}^2}{c^2}. \tag{14}$$

So finally we get the GR result

$$\frac{d\tau}{dt} = \sqrt{1 + \frac{2\Phi}{c^2} - \frac{v_{orbit}^2}{c^2}} \tag{15}$$

with $d\tau$ as the clock-rate of a standard clock A in a geodetic orbit and dt as the 'universal' clock-rate G of a standard clock at rest in infinity, the only condition for which $d\tau = dt$. The result of Eqn. (15) is the basic relativistic correction used in GNSS clock frequencies, with the first usually presented as the gravity effect or gravitational potential correction and the second as the velocity effect or the correction due to Special Relativity (Ashby 2002; Hećimović 2013; Delva & Lodewyck 2013).

Given the classical definitions of $K = \frac{1}{2}mv_{orbit}^2$ and $V = m\Phi$, we get

$$\frac{d\tau}{dt} = \sqrt{1 - \frac{2L}{U_0}}. \tag{16}$$

All the satellites of a GNSS system are being installed on a similar orbit and thus syntonized relative to one another because they share the same high and velocity and have constant L and $\frac{d\tau}{dt}$ on those orbits. But different GNSS systems, as for example GPS compared to GALILEO, are functioning on different orbits with different velocities and those systems aren't syntonized relative to one another. This non-syntonization between satellites on orbits with different heights and virial theorem connected velocities is an all to real technical obstacle for the effort towards realizing an integration of the different GNSS systems into one single global network. For satellites for which the virial theorem holds, the Lagrangian isn't a constant on orbits with different radii. Thus, with $\frac{\Delta L}{\Delta r} \neq 0$, atomic clocks moving in free fall on those different radii aren't syntonized. For GNSS systems, the virial theorem constitutes a problem, not an asset.

6. A COMPLETELY SYNTONIZED MODEL GALAXY

Fundamental in the approach of this paper is to analyze gravity using relative frequency shifts, and thus $\frac{d\tau}{dt}$, as one of the basic experimental inputs. Such a method is looming in today's geodesy. In modern gravitational geodesy scientists are investigating the relativistic frequency shift as a new observable type for gravity field recovery (Mayrhofer & Pail 2012). Driven by this development, modern geodesy is about to go through a change from the Newtonian paradigm to Einstein's theory of general relativity (Kopeikin et al. 2017). A new generation of atomic clock is the game changer for this new domain of chronometric geodesy, and requires additional new techniques to be developed in the field of frequency transfer and comparison (Delva & Lodewyck 2013). The paradigm shift towards gravitational divergence recovery is based on the principle of frequency comparison between two clocks on different space-time locations in order to measure the frequency shift between them (Delva & Lodewyck 2013). The knowledge of the Earth's gravitational field has often been used to predict frequency shifts between distant clocks. In relativistic geodesy, the problem is reversed and the measurement of frequency shifts between distant clocks now provides knowledge of the gravitational field (Delva & Lodewyck 2013). This reversal is also present in my postulate of the 'constant Lagrangian' model. A constant Lagrangian implies a zero divergence in the syntonization of atomic oscillators and thus an absence of gravitational stress. A divergence in the Lagrangian implies a divergence in the time dilation factor $\frac{d\tau}{dt}$ and thus a non-zero gravitational stress.

The key to this paper's approach is to extend this clock frequency perspective towards gravity from geodesy to galaxies. When I connected

$$\frac{d\tau^2}{dt^2} = 1 + \frac{2\Phi}{c^2} - \frac{v_{orbit}^2}{c^2} = 1 - \frac{2L}{U_0} \tag{17}$$

to the problem of the galactic rotation curve, I realized that the flat rotation curve implies atomic clock syntonization in those areas. In those outer regions, the gravitational potential can be assumed to be approximately zero and the velocity constant. This made me curious as to the clock-rate status in the inner regions. It is intriguing to realize that you can jump from orbit to orbit and still encounter a constant clock-rate on all the orbiting satellites you encounter on an imaginary voyage through the outer regions of galaxies. Those flat rotation rate zones are the GNSS engineer's dream come true. This implies that precisely in those regions where the classical virial theorem seems in trouble, $L \simeq constant$, not just in one single orbit *but also between different orbits*.

It should be clear that for those geodetic orbits, the classical virial theorem, which in its most essential form states that $F_{gravity} = F_{centripetal}$, becomes meaningless because on circular geodetics this reduces to the empty expression $0 = 0$. From the energy perspective, by what mechanism should masses in orbital collapse in the outer region of galaxies dissipate half of the potential energy? It seems that the virial theorem isn't fundamental, but in need of a dissipative mechanism in order to assert itself. Without such a (thermo)dynamics, conservation of mechanical energy in orbital collapse could well be the rule, with as a consequence that all the potential gravitational energy is transformed into orbital kinetic energy: a 'constant Lagrangian' model.

In order to study the relativistic clock-rate behavior in the inner regions of galaxies, I had to construct a model galaxy. My model galaxy is build of a model bulge with mass M and radius R and a Schwardschild metric emptiness around it. The model bulge has constant density $\rho_0 = \frac{M}{V} = \frac{3M}{4\pi R^3}$ and its composing stars rotate on geodetics in a quasi-solid way. So all those stars in the bulge have

equal angular velocity on their geodetic orbits, with $v = \omega r$. On the boundary between the quasi solid spherical bulge and the emptiness outside of it, the orbital velocities are behaving smoothly. So the last star in the bulge and the first star in the Schwarzschild region have equal velocities and potentials. I also assume that the Newtonian potential itself is unchanged and unchallenged, remains classical in the whole galaxy and its surroundings. Such a model galaxy doesn't, for the moment, have a SMBH in the center of its bulge and it only has some very lonely stars in the space outside the bulge.

The gravitational potential in such a case is well known. Inside the sphere the potential is

$$\Phi = -\frac{GM}{2R}\left(3 - \frac{r^2}{R^2}\right), \tag{18}$$

and outside the sphere the potential is

$$\Phi = -\frac{GM}{r}. \tag{19}$$

If this sphere would be in a quasi solid condition for which the classical virial theorem would hold, so $2K = -V$, then on the boundary $r = R$ we would have $\frac{K}{m} = \frac{GM}{2R}$ and $\frac{L}{m} = \frac{K-V}{m} = \frac{3GM}{2R}$. At the center of the rotating sphere, $K = 0$ and we also have $\frac{L}{m} = \frac{3GM}{2R}$.

From $r = 0$ to $r = R$, the potential Φ increased as r^2. The kinetic energy does the same because $v^2 = \omega^2 r^2$. One can conclude that they increase identical and that $L = K - V$ is a constant inside the quasi-solid sphere. We can write for the region from $r = 0$ to $r = R$

$$\frac{L}{m} = \frac{v_{orbit}^2}{2} + \frac{GM}{r} = \frac{3GM}{2R} = constant. \tag{20}$$

As a result, inside such a model bulge, L is a constant of the motion of a mass m, not only in one orbit but also between orbits. All the clocks inside such a model bulge would be syntonized.

Thus, in the model galaxy that I am about to construct, we have $L = constant$ inside the model bulge and we have $L = constant$ in the outer regions where the rotational velocity curve flattens and the Newtonian potential turns negligibly small. So let's be bold and declare $L = K - V = constant$ in the entire galaxy, without changing the Newtonian potential. What would the implications be?

We would get $K = L + V$ and $L = V(r = 0)$ so for the region $0 \leq r \leq R$ we get

$$v_{orbit}^2 = \frac{GM}{R} \cdot \frac{r^2}{R^2} \tag{21}$$

and outside the model bulge, where $R \leq r \leq \infty$, we have

$$v_{orbit}^2 = \frac{3GM}{2R} - \frac{GM}{r}. \tag{22}$$

In Fig.(5) I sketched the result, with $-V = +K_{escape}$.

From the perspective of a free fall Einstein elevator observer, the free fall on a radial geodetic from infinity towards the center of the bulge, the other free fall tangential geodetics seem to abide the law of conservation of energy, because the escape kinetic energy plus the orbital kinetic energy is a constant on my model galaxy with galactic constant L. An Einstein elevator system with test mass m that would be put in an orbital collapse situation, magically descending from orbit to orbit in a

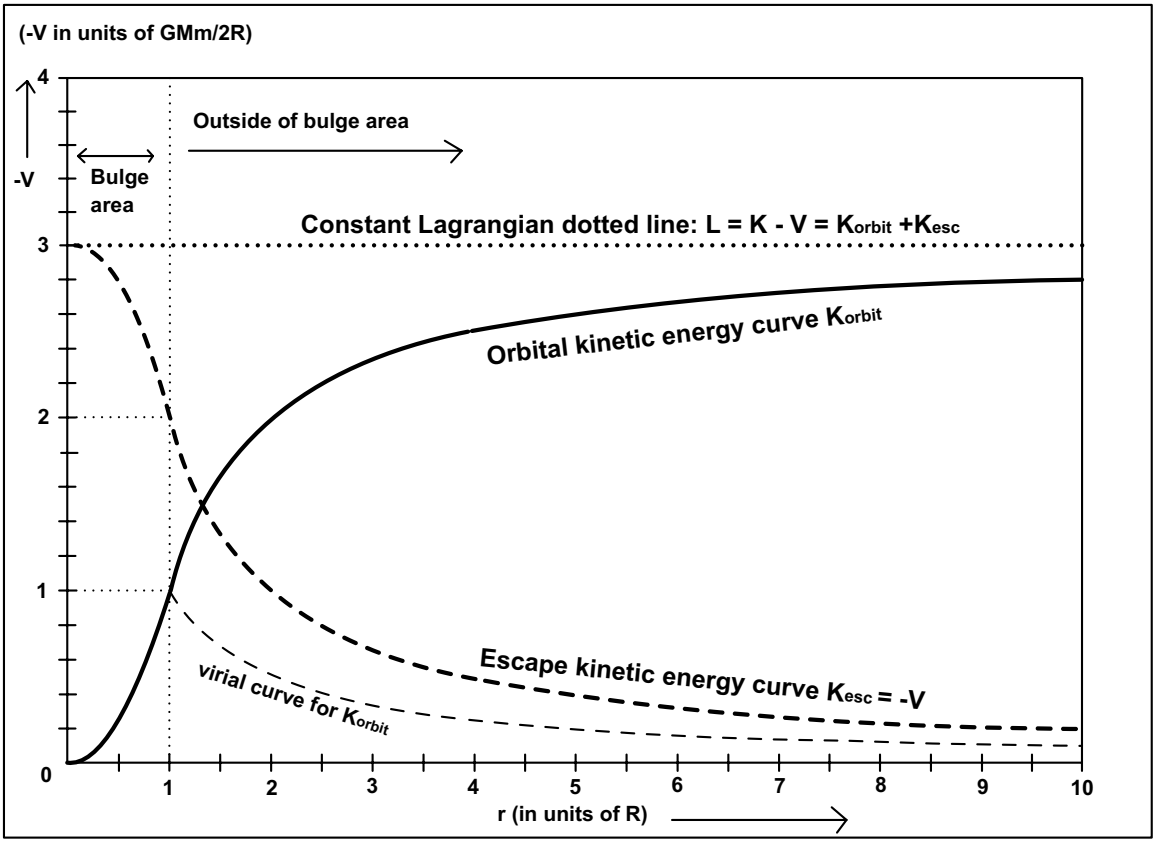

Figure 5. The square of the orbital velocity profile in the model galaxy with $L = constant$.

process in thermodynamic equilibrium, would have constant total kinetic energy, from the radial free fall perspective. This can be expressed as $L = K_{orbit} - V = K_{orbit} + K_{escape} = K_{final}$.

Such a model galaxy would also be a GNSS engineer's dream come true because the whole model galaxy is in one single syntonized mode, a clock-rate halo or time-bubble, defined by

$$\frac{d\tau}{dt} = \sqrt{1 - \frac{2L}{U_0}}. \tag{23}$$

Given the Baryonic Tully-Fisher relation in Milgrom's version $v_{final}^4 = Ga_0M$ with $2\pi a_0 \approx cH_0$, with a_0 as Milgrom's galactic minimum acceleration and H_0 as the Hubble constant, we get as a galactic clock-rate fix

$$\frac{d\tau}{dt} = \sqrt{1 - \frac{2L}{U_0}} = \sqrt{1 - \frac{v_{final}^2}{c^2}} = \sqrt{1 - \sqrt{\frac{v_{final}^4}{c^4}}} = \tag{24}$$

$$\sqrt{1 - \sqrt{\frac{Ga_0M}{c^4}}} = \sqrt{1 - \sqrt{\frac{GH_0M}{2\pi c^3}}} = \sqrt{1 - \sqrt{\frac{M}{2\pi M_U}}}, \tag{25}$$

in which I used $L = 3GM/R = K_{final} = \frac{1}{2}mv_{final}^2$ and $M_U = \frac{c^3}{GH_0}$. This last constant can be referred to as an apparent mass of the Universe, a purely theoretical number constant, see (Mercier 2015).

In a model Universe, this would imply that my model galaxy would realize a proper time bubble with clock-rate $d\tau$ relative to the universal clock-rate dt in proportion to the masses of galaxy M

and Universe M_U. In the theoretical environment of my model galaxy, the Baryonic Tully-Fisher relationship implies that the galactic clock-rate is fixed through the mass of my model galaxy and that this fix is a cosmological one. So what is a universal acceleration minimum a_0 in MOND can be interpreted as a universally correlated (through M_U) but still local (through M) clock-rate syntonization in my model galaxy geodetic environment.

7. GALAXIES WITH A SINGLE FIT ROTATION CURVE

Having determined the model galactic velocity rotation curve based on the Lagrangian as a galactic constant of orbital motion, the question is to what extend real galaxies can be modeled in this way. In my Lagrangian approach I analyze the plot of v_{orb}^2, in $(km/s)^2$ against r, in kpc. This in contrast to the usual rotation curves where v_{orb}, in (km/s) is plotted against r, in kpc. In the Lagrangian approach, the energies, not the velocities, are primary.

In each plot the experimental values are given in red stars with vertical error bars and the theoretical model values as a curved fit. The fitting plot is with one single fit for M, in units of $10^{10} Msolar$, and R, in units of kpc. The most important cut in the model is the change from the model bulge to the model empty space around it, which happens at the chosen value for R. In the model bulge, $V_{orb}^2 \propto r^2$, outside the model bulge $V_{orb}^2 \propto -r^{-1}$.

In this section, I use the SPARC database, including the error margins, as provided by (Lelli et al. 2016). This database functions as a random set relative to my model. I analyzed, fitted, the full set of 175 galaxies at the SPARC database, as provided by (Lelli et al. 2016) in the file Rotmod-LTG.zip. The SPARC website also provides a luminosity and mass distribution analysis of those 175 galaxies. It is to the reader to compare the results of my fits with the surface brightness and mass distribution graphs of SPARC (from the MassModels-LTG.zip file). As an inductive first indication, the fits of this database shows that, at least, huge stretches of almost all galaxy rotation curves can be plotted on a constant Lagrangian curve.

While fitting the SPARC database, I realized that an offset of the kinetic energy at $r = 0$ would improve the fit for many galaxy rotation curves. This offset is given in the graphs as the value of V_0. With this offset, three variables determine the fit, the mass M_1, the change from bulge to empty space R_1 and the offset of the kinetic energy at the origin represented by V_0^2.

With these three variables, of the 175 galaxies, 77 allowed a single fit rotation curve, so about 44 percent. Of these 77 galaxies, 21 didn't need an offset for v^2 so the fit was realized with only two variables, M and R. Another 20 galaxies didn't need the offset to arrive at a fit, but the offset significantly improved the fit, so I applied it to arrive at a minimum value of the RMWRSS.

This amazing result rules out stochastic coincidence as an explanation of those fits. Relative to the model, those 175 galaxies were a random set. The restrictions for a single fit (of almost all measurements) within the error margins are such that a 44 percent positive match rules out the possibility of a coincidental correlation without any causation. In the next pages I present 3 selected galaxies of the 77 with a nice single fit. In Appendix A, all the 77 single fits are given. All the plots are produced in Microsoft Excel, which for a High School teacher is the standard available software.

The second graph next to the fit presents the weighted residual of each measurement. The Root Mean Weighted Residual Sum Squares (RMWRSS) of the fit is calculated with each plot. The combination of the second graph and the RMWRSS gives a quantative expression of the quality of the fit. Of course, the more measurements of the galaxy rotation curve are given, and the more accurate these measurements are, the more impressive the fit will be, given an equal RMWRSS.

In the results of Fig.(7, UGC01281) the three aspects of the model curve are clearly present. First the model bulge patter is clearly present in the ascending parabolic part of the curve. This part of the model is classical because it combines the virial theorem and the constant Lagrangian. In my model, there shouldn't be need for any Dark Matter inside the bulge, because the behavior is purely classical. Then secondly the shift from bulge to free space as a continuous increasing function instead of the abrupt decrease as would be expected classically with the virial theorem. Thirdly is the type of ascending towards a maximum. This part of the graph is more clearly visible in Fig.(A, F579-V1).

Whatever the theory applied, these single fit galaxies have realized a constant Lagrangian structure and are syntonized over the entire rotation curve. This result is a consequence of the fit and independent of my justifications of the model. One should realize the consequence: if we were able to launch GNSS satellites in orbit over the entire rotation curve of those galaxies, all the atomic clocks in those standard satellites would be syntonized. If we could express the degree of syntonization on a galactic velocity curve in terms of entropy, these single fit galaxies reach the lowest possible time-like entropy because they achieve the highest order as to the syntonization of their 'on board' atomic clocks.

If we examen the surface brightness and mass distribution graphs of these galaxies, (from the MassModels-LTG.zip file), there is one dominant denominator: for many of them the measured rotation curves of these galaxies does not extend beyond the measured range of the surface brightness.

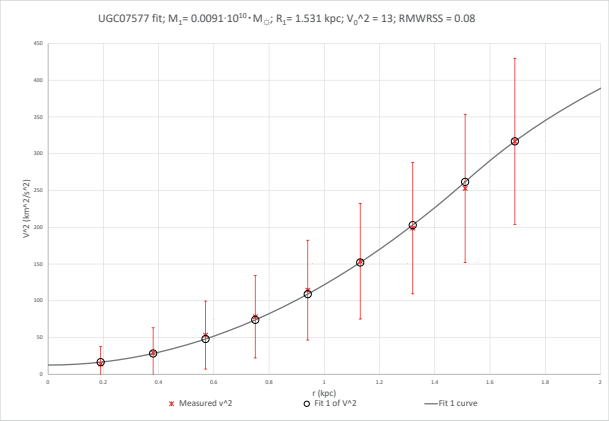

UGC07577

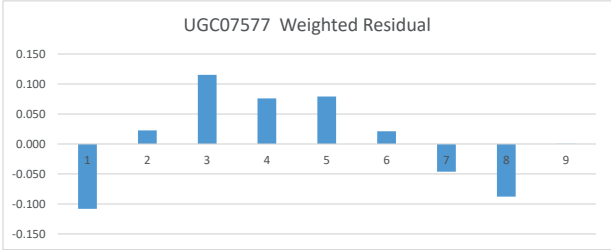

UGC07577 WR; RMWRSS = 0.08

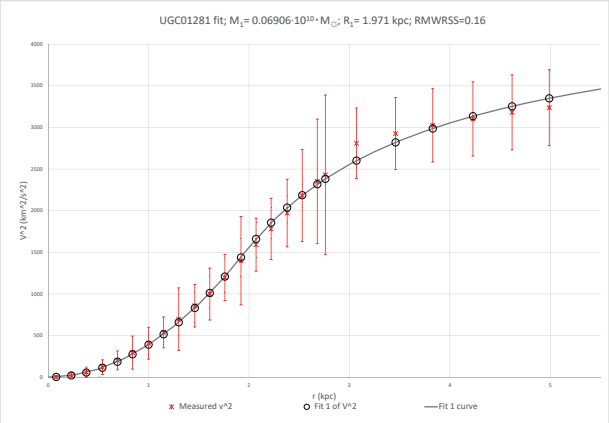

UGC01281

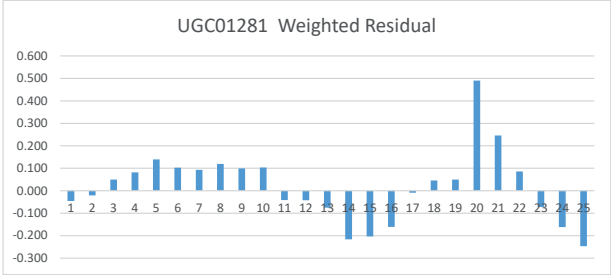

UGC01281 WR; RMWRSS = 0.16

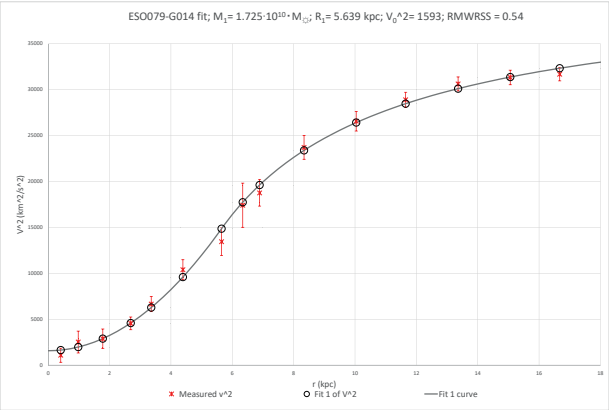

ESO079-G014

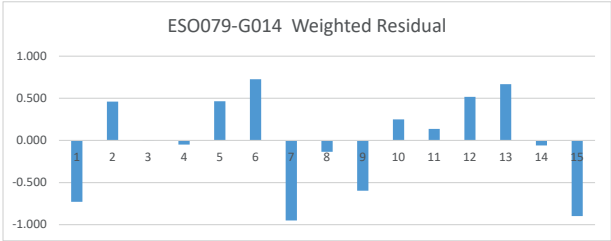

ESO079-G014 WR; RMWRSS = 0.54

8. THE NON-SINGLE FIT GALAXIES

8.1. *Almost single fit galaxies*

The first category in the non-single fit galaxies are the ones that almost allowed a single fit, but where the error margins prevented such a decision. There are 18 galaxies in this category. These 'deviations' from a single model curve presented itself for example at the bulge part closest to the center of those galaxies. See Fig.(6, UGC06399)as an example. Others had an outer range measurement that didn't follow the fitting curve. And then there were the erratic not fitting ones. Some of the non-single fit galaxies had the RMWRSS still below unity but with one or more measurements having a weighted residual relative to the fitting curve above unity.

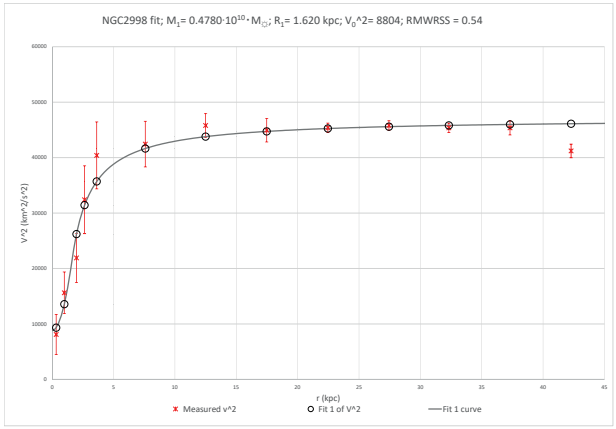

NGC2998

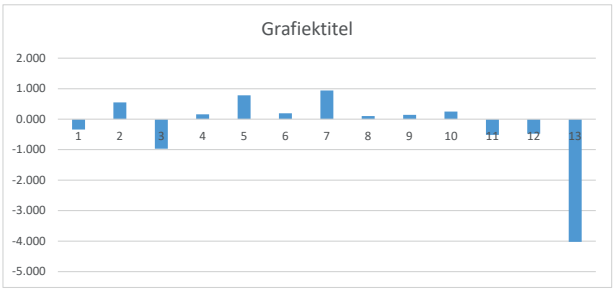

NGC2998-WR; RMWRSS = 0.54

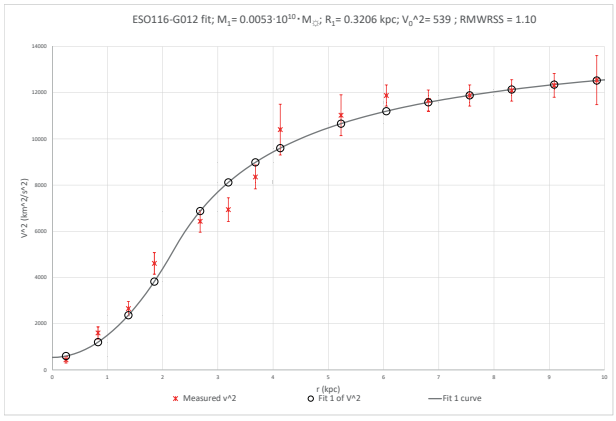

ESO116-G012

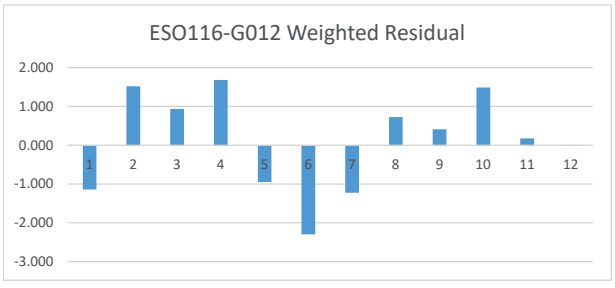

ESO116-G012-WR; RMWRSS = 1.10

Figure 6. Galaxies with an 'almost' single fit.

8.2. *Abrupt transition crossover dual Lagrangian fit galaxies*

The second category in the dual fit galaxies are the ones that have an abrupt transition from one Lagrangian fit to the next. See Fig.(7) as an example. There are 13 galaxies in this category. See Appendix C. In many cases, the abrupt transition is corresponding to a change in the composition

of the galaxy. For example the ending of a strong surface brightness and the beginning of the gas filled outer regions of the galaxy.

In the case of the upwards Lagrangian crossing over from below as in Fig.(7), the galaxy's time-rate shifts to a higher frequency. The frequency shifts are rather abrupt, effectively splitting these galaxies in two clock-rate time zones.

In the example of Fig.(7, NGC0247), the crossover coincides with the new R_2, so it marks a new end of the 'bulge' or the beginning of a new 'outside the bulge' area. The additional galaxy fits of this type can be found in Appendix C. In the velocity rotation curves of SPARC, the two zones are also recognizable, but not so distinctly as in the squared velocity rotation curves, especially when fitted along constant Lagrangian curves.

In the upwards abrupt transition, the rotation curve starts of as a model galaxy including a model bulge ending at R_1 with inside mass M_1 and an outside area where the virial theorem seems invalidated and the constant Lagrangian alone determines the shape of the curve. In the model galaxy there is by definition only an insignificant amount of mass outside the model bulge but in real galaxies the mass outside the bulge can be much more than the mass of the bulge, as is the case for galaxies with a substantial disk.

My interpretation of the upwards abrupt Lagrangian transition is that the galaxies dynamics allowed for or favored a sudden reset because the upward crossover happens to coincide with the new bulge radius R_2, identifying a higher mass M_2 inside R_2. The additional mass outside R_1 first follows the model curve beyond R_1 but eventually the accumulated new mass disrupts the initial 'constant Lagrangian' curve. But the model curve doesn't break down, it just resets itself by defining a new bulge with radius R_2 which includes all the additional mass into M_2. It is as if a thin spherical shell with a high density mass $M_2 - M_1$ appears at R_2, causing this abrupt transition.

Because the two constant Lagrangian curves co-define atomic clock-rate frequencies, this crossover partitions the galaxy in two distinct clock-rate zones or 'time bubbles'. It results in a lower atomic frequency or clock-rate time-bubble inside a higher atomic frequency or clock-rate time-bubble.

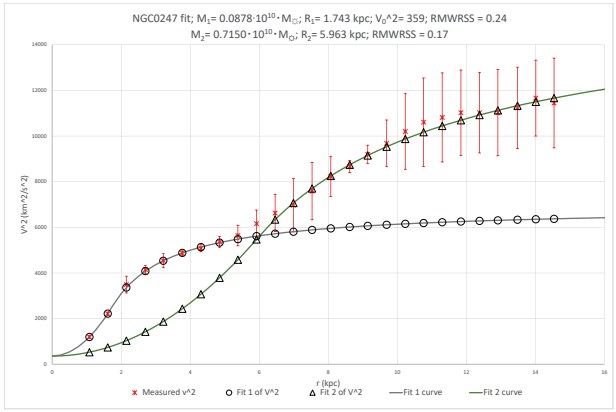

NGC0247

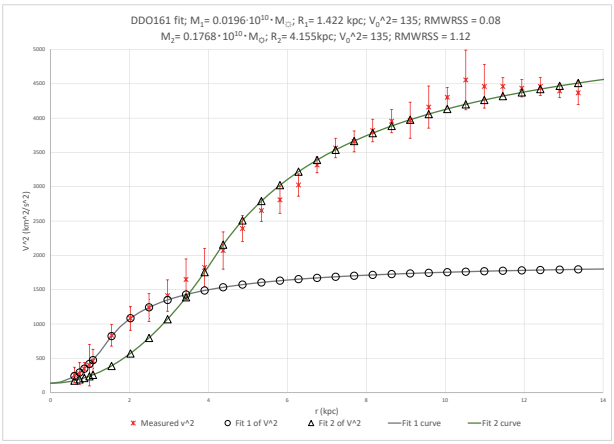

DDO161

Figure 7. Galaxies with an upwards abrupt crossover transition.

8.3. *Receding to a final energy (almost) single fit galaxies*

While fitting the curves with a constant Lagrangian function, MS Excel surprised me by fitting some galaxy velocity curves with negative $M$and R. For the absolute values of M and R in the region outside the bulge, this changes the curve into

$$v_{orbit}^2 = \frac{3GM}{2R} + \frac{GM}{r}, \tag{26}$$

so with a kinetic energy decreasing Newtonian like to a final value. In a genuine Newtonian regime, this should decrease to zero, but in the galaxy rotation curve it decreases to a fixed value from above. It still can be interpreted as a Newtonian like regime. In Fig.(8) a typical example is given. See Appendix D for all 3 galaxies of this subsection.

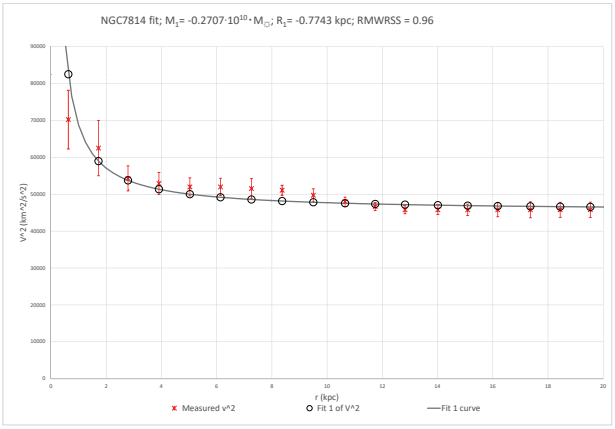

NGC7814

Figure 8. Galaxy with an semi-Newtonian regime.

8.4. *Gaxies with a Lagrangian to semi-Newtonian transition*

After I realized that some galaxies could be fitted on a semi-Newtonian curve, I recognized such semi-Newtonian curves in other galaxy velocity plots. I first categoriezed the single transition galaxies. This subsection contains 23 galaxies. In Fig.(9, UGC05986) a typical example is given. The characteristic of this subtype is that the transition mainly occurs in the larger scale velocity curves, roughly in between $10kpc$ and $100kpc$. See Appendix E for the remaining galaxies of this subsection.

8.5. *Triple fit galaxies and beyond*

This subsection contains 12 galaxies. In the example of Fig.(10, NGC7331) a typical galaxy in this category is given. See Appendix F for the remaining galaxies of this subsection. The galaxy NGC7331 is chosen because of its small error margins. Those small margins greatly reduce the freedom of interpretation while fitting the experimental curve. Most of these galaxies have rotation curves that reach beyond $50kpc$.

The galaxies of this category start with a Lagrangian curve and then suddenly start to drift downwards in a semi-Newtonian like fashion and on a large scale, $\simeq 10kpc$, dimension, until a new upwards

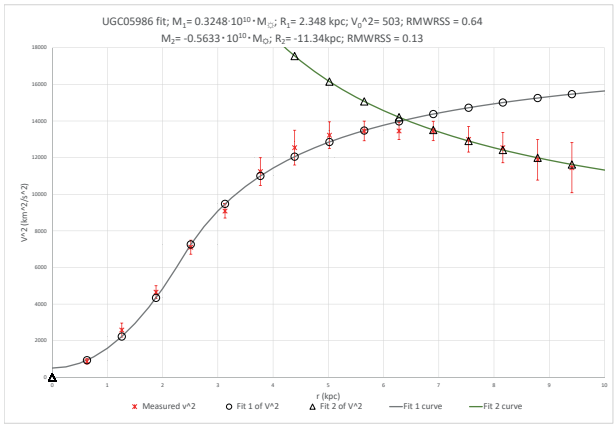

UGC05986

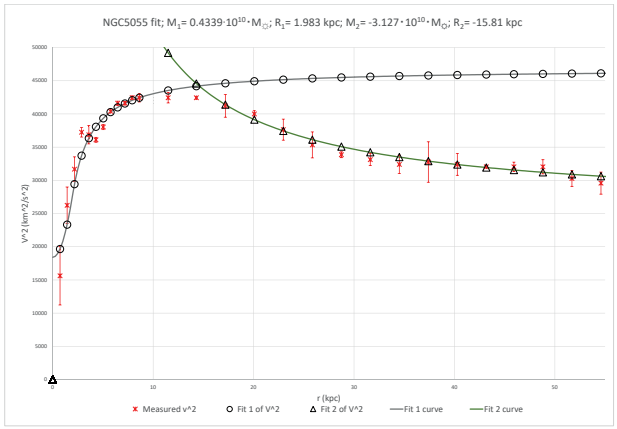

NGC5055

Figure 9. Galaxies with a Lagrangian to a semi-Newtonian transition.

moving constant Lagrangian curve is found. The direction of the drift implies that from orbit to orbit energy is being or has been dissipated in a virial like way. These downward drift zones should therefore show a thermodynamically higher activity than the surrounding constant Lagrangian zones. Those zones should be the more turbulent zones of those galaxies because with a non-zero $\frac{\Delta L}{\Delta r}$, the Newtonian force of gravity F_g should also be non-zero in that zone and matter should not be moving on geodetic orbits. It should be a zone with non-zero gravitational stress between orbits. But because the galaxies almost always achieve to return to a non-virial constant Lagrangian curve, a purely Newtonian regime should not be expected in such zones. Those zones might be characterized as drifting in between a Hubble expansion dynamics and a Newtonian contraction dynamics, because the Lagrangian isn't a constant so gravitational stresses should be expected but the drifting down seems too slow for a full reaffirmation of the virial theorem.

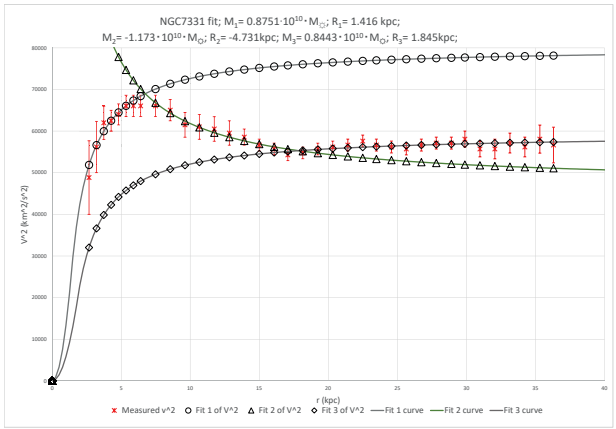

NGC7331

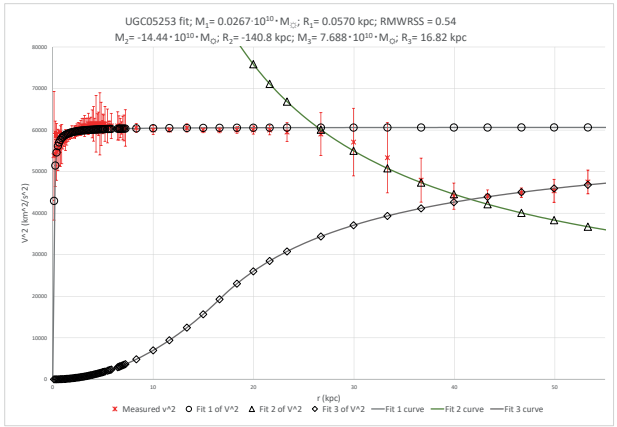

UGC05253

Figure 10. Triple fit galaxies

8.6. *The rest of the galaxies*

This category contains 27 galaxies. For these 27 galaxies, a partial fit was almost always possible. For UGC08286 it might have been better not to present a fit at all, see Fig.(11, NGC2683). See the appendix G for the rest of the galaxies of this category. Most of the galaxies in this section could be appointed to one of the previous categories but not without the cost of seeming over eager to impose order, even when disorder dominates. This means that 10 percent of the galaxies couldn't be easily put into on of the proposed categories.

Some of these galaxies where so chaotic that any fit might seem appropriate, thus also no fit at all. Some of them could without to much imagination, but at the cost of significantly less error margin rigor, be categorized into one of the previous sections. The scientific integrity demands that when the SPARC database of 175 galaxies are subjected to an independent model, that the 'failures' and the difficulties to model reality will be recognized as such.

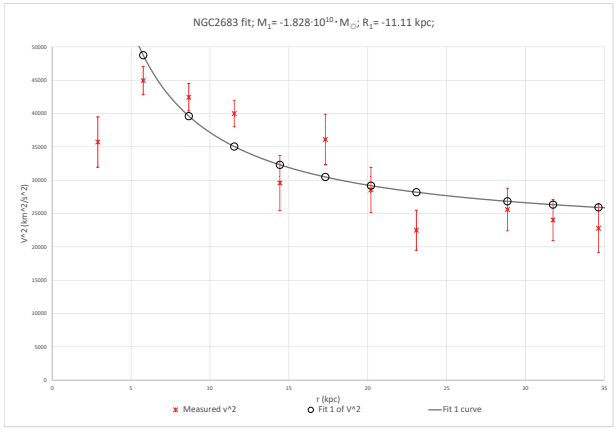

NGC2683

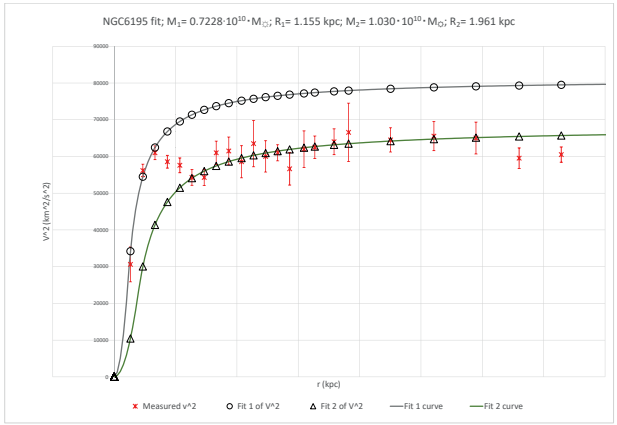

NGC6195

Figure 11. The almost no-fit galaxies

9. CONCLUSION

The least daring conclusion of this paper is that complete to huge stretches of galaxy rotation curves can be effectively plotted on constant Lagrangian curves. On these stretches atomic clocks are highly syntonized, creating effective time-rate zones and bubbles.

Of the 175 galaxies, 77 allowed a single fit rotation curve, so about 44 percent. Another 18 galaxies could almost be plotted on a single fit. Then 13 galaxies could be fitted really nice on crossing dual curves. The reason for the appearance of this dual curve, in its two versions, could be given and related to the galactic constitution and dynamics.

Three galaxies could be fitted on a semi-Newtonian curve.

Another 23 galaxies could be fitted on a Lagrangian to semi-Newtonian transition. Then 12 galaxies could be fitted on a transition from one Lagrangian to the next through a semi-Newtonian transition, tripple fit LNL galaxies. Then 27 galaxies where to chaotic to be catetorized and the attempt to fit the velocity rotation curve should be aborted.

In my opinion, the success of the 'constant Lagrangian' approach indicates that the problem of the galaxy rotation curves can be solved on the basis of the principle of conservation of energy.

Inside a model bulge, thermodynamic and stellar processes allow for a side by side existence of the virial theorem and the constant Lagrangian condition. Outside the model bulge, orbital collapse conditions are mostly such that these conditions do not allow the collapsing matter to dissipate half of the gravitational energy. This invalidates the virial theorem, which is then replaced by the constant Lagrangian condition.

From a radial free fall perspective, the last condition is just a conservation of energy expression. From a General Relativity perspective, a constant Lagrangian condition implies a zero force of gravity and that in turn means that a metric approach is allowed and needed. But on stretches of galactic curves where the Lagrangian isn't a constant from orbit to orbit, gravitational stresses are present and the application of General Relativity should be expected to meet its limitations. Those regions can be seen as intermediates between Newton and Einstein. That might also be the reason for the partial successes of MOND.

REFERENCES

Ashby, N. 2002, Physics Today, 55, 41

de Haas, E. P. J. 2014, Canadian Journal of Physics, 92, 1082

de Haas, E. P. J. 2018a, Preprint on viXra.org:Astrophysics, vixra:1805.0168

—. 2018b, Preprint on viXra.org:Astrophysics, vixra:1804.0386

—. 2018c, Preprint on viXra.org:Astrophysics, vixra:1804.0328

—. 2018d, Preprint on viXra.org:Astrophysics, vixra:1805.0047

Delva, P., & Lodewyck, J. 2013, in Workshop on Relativistic Positioning Systems and their Scientific Applications Brdo, Slovenia, September 19-21, 2012, arXiv:1308.6766 [physics.atom-ph]

Hećimović, Ž. 2013, Tehnički vjesnik, 20, 195

Koopmans, L., et al. 2009, Astrophysical Journal, arXiv:astro-ph/0902.3186v2

Kopeikin, S. M., Vlasov, I. Y., & Han, W. B. 2017, ArXiv e-prints, arXiv:1708.09456 [gr-qc]

Lelli, F., McGaugh, S. S., & Schombert, J. M. 2016, The Astronomical Journal, 152, 157

Mayrhofer, R., & Pail, R. 2012, in International Association of Geodesy Symposia, Vol. 136, Geodesy for Planet Earth, ed. S. Kenyon (Springer International Publishing), 231–238, switzerland

McGaugh, S. S. 2005, The Astrophysical Journal, 632, 859, arXiv:astro-ph/0506750v2

Mercier, C. 2015, Website access (accessed on April, 14, 2018)

Milgrom, M. 1983a, The Astrophysical Journal, 270, 371, Astronomy Abstract Service pdf

—. 1983b, The Astrophysical Journal, 270, 365, Astronomy Abstract Service

Misner, C., Thorne, K., & Wheeler, J. 1973, Gravitation (San Francisco: Freeman and Company)

Ohanian, H., & Ruffini, R. 2013, Gravitation and Spacetime, 3rd edn. (New York: Cambridge University Press)

Oort, J. H. 1932, Bulletin of the Astronomical Institutes of the Netherlands, 6, 249

Rubin, V., Thonnard, N., & Ford, W. J. 1978, Astrophysical Journal, Part 2 - Letters to the Editor, 225, L107

—. 1980, Astrophysical Journal, 238, 471

Ruggiero, M. L., Bini, D., Geralico, A., & Tartaglia, A. 2008, Classical and Quantum Gravity, 25, 205011, arXiv:0809.0998 [gr-qc]

Singer, S. F. 1956, Phys. Rev., 104, 11

Straumann, N. 1984, General Relativity and Relativistic Astrophysics (Berlin: Springer-Verlag)

The ATLAS Collaboration. 2018, The European Physical Journal C, 78, 18

Tully, R. B., & Fisher, J. R. 1977, Astronomy and Astrophysics, 54, 661

Weinberg, S. 1972, Gravitation and cosmology: principles and applications of the general theory of relativity (New York: Wiley & Sons)

Zwicky, F. 1933, Helvetica Physica Acta, 6, 110

—. 1937, Astrophysical Journal, 86, 217

APPENDIX

A. THE SINGLE FIT SELECTION.

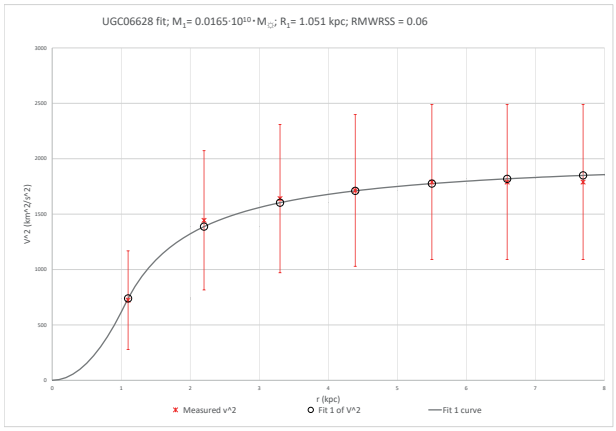

UGC06628

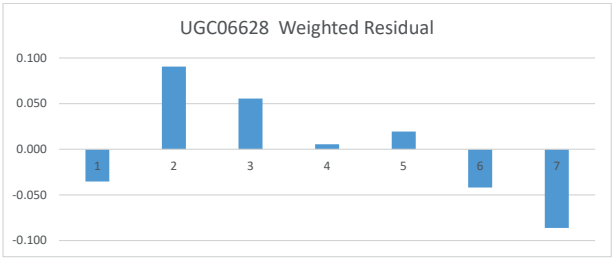

UGC06628 WR; RMWRSS = 0.06

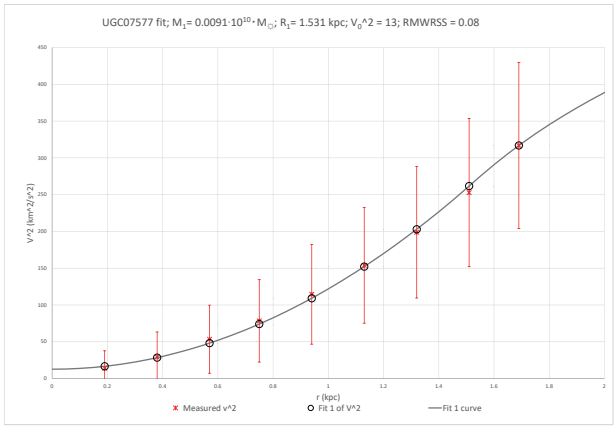

UGC07577

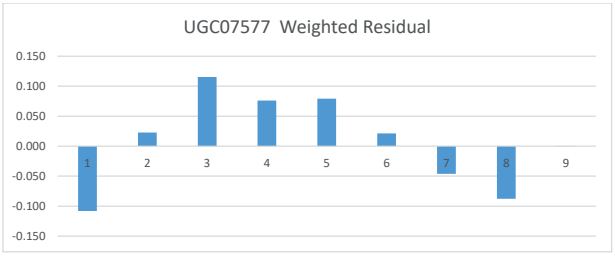

UGC07577 WR; RMWRSS = 0.08

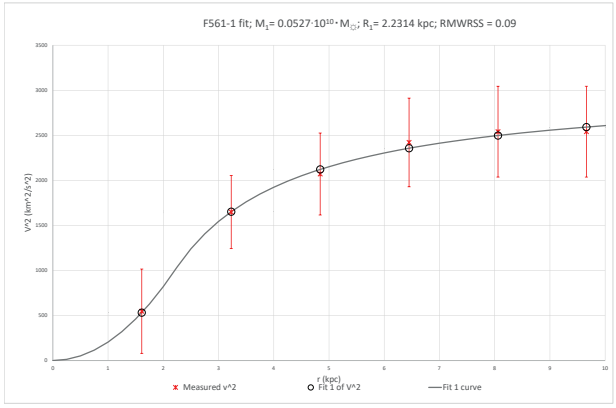

F561-1

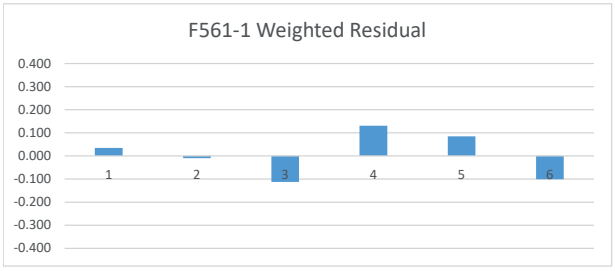

F561-1 WR; RMWRSS = 0.09

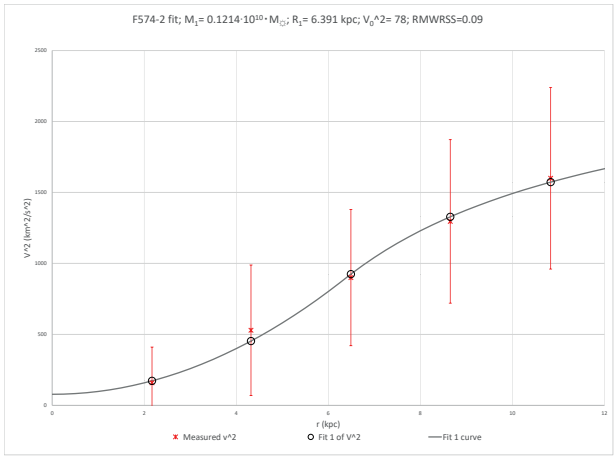

F574-2

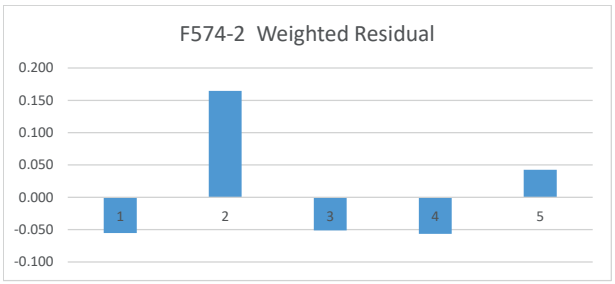

F574-2 WR; RMWRSS = 0.09

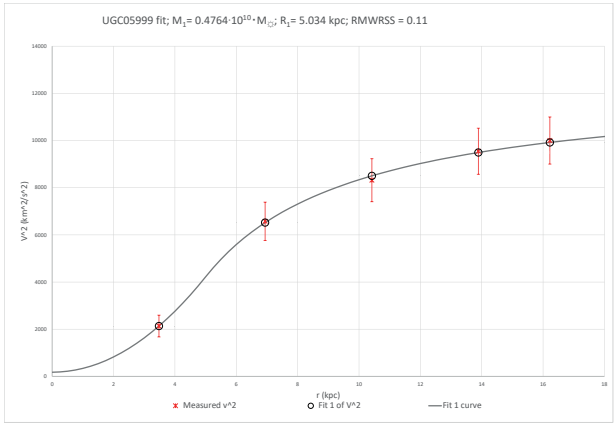

UGC05999

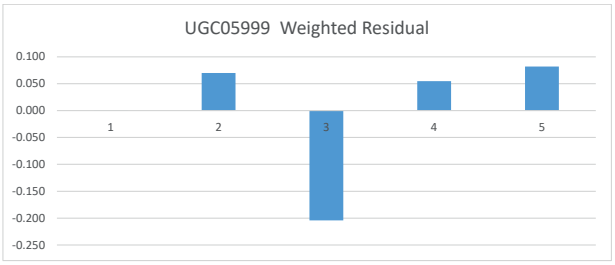

UGC05999 WR; RMWRSS = 0.11

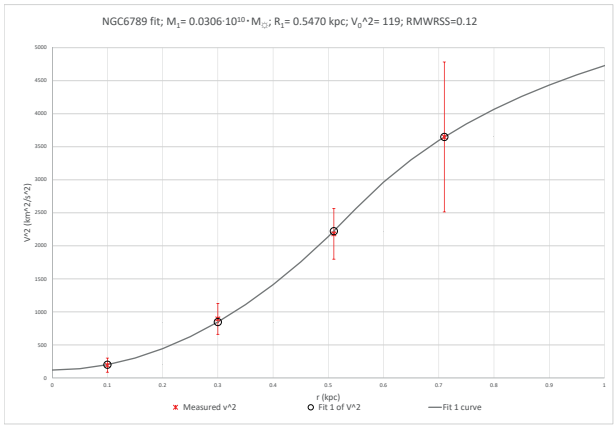

NGC6789

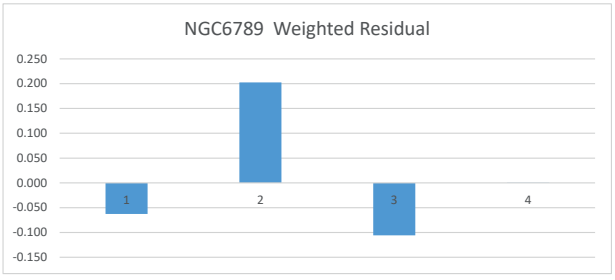

NGC6789 WR; RMWRSS = 0.12

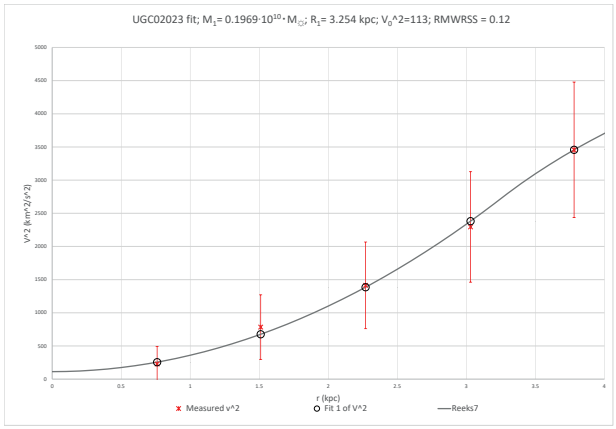

UGC02023

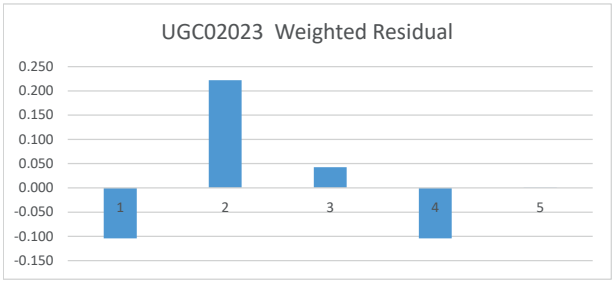

UGC02023 WR; RMWRSS = 0.12

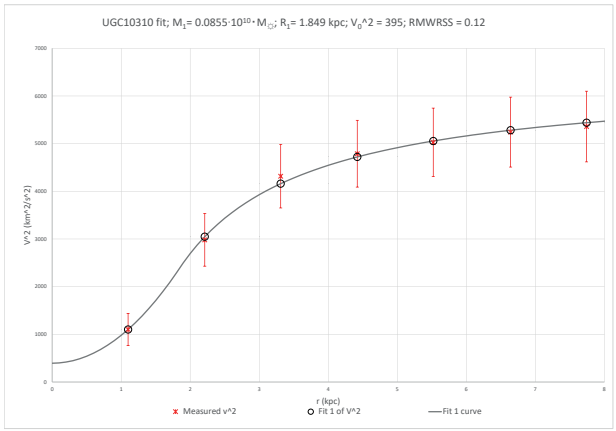

UGC10310

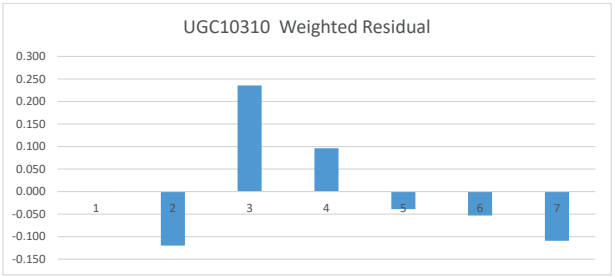

UGC10310 WR; RMWRSS = 0.12

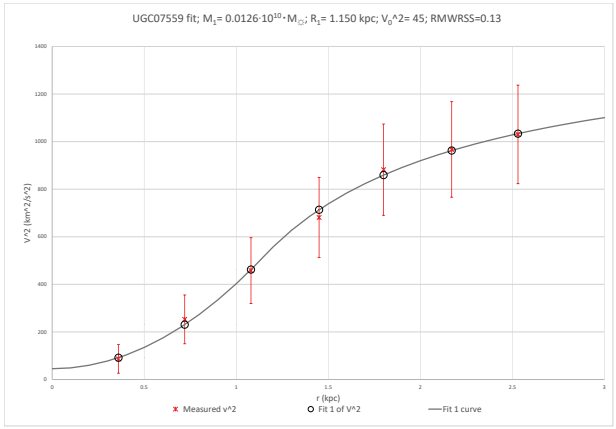

UGC07559

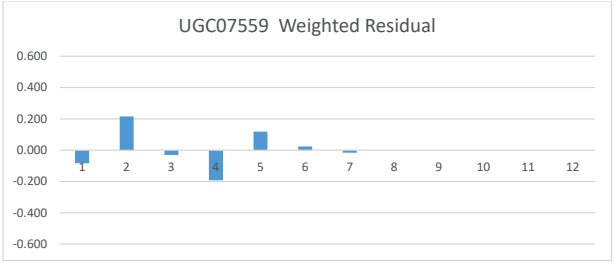

UGC07559 WR; RMWRSS = 0.13

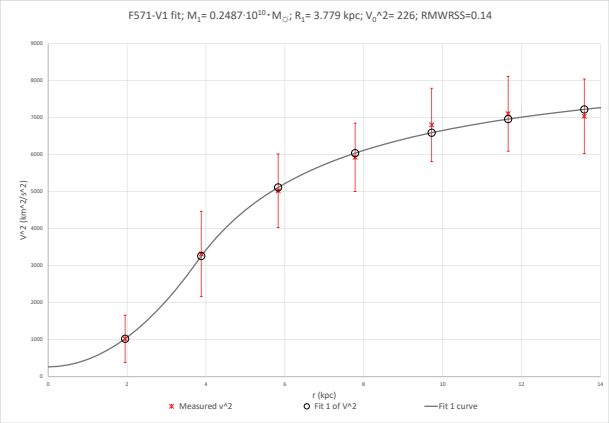

F571-V1

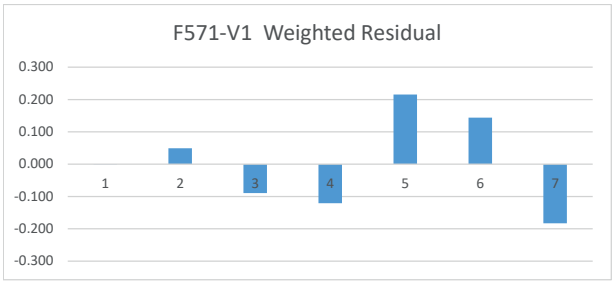

F571-V1 WR; RMWRSS = 0.14

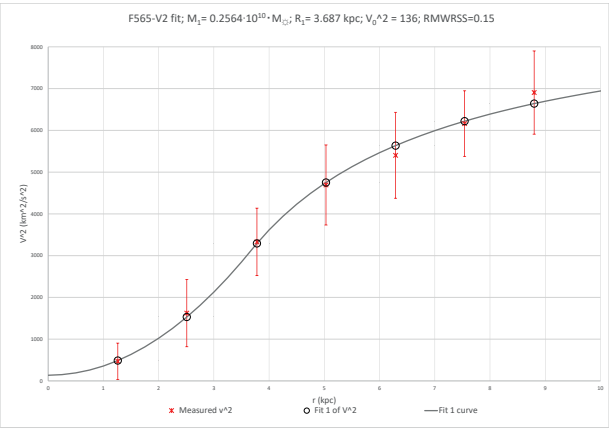

F565-V2

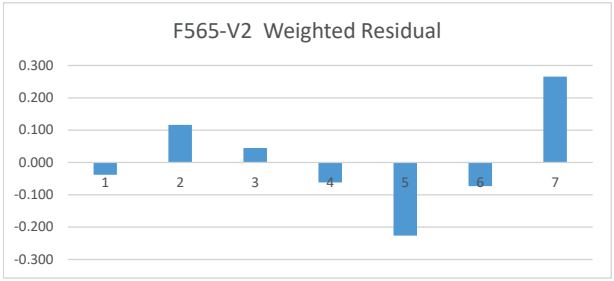

F565-V2 WR; RMWRSS = 0.15

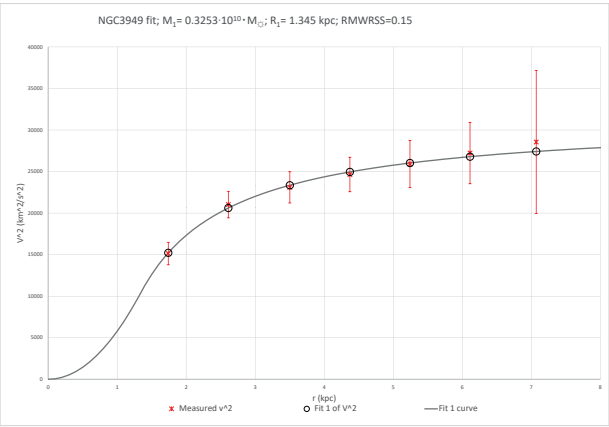

NGC3949

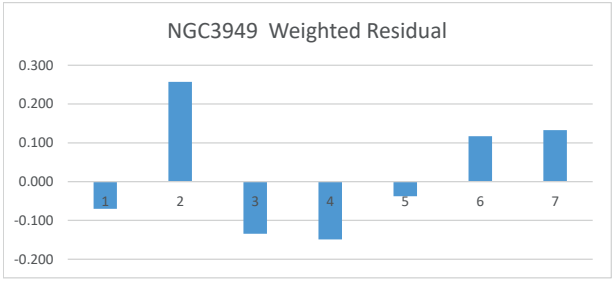

NGC3949 WR; RMWRSS = 0.15

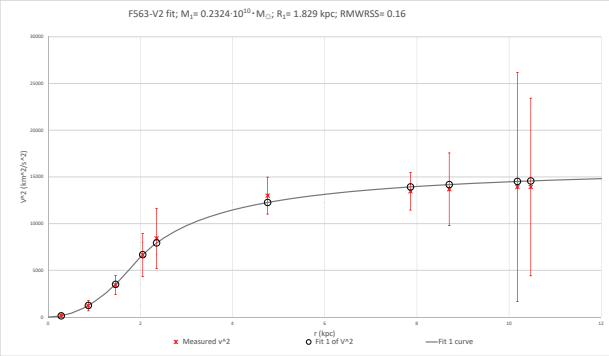

F563-V2

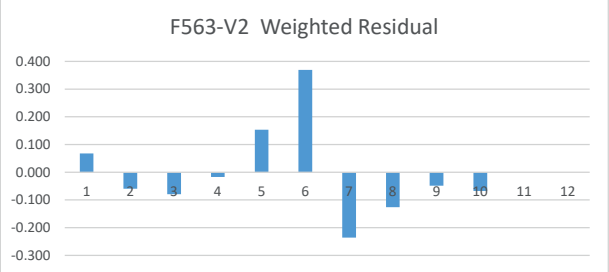

F563-V2 WR; RMWRSS = 0.16

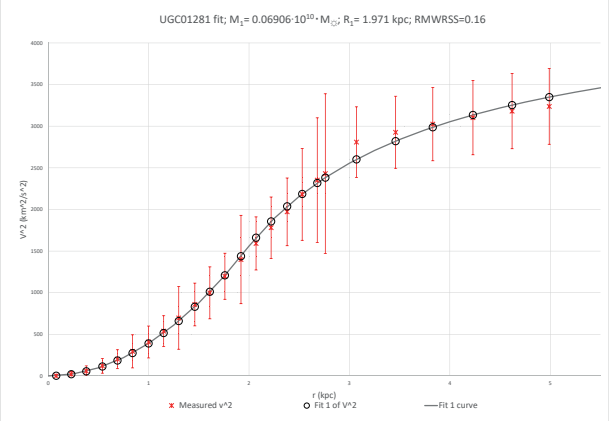

UGC01281

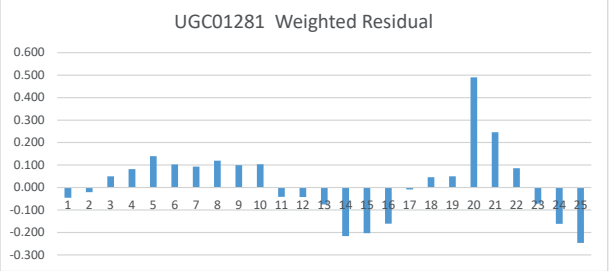

UGC01281 WR; RMWRSS = 0.16

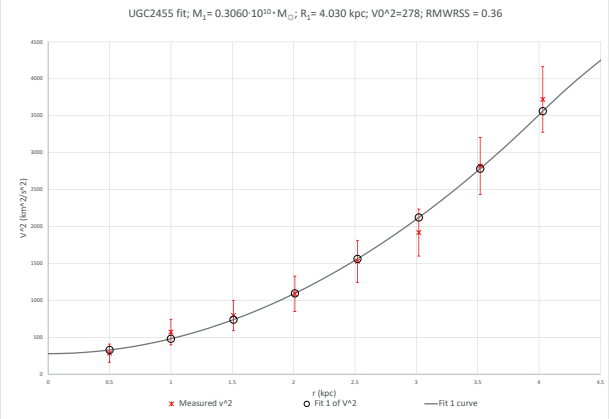

UGC02455

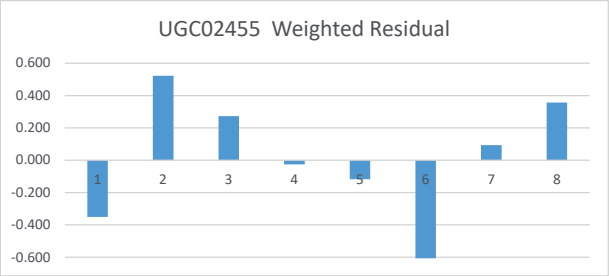

UGC02455 WR; RMWRSS = 0.16

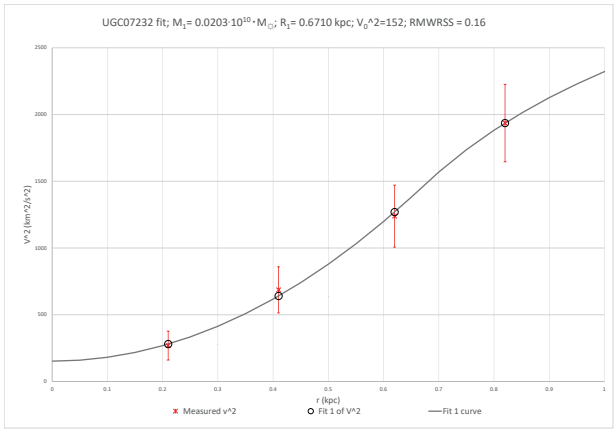

UGC07232

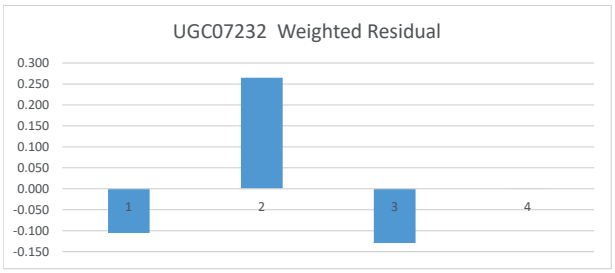

UGC07232 WR; RMWRSS = 0.16

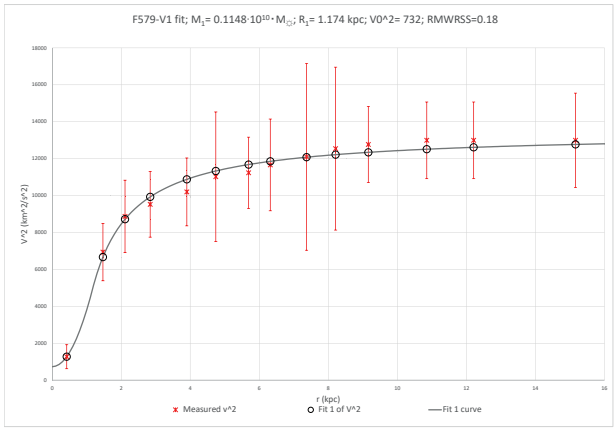

F579-V1

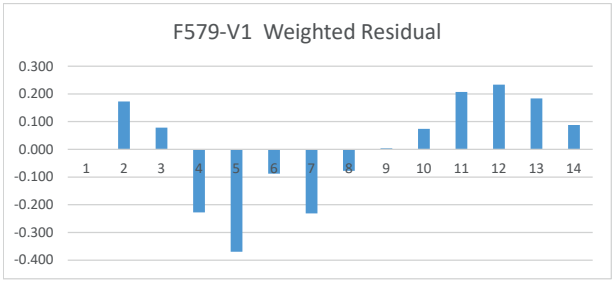

F579-V1 WR; RMWRSS = 0.18

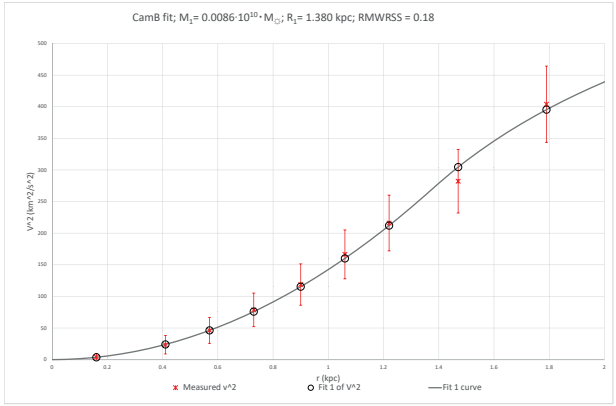

CamB

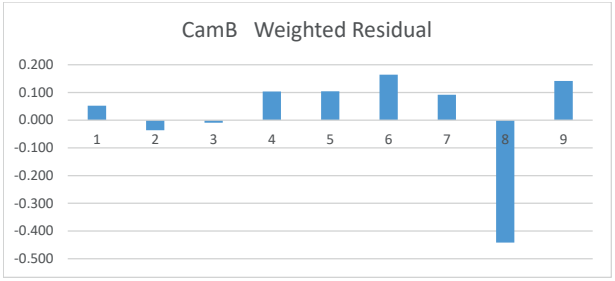

CamB WR; RMWRSS = 0.18

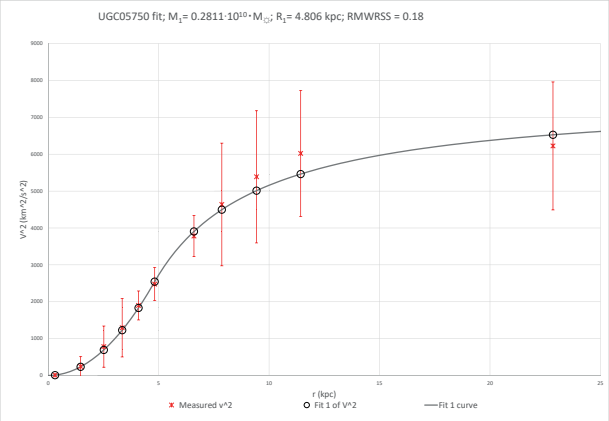

UGC05750

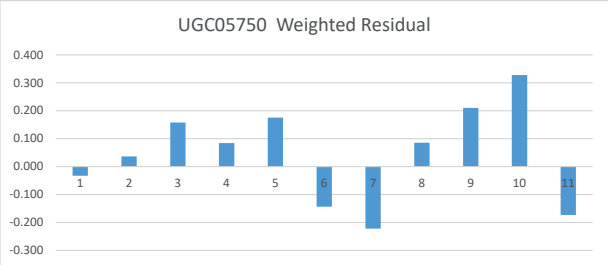

UGC05750 WR; RMWRSS = 0.18

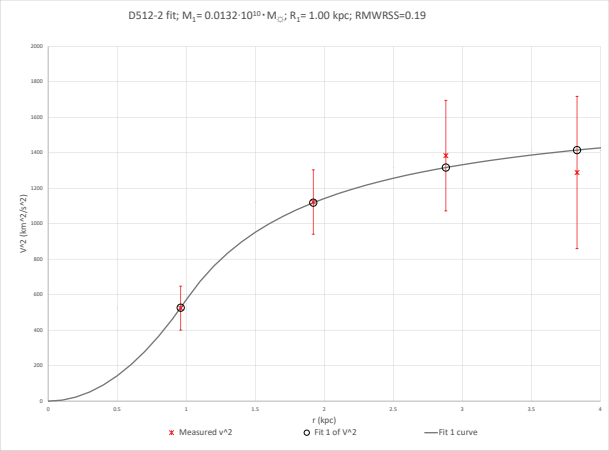

D512-2

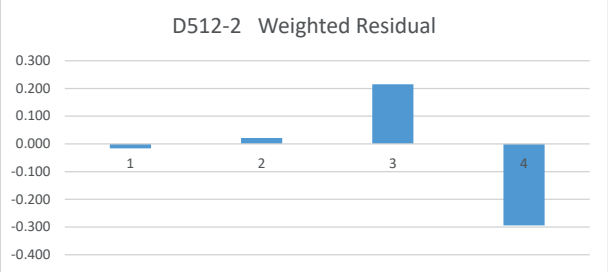

D512-2 WR; RMWRSS = 0.19

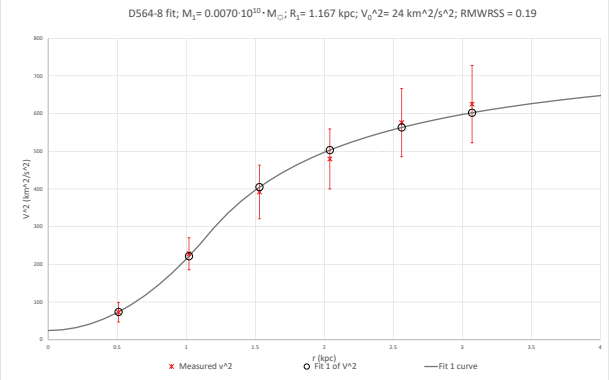

D564-8

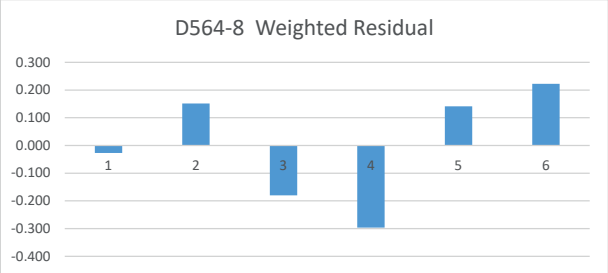

D564-8 WR; RMWRSS = 0.19

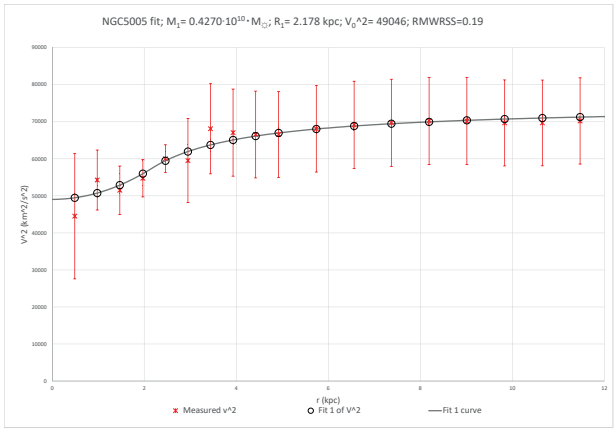

NGC5005

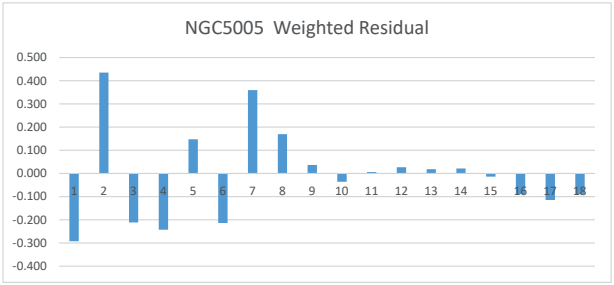

NGC5005 WR; RMWRSS = 0.19

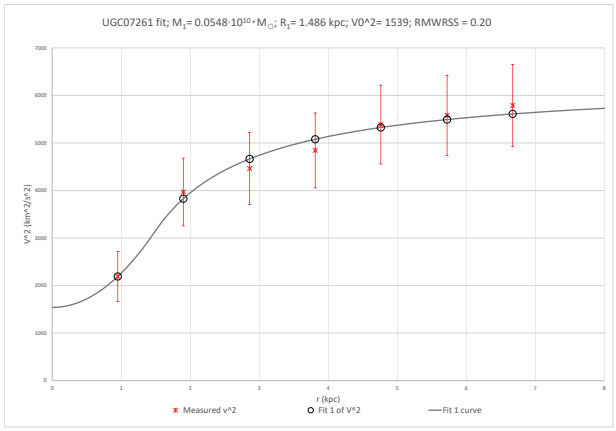

UGC07261

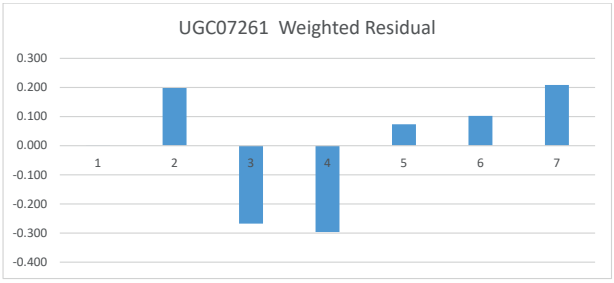

UGC07261 WR; RMWRSS = 0.20

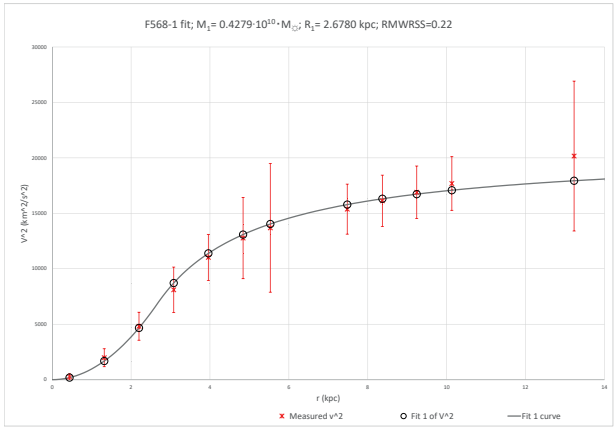

F568-1

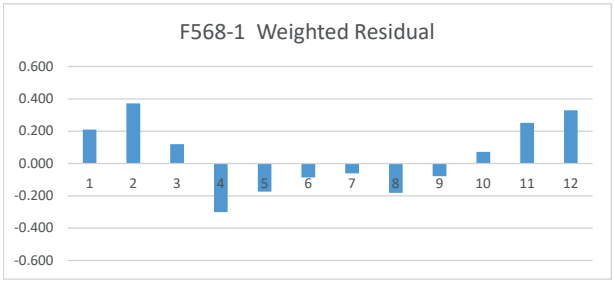

F568-1 WR; RMWRSS = 0.22

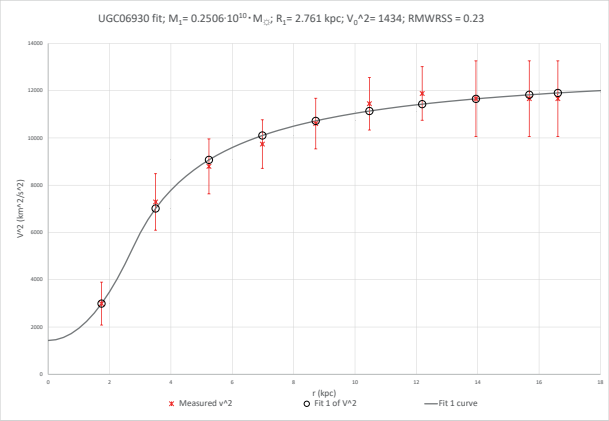

UGC06930

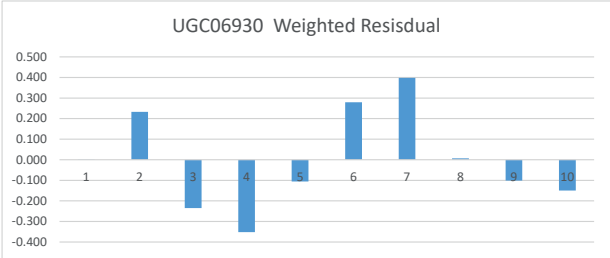

UGC06930 WR; RMWRSS = 0.23

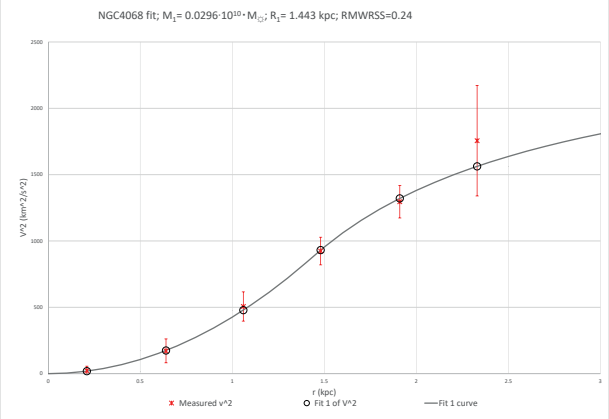

NGC4068

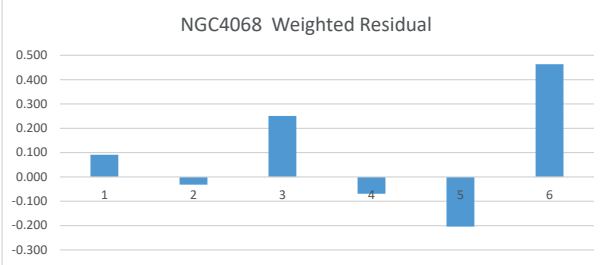

NGC4068 WR; RMWRSS = 0.24

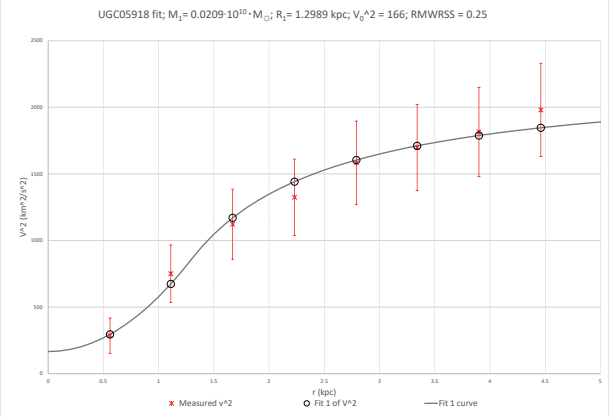

UGC05918

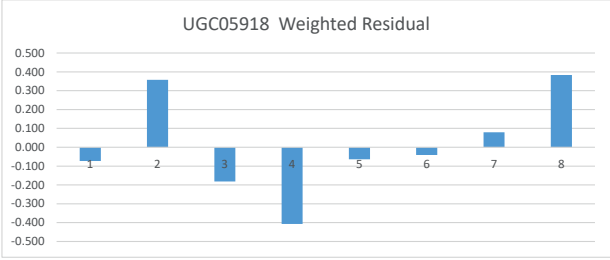

UGC05918 WR; RMWRSS = 0.25

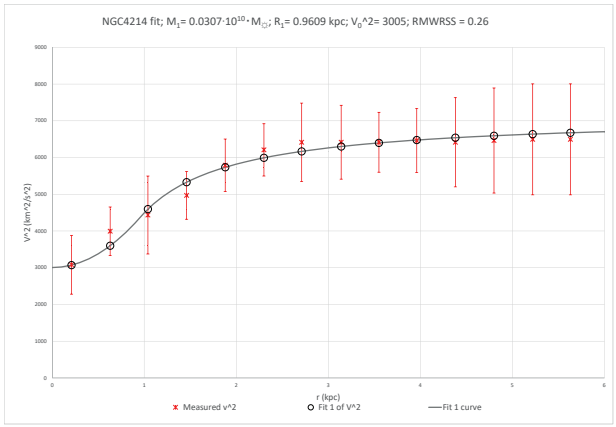

NGC4214

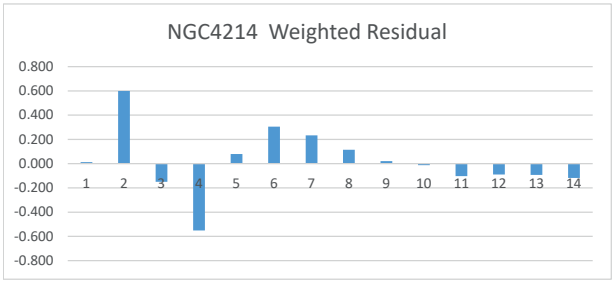

NGC4214 WR; RMWRSS = 0.26

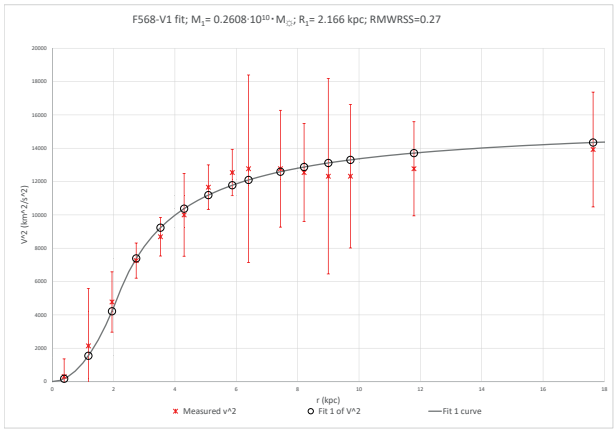

F568-V1

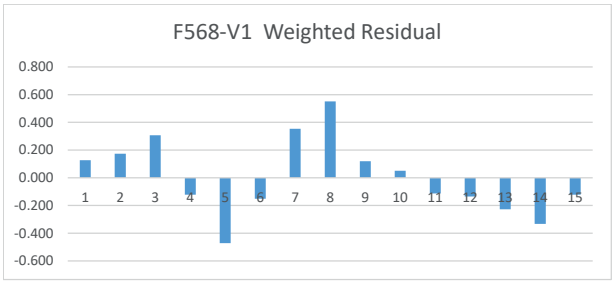

F568-V1 WR; RMWRSS = 0.27

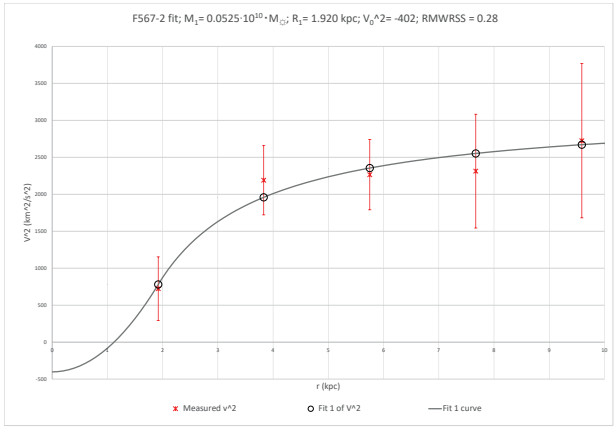

F567-2

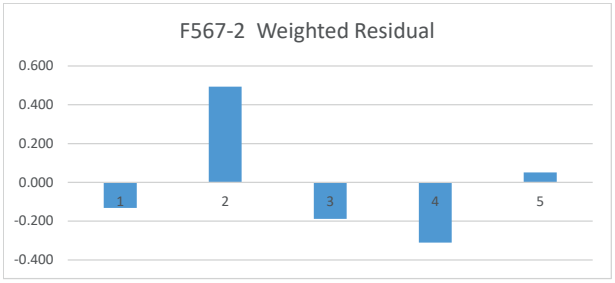

F567-2 WR; RMWRSS = 0.28

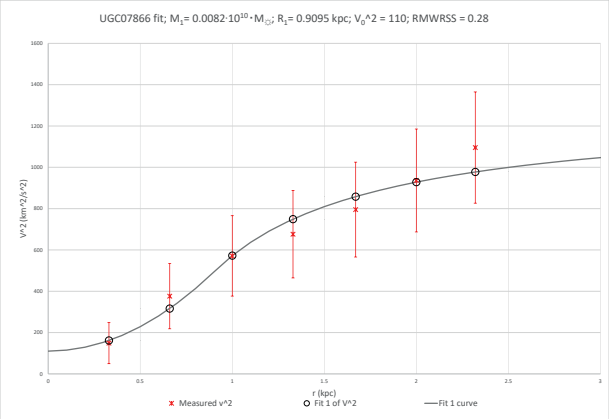

UGC07866

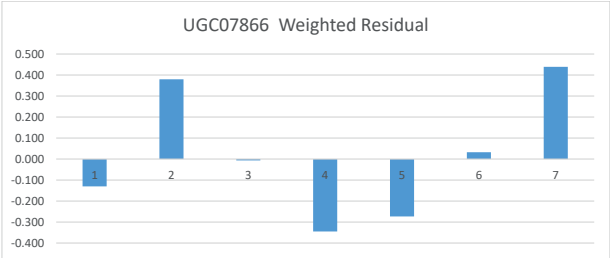

UGC07866 WR; RMWRSS = 0.28

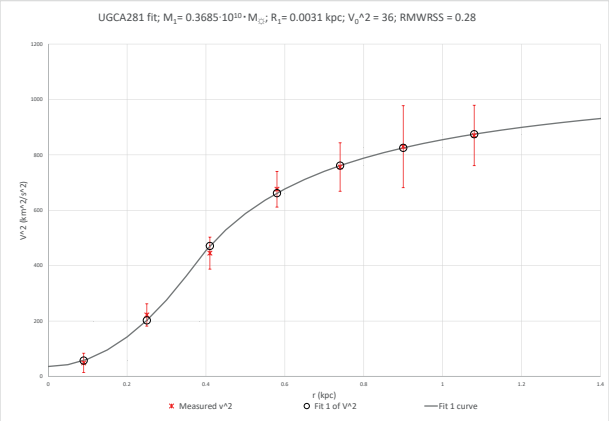

UGCA281

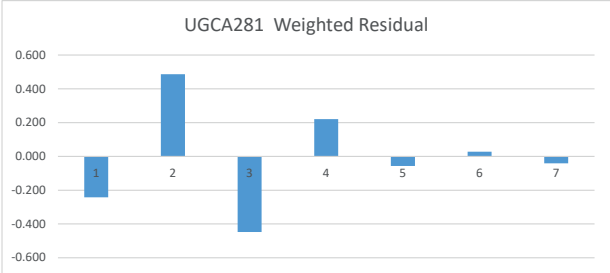

UGCA281 WR; RMWRSS = 0.28

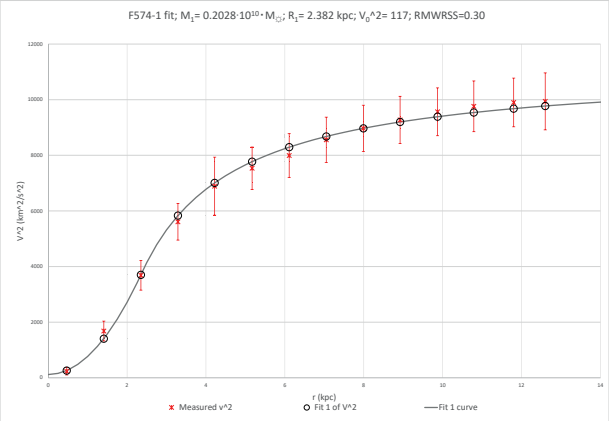

F574-1

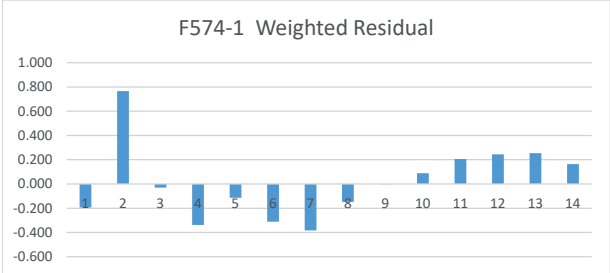

F574-1 WR; RMWRSS = 0.30

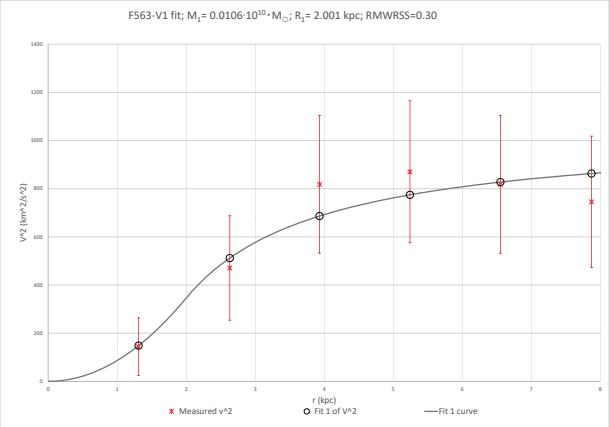

F563-V1

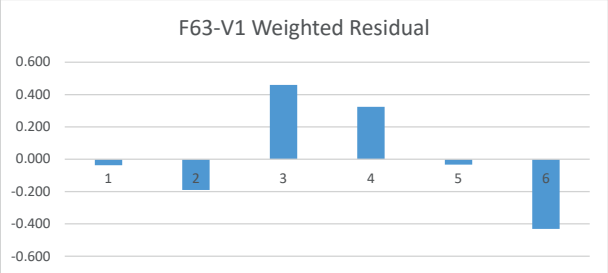

F563-V1 WR; RMWRSS = 0.30

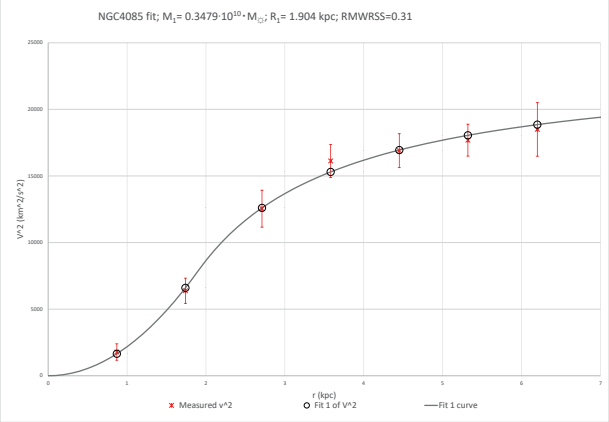

NGC4085

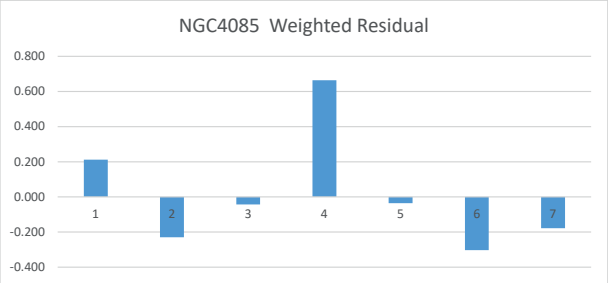

NGC4085 WR; RMWRSS = 0.31

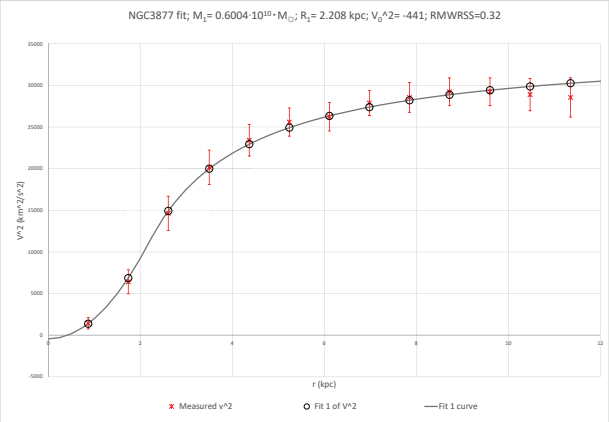

NGC3877

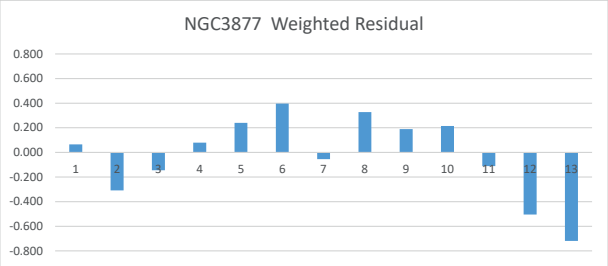

NGC3877 WR; RMWRSS = 0.32

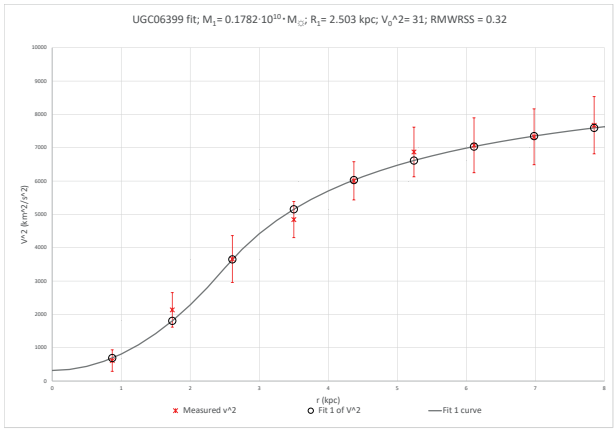

UGC06399

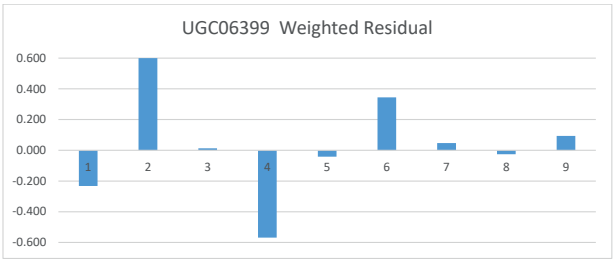

UGC06399 WR; RMWRSS = 0.32

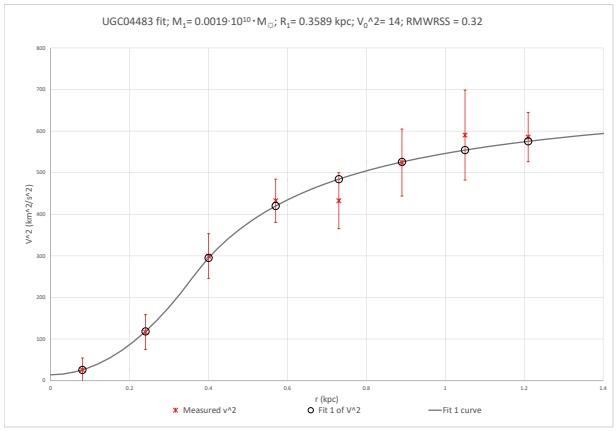

UGC04483

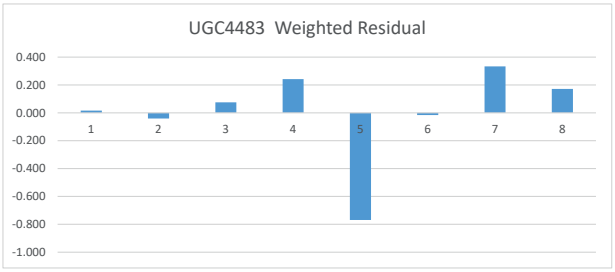

UGC04483 WR; RMWRSS = 0.32

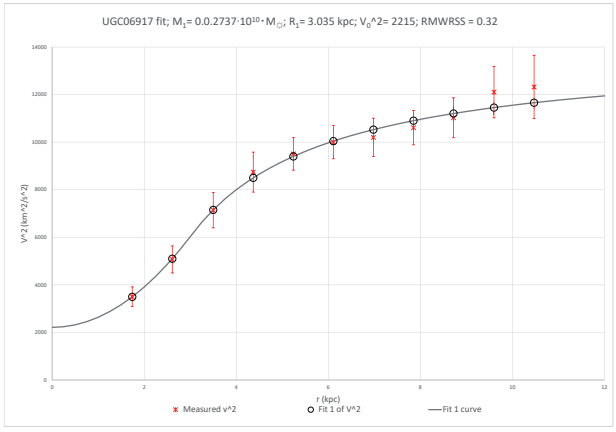

UGC06917

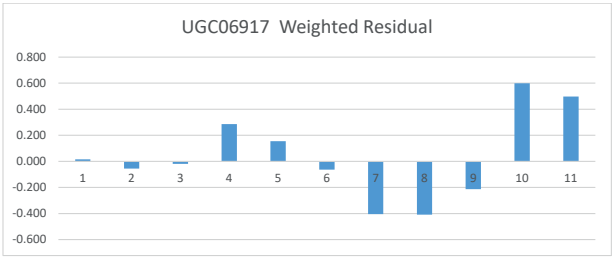

UGC06917 WR; RMWRSS = 0.32

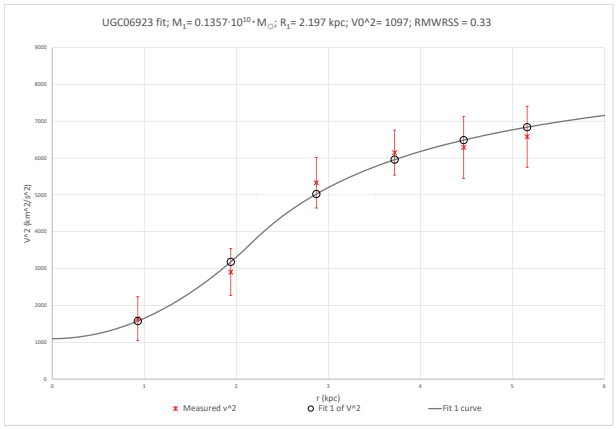

UGC06923

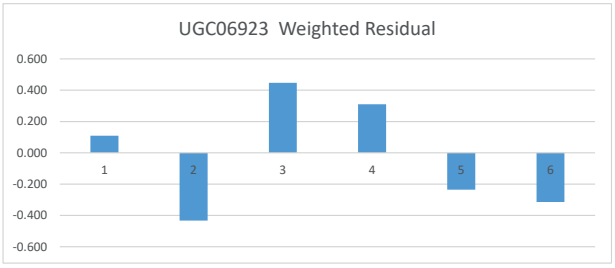

UGC06923 WR; RMWRSS = 0.33

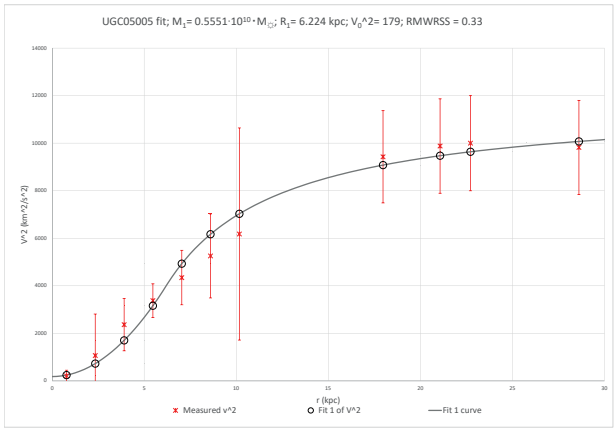

UGC05005

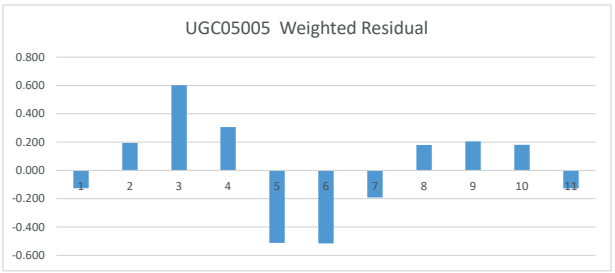

UGC05005 WR; RMWRSS = 0.33

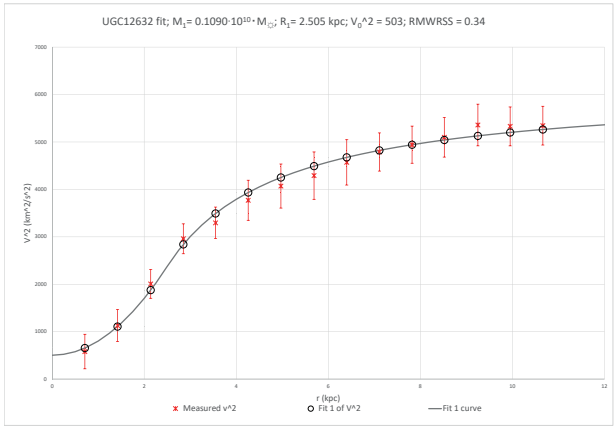

UGC12632

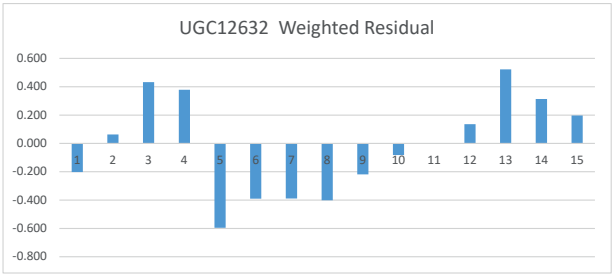

UGC12632 WR; RMWRSS = 0.34

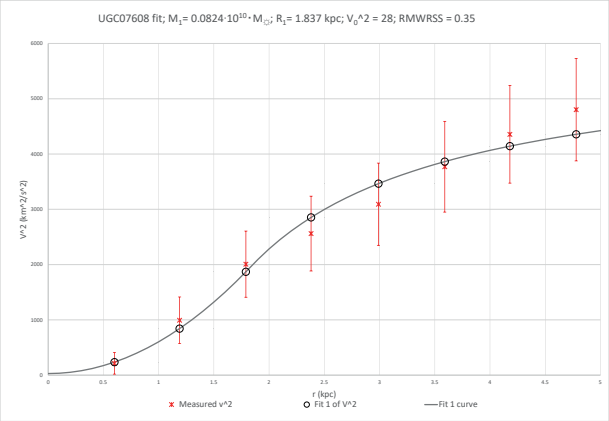

UGC07608

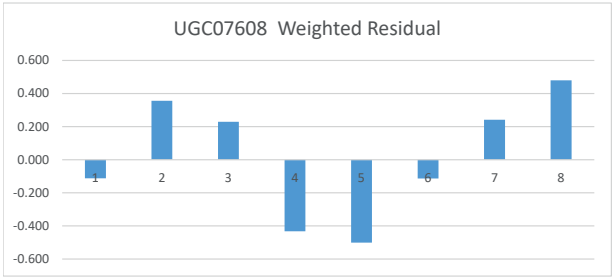

UGC07608 WR; RMWRSS = 0.35

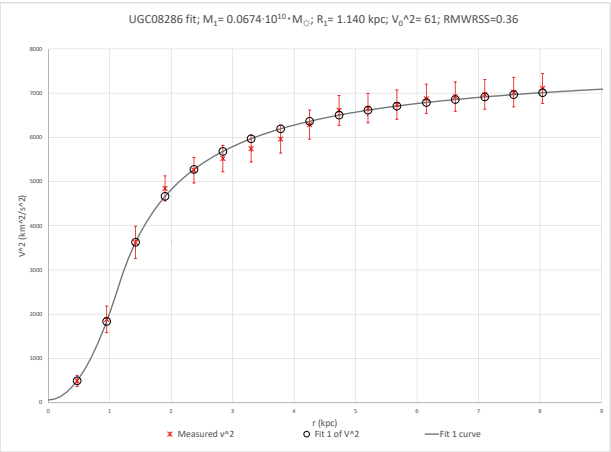

UGC08286

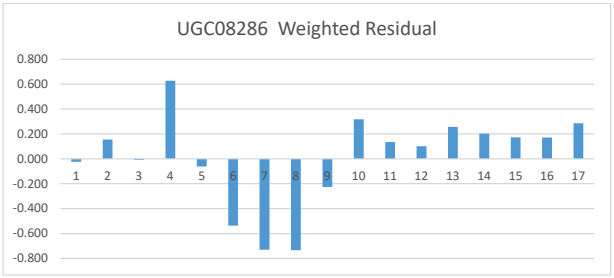

UGC08286 WR; RMWRSS = 0.36

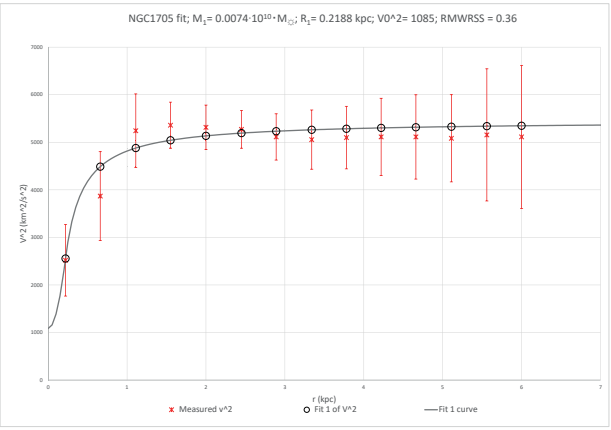

NGC1705

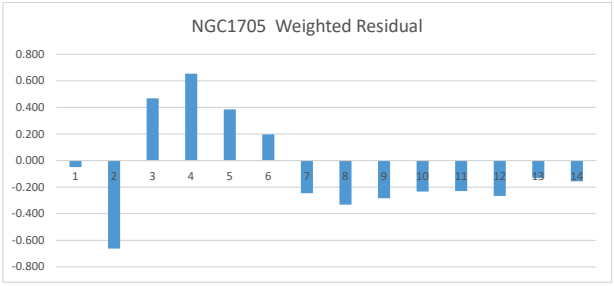

NGC1705 WR; RMWRSS = 0.36

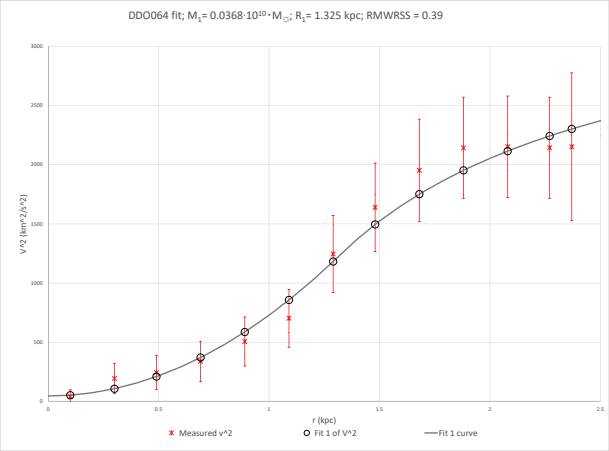

DDO064

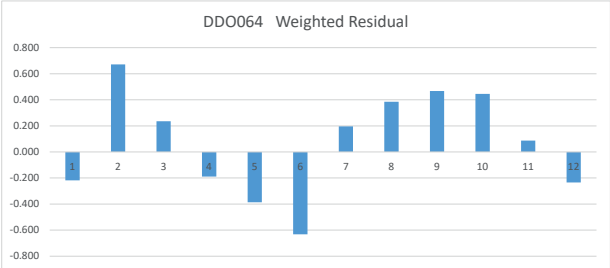

DDO064 WR; RMWRSS = 0.39

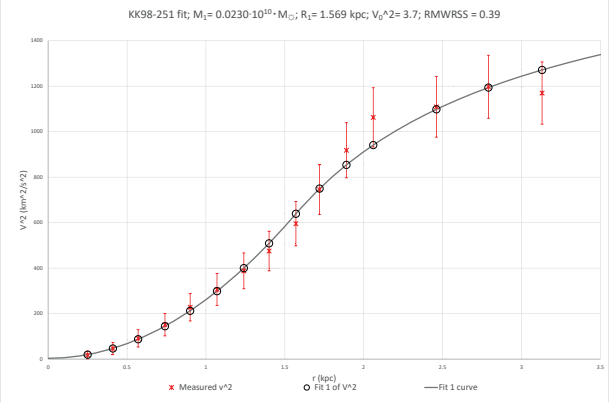

KK98-251

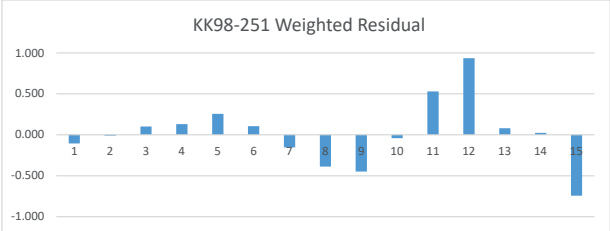

KK98-251 WR; RMWRSS = 0.39

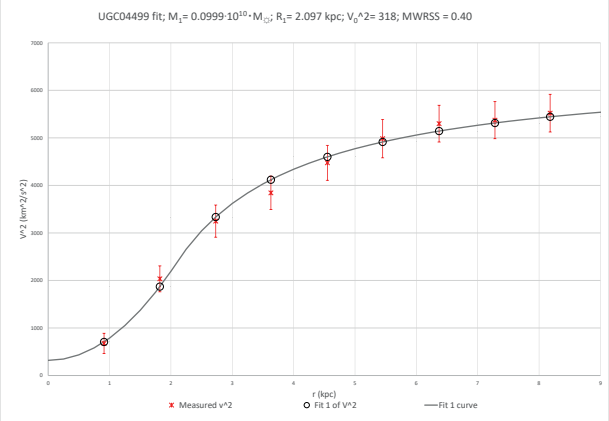

UGC04499

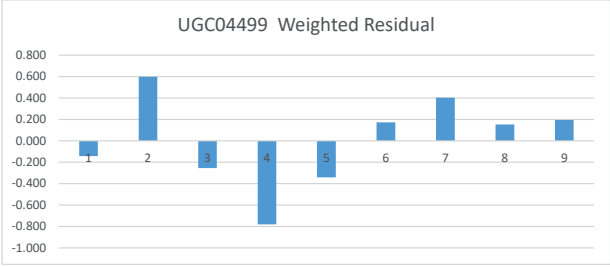

UGC04499 WR; RMWRSS = 0.40

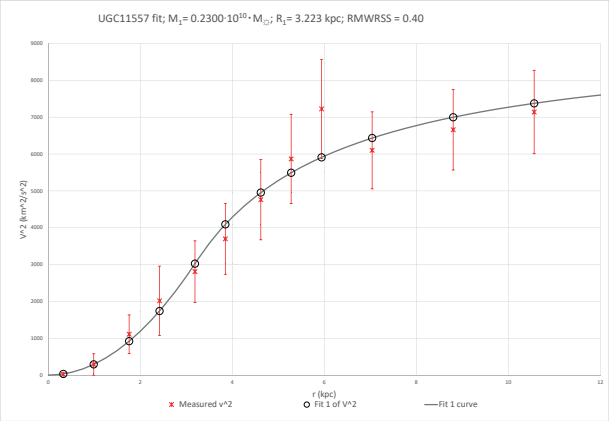

UGC11557

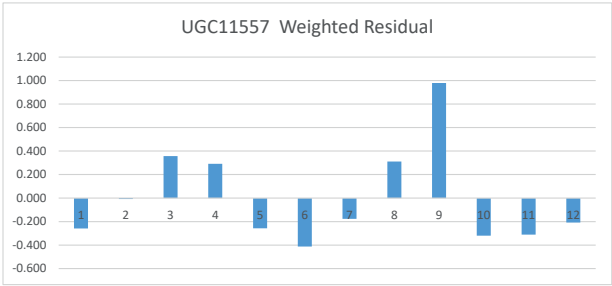

UGC11557 WR; RMWRSS = 0.40

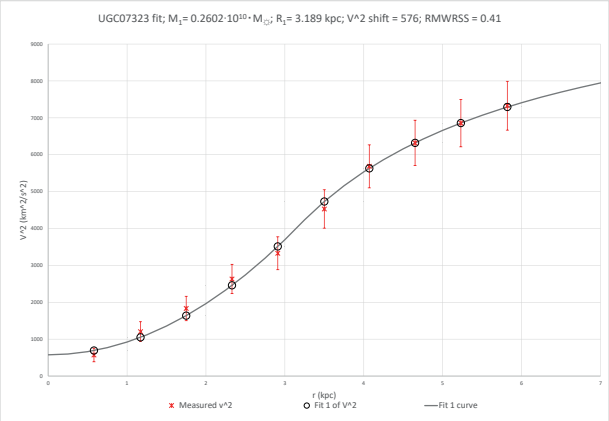

UGC07323

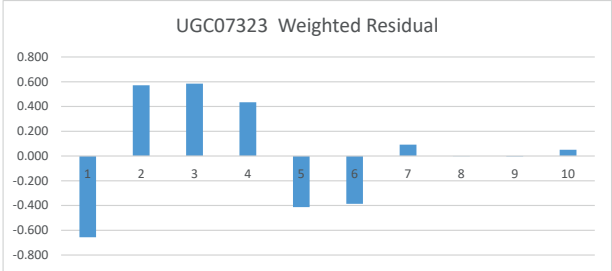

UGC07323 WR; RMWRSS = 0.41

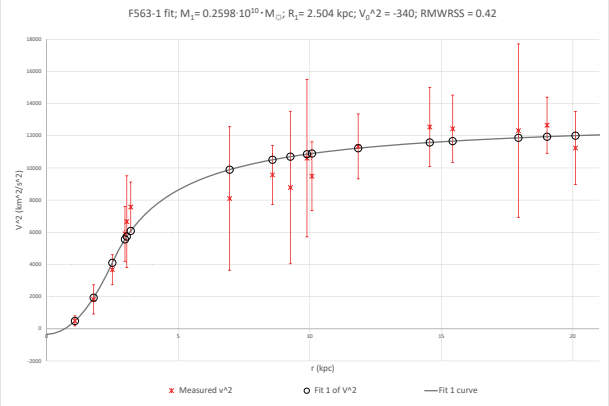

F563-1

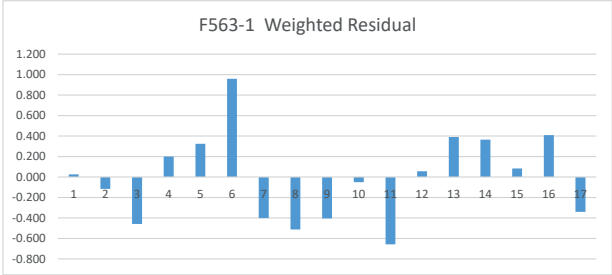

F563-1 WR; RMWRSS = 0.42

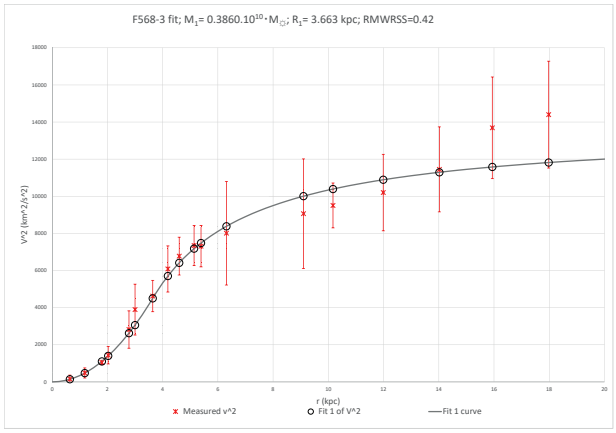

F568-3

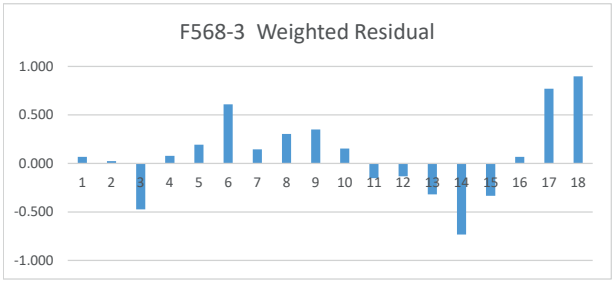

F568-3 WR; RMWRSS = 0.42

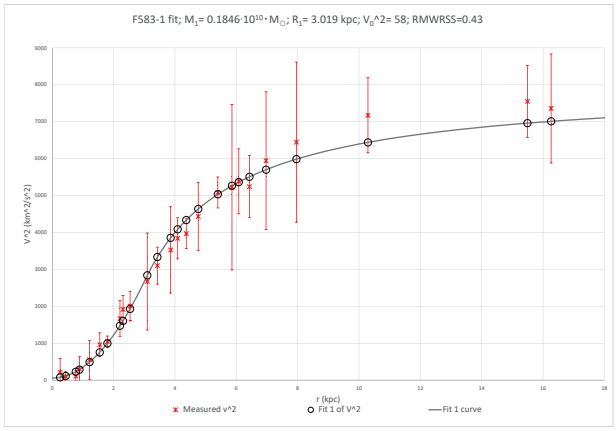

F583-1

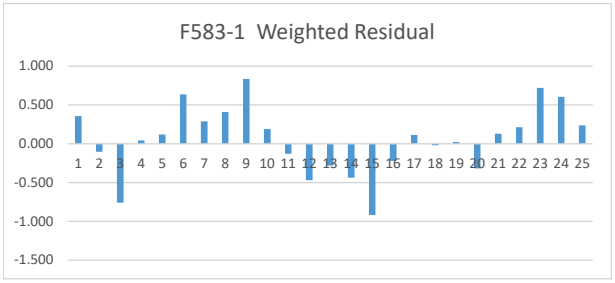

F583-1 WR; RMWRSS = 0.43

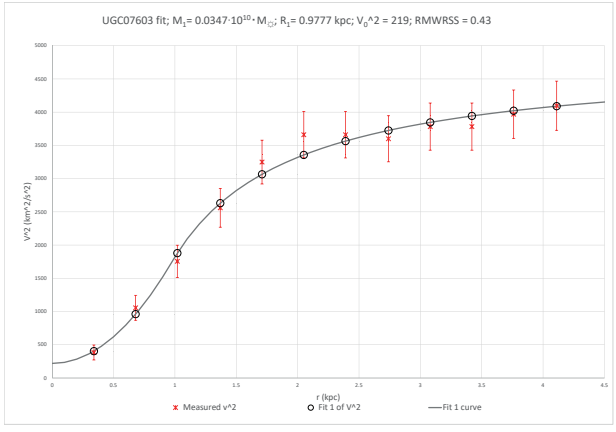

UGC07603

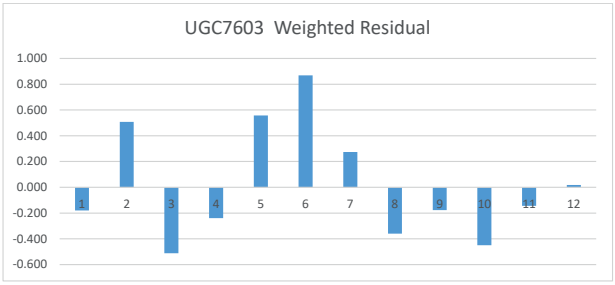

UGC07603 WR; RMWRSS = 0.43

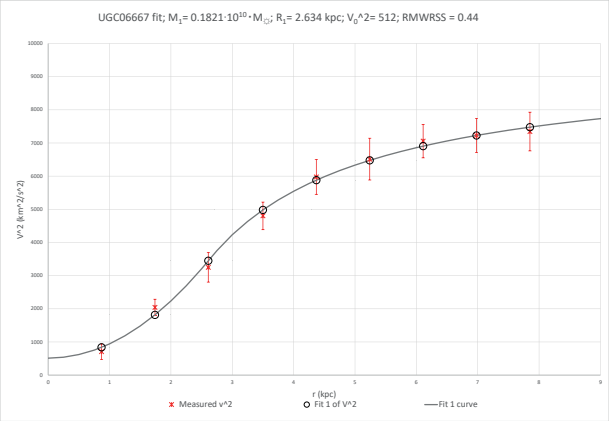

UGC06667

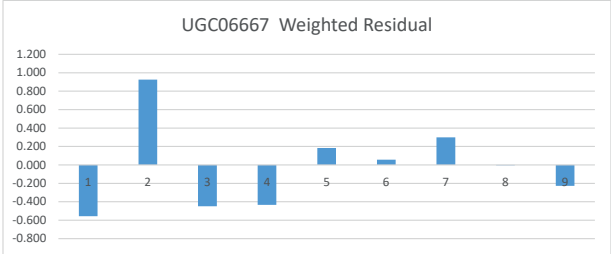

UGC06667 WR; RMWRSS = 0.44

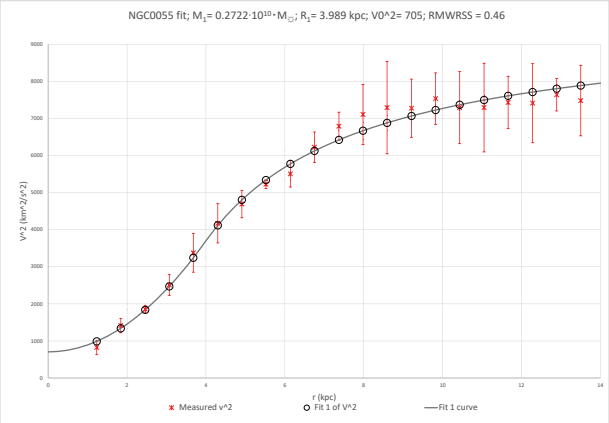

NGC0055

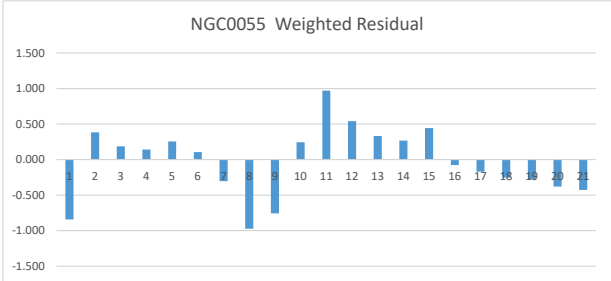

NGC0055 WR; RMWRSS = 0.46

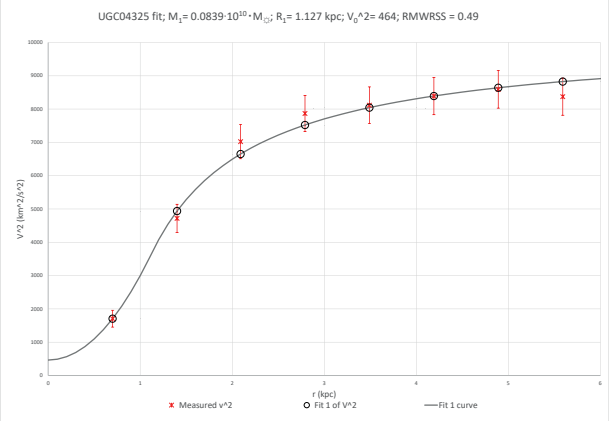

UGC04325

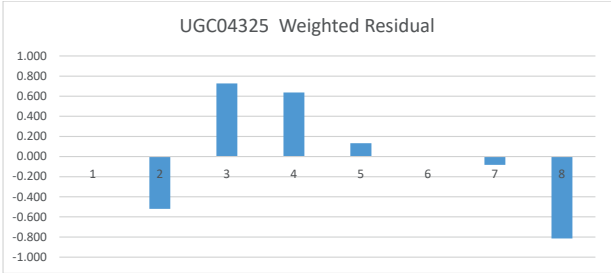

UGC04325 WR; RMWRSS = 0.46

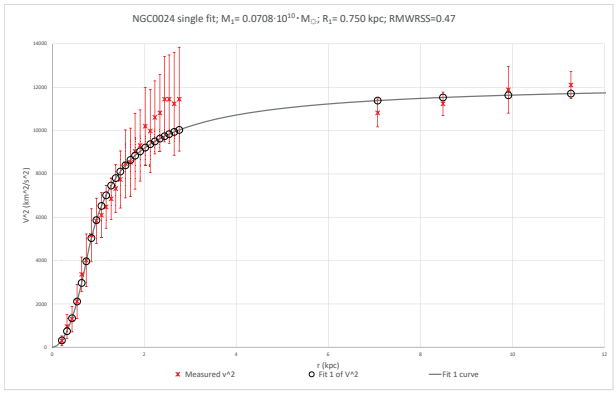

NGC0024

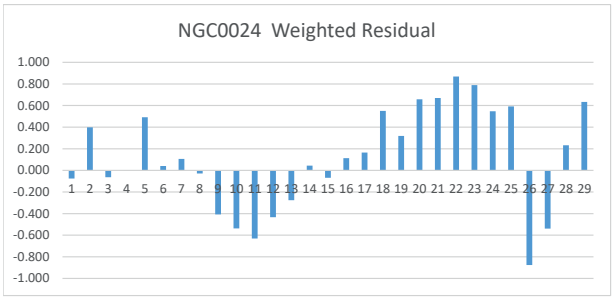

NGC0024 WR; RMWRSS = 0.47

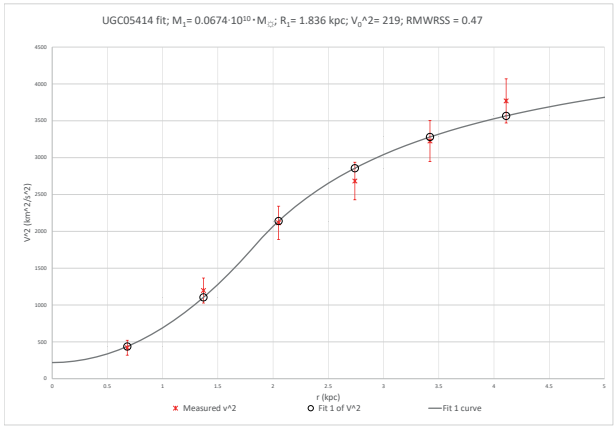

UGC05414

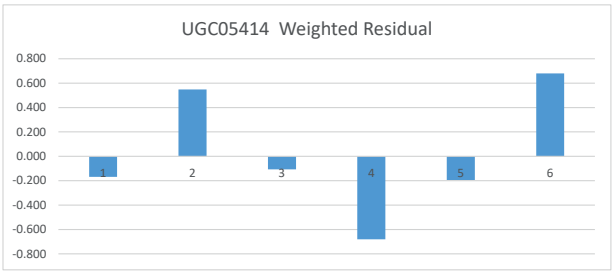

UGC05414 WR; RMWRSS = 0.47

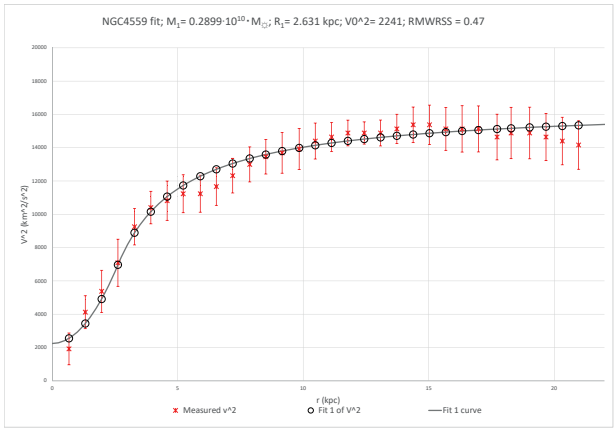

NGC4559

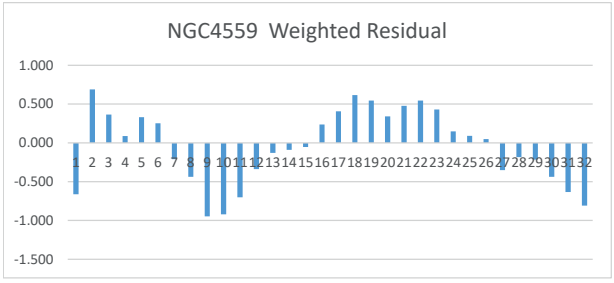

NGC4559 WR; RMWRSS = 0.47

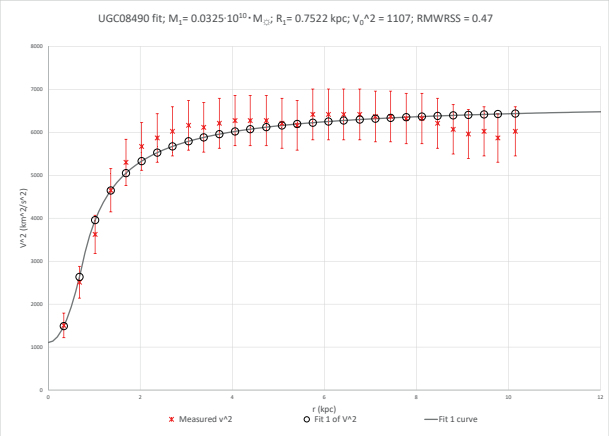

UGC08490

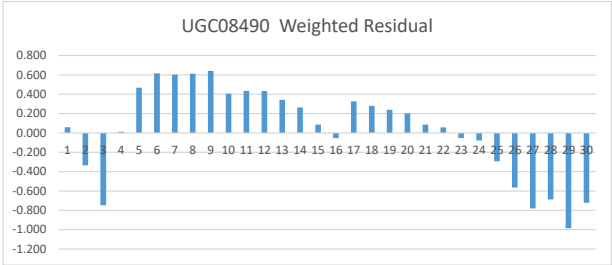

UGC08490 WR; RMWRSS = 0.47

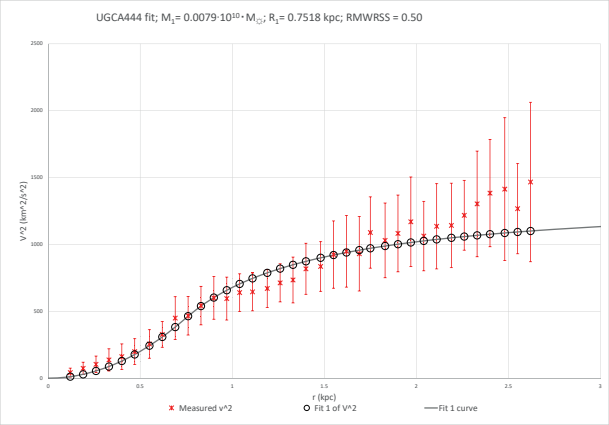

UGCA444

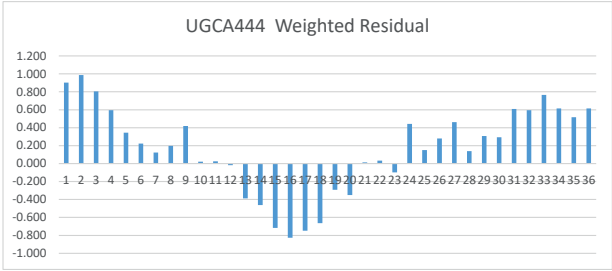

UGCA444 WR; RMWRSS = 0.50

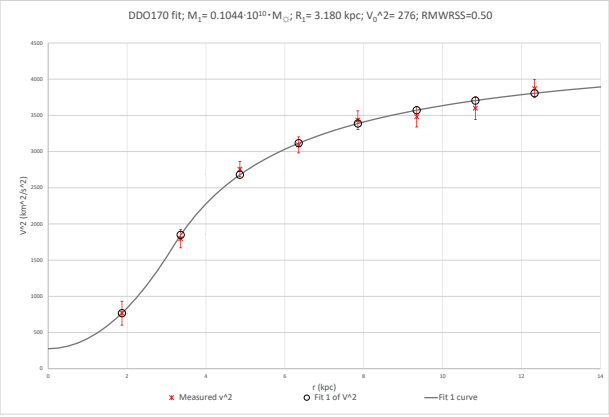

DDO170

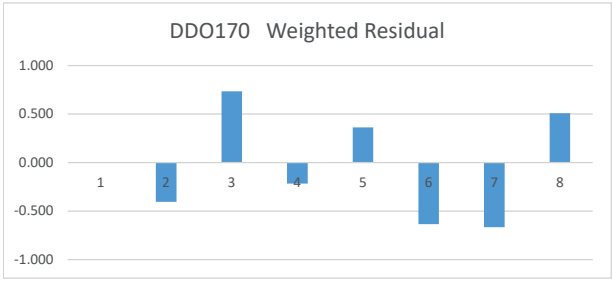

DDO170 WR; RMWRSS = 0.50

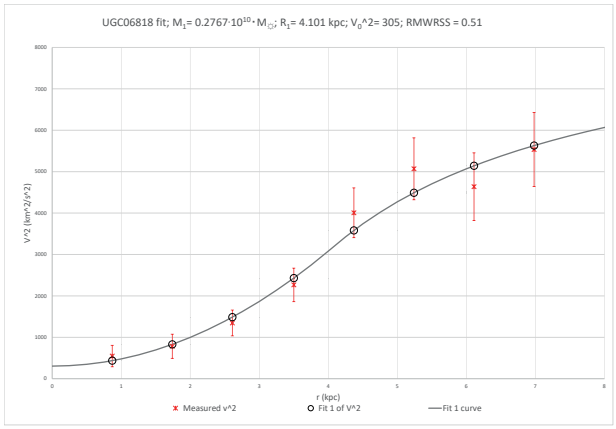

UGC06818

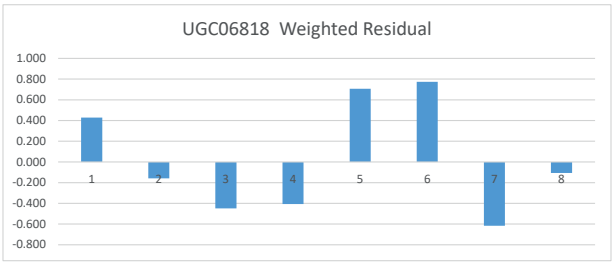

UGC06818 WR; RMWRSS = 0.51

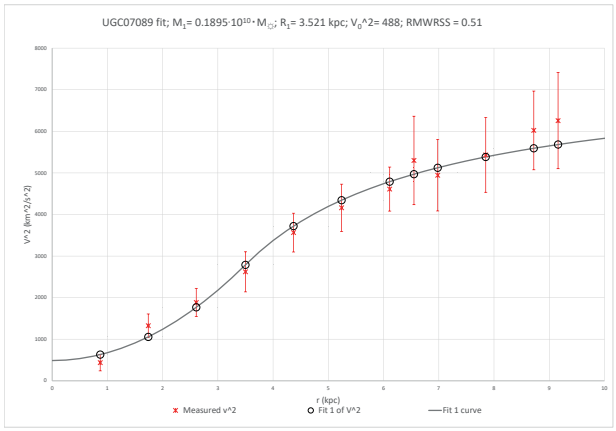

UGC07089

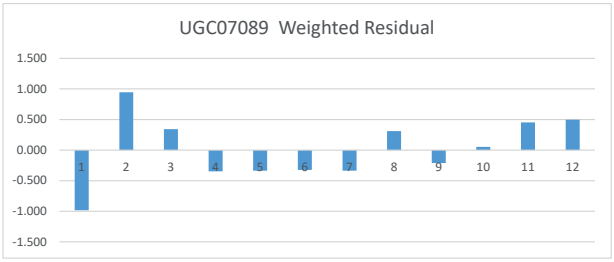

UGC07089 WR; RMWRSS = 0.51

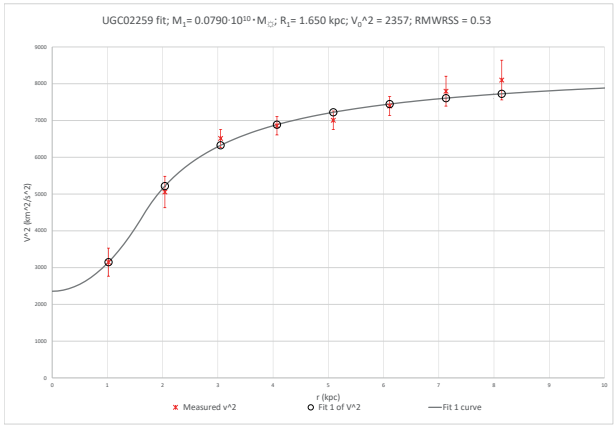

UGC02259

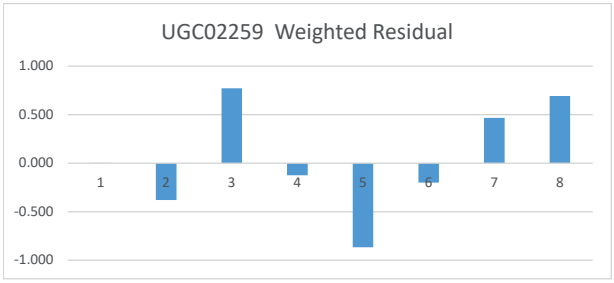

UGC02259 WR; RMWRSS = 0.53

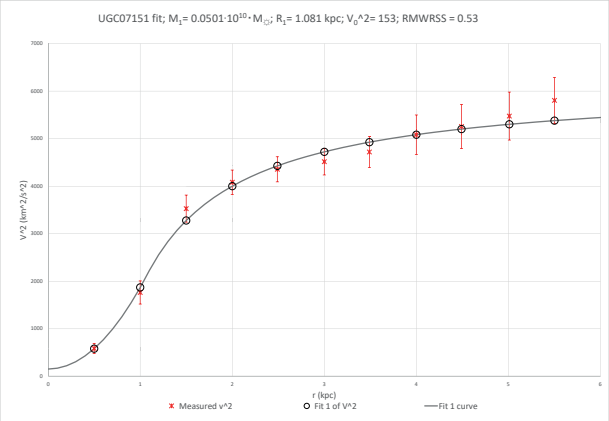

UGC07151

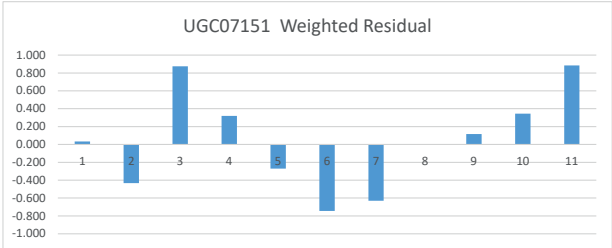

UGC07151 WR; RMWRSS = 0.53

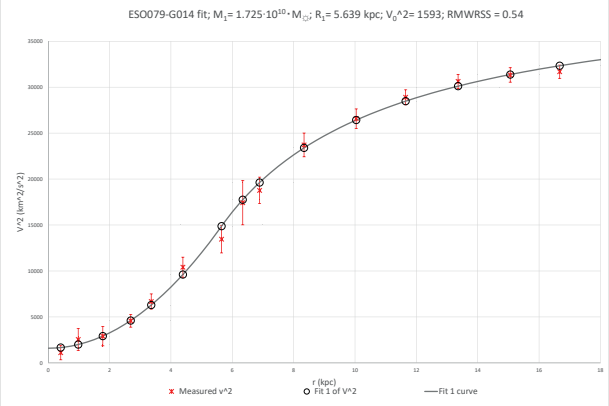

ESO079-G014

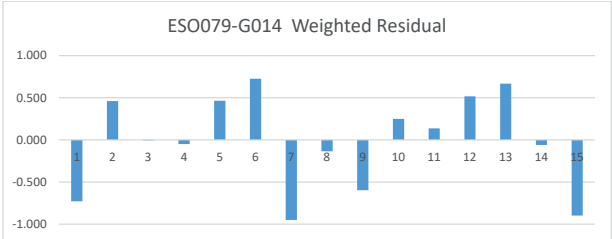

ESO079-G014 WR; RMWRSS = 0.54

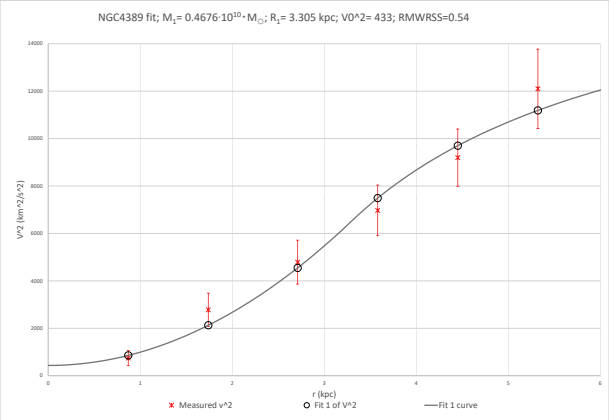

NGC4389

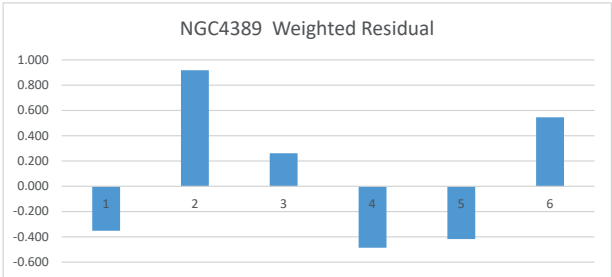

NGC4389 WR; RMWRSS = 0.54

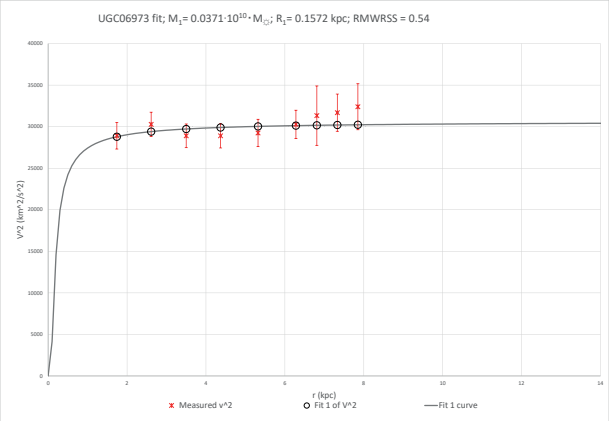

UGC06973

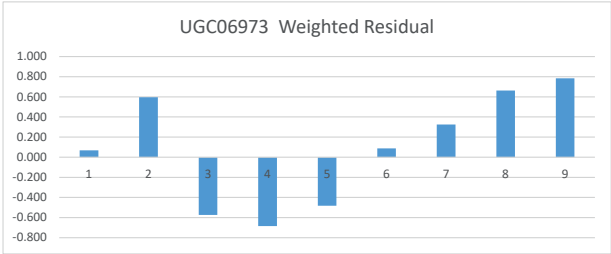

UGC06973 WR; RMWRSS = 0.54

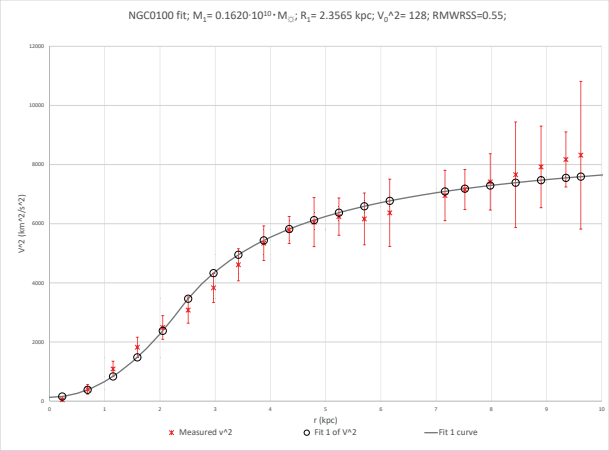

NGC0100

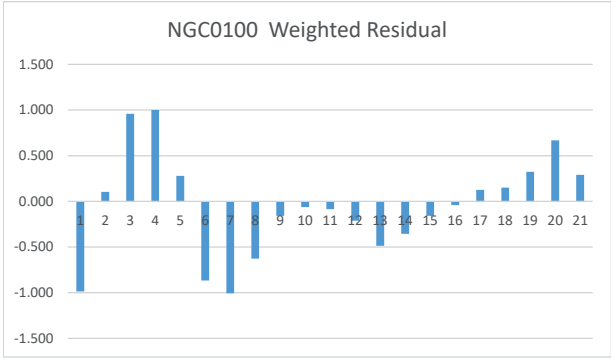

NGC0100 WR; RMWRSS = 0.55

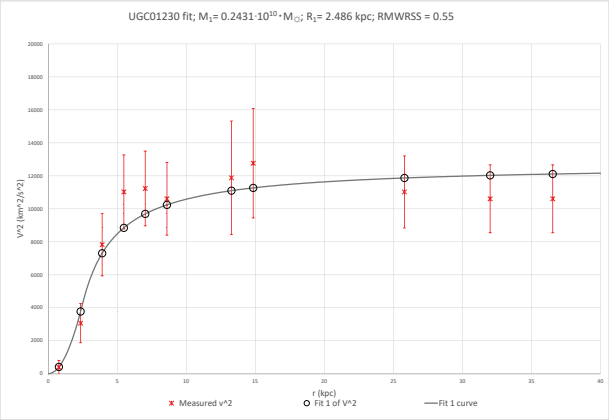

UGC01230

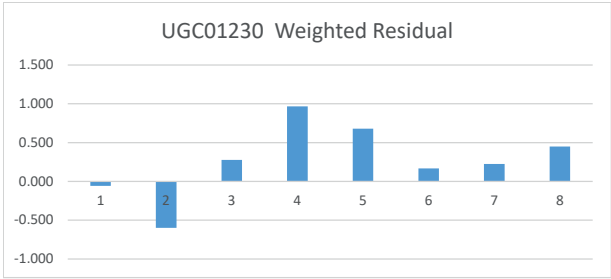

UGC01230 WR; RMWRSS = 0.55

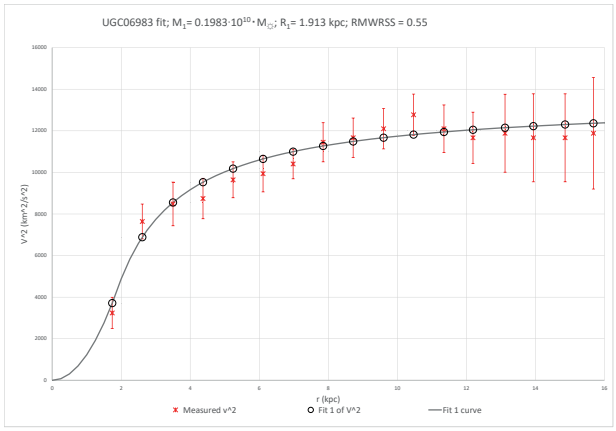

UGC06983

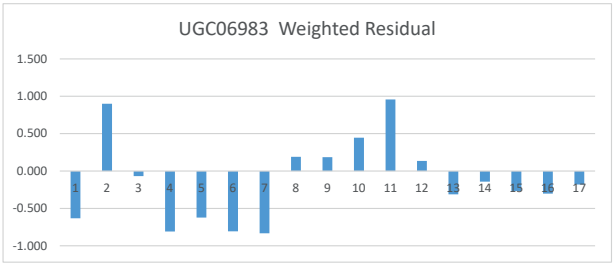

UGC06983 WR; RMWRSS = 0.55

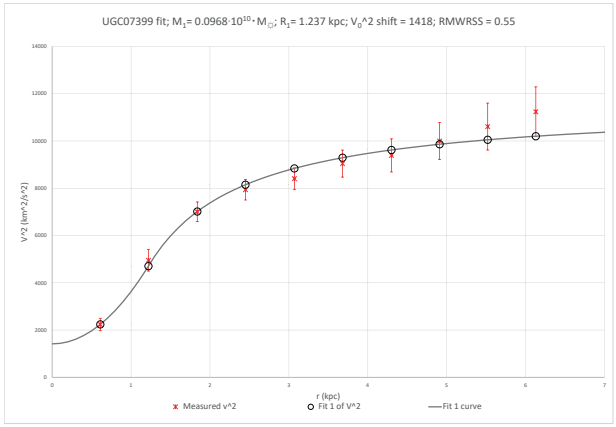

UGC07399

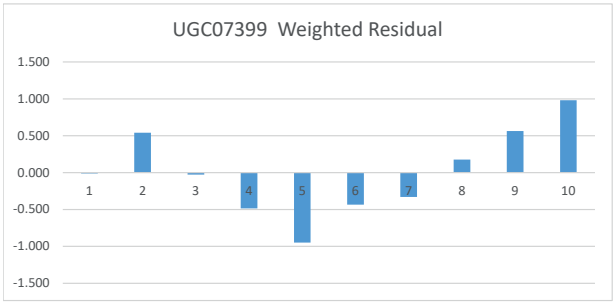

UGC07399 WR; RMWRSS = 0.55

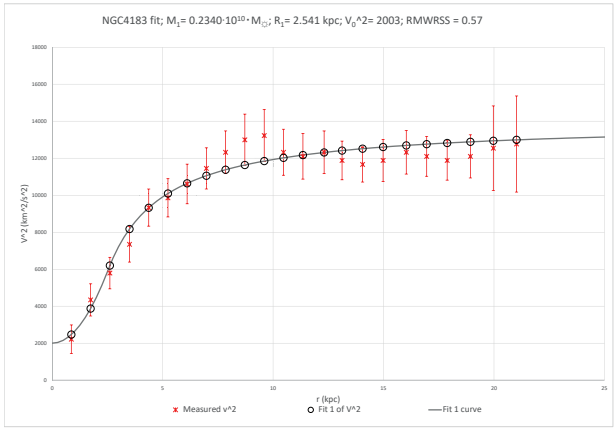

NGC4183

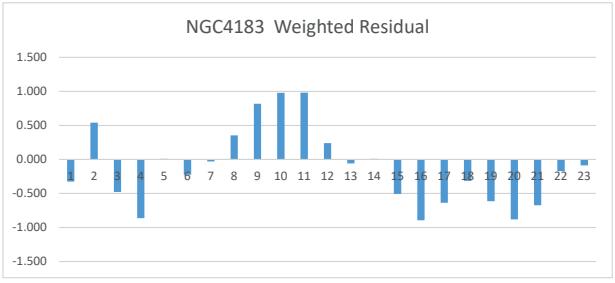

NGC4183 WR; RMWRSS = 0.57

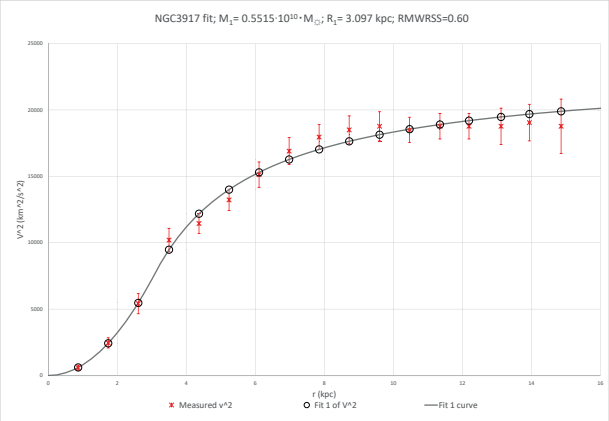

NGC3917

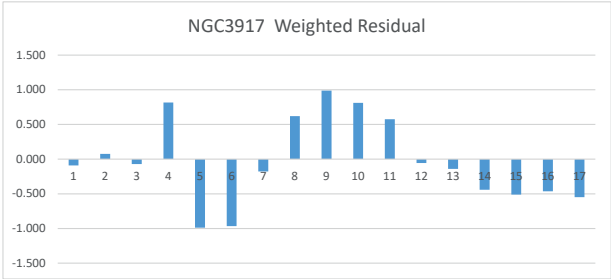

NGC3917 WR; RMWRSS = 0.60

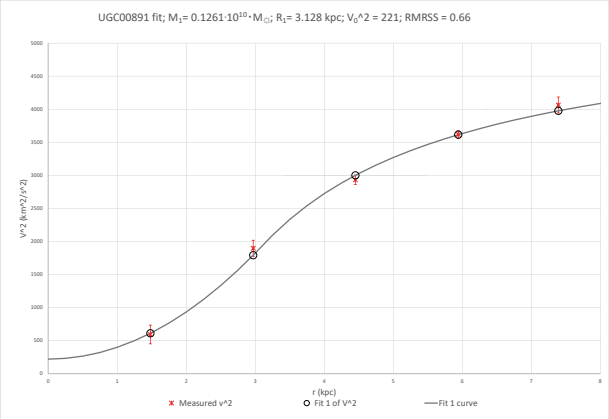

UGC00891

UGC00891 WR; RMWRSS = 0.66

B. THE ALMOST SINGLE FIT SELECTION.

First there are the one of galaxies. With galaxies NGC2998, UGC00731, UGC07524 and UGCA442, one measurement has been ignored in fitting the curve and calculating the RMWRSS. Then there are the galaxies that have more measurements with the error bars outside the fit, but that still have a RMWRSS below 1 and reasonably follow the pattern of the single Lagrangian curve. At the end, the galaxies with a RMWRSS above 1, but for which a multiple curve fit would be too arbitrary due to lack of sufficient measurements for the second fit.

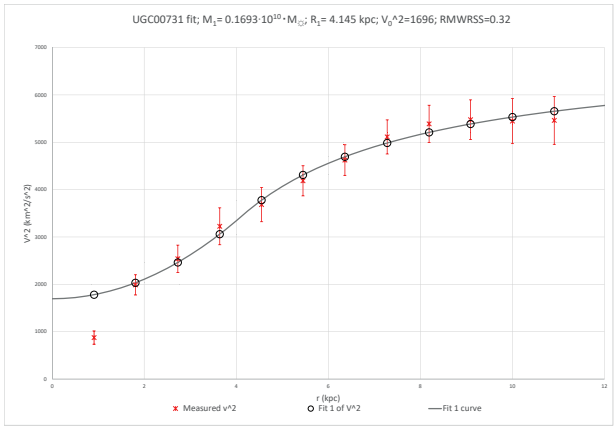

UGC00731

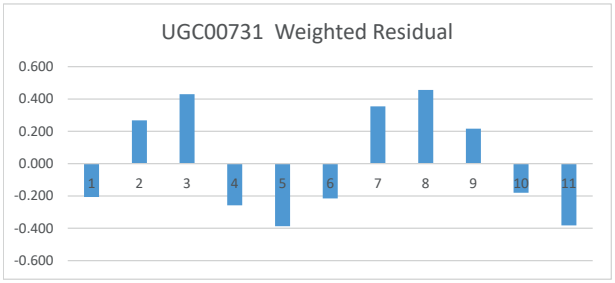

UGC00731-WR; RMWRSS = 0.32

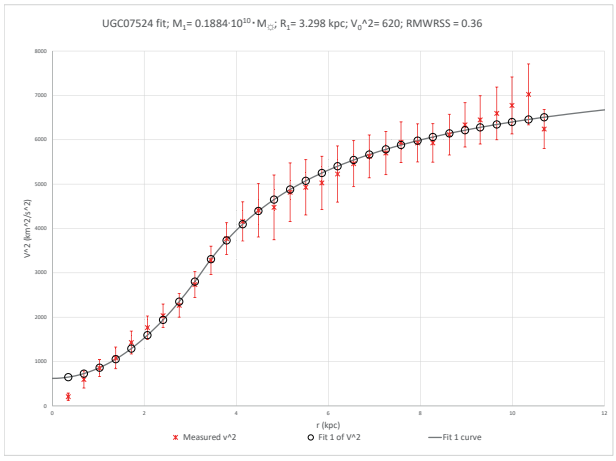

UGC07524

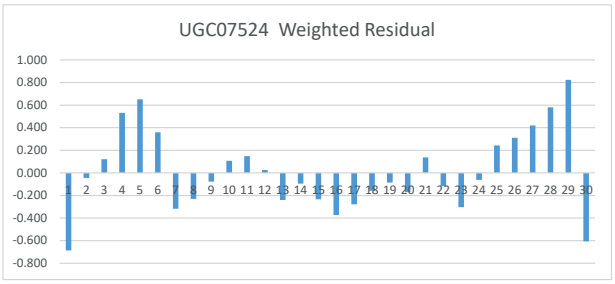

UGC07524-WR; RMWRSS = 0.36

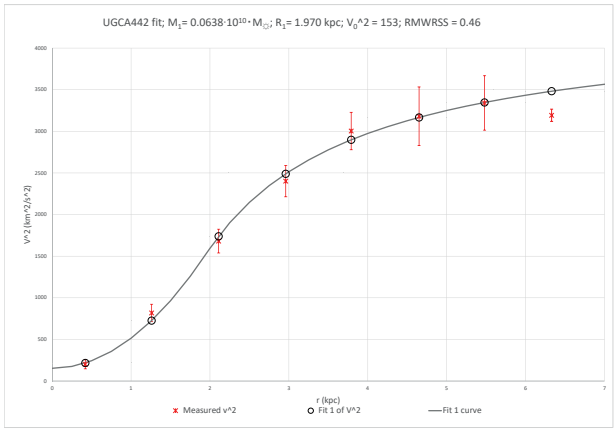

UGCA442

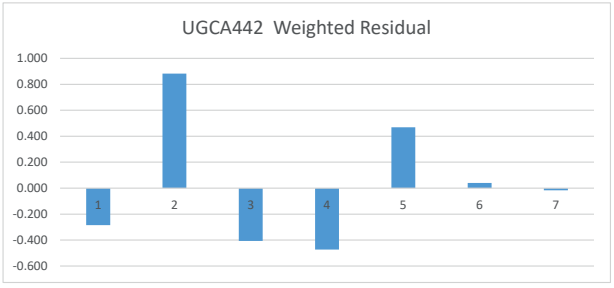

UGCA442-WR; RMWRSS = 0.46

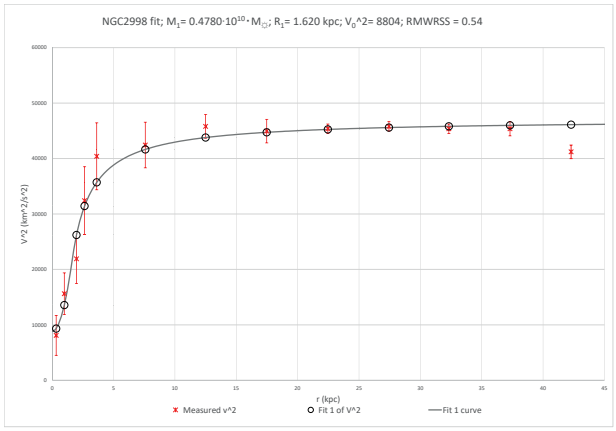

NGC2998

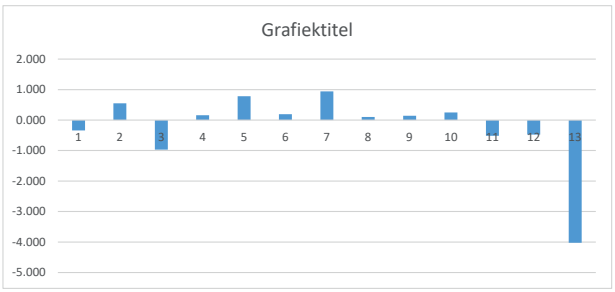

NGC2998-WR; RMWRSS = 0.54

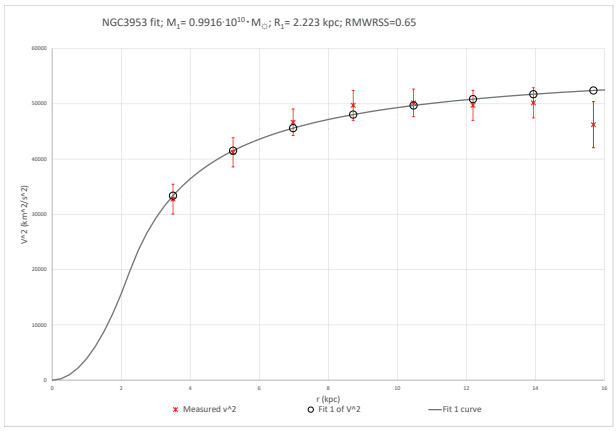

NGC3953

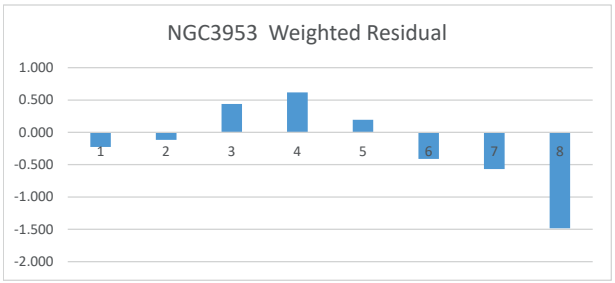

NGC3953-WR; RMWRSS = 0.65

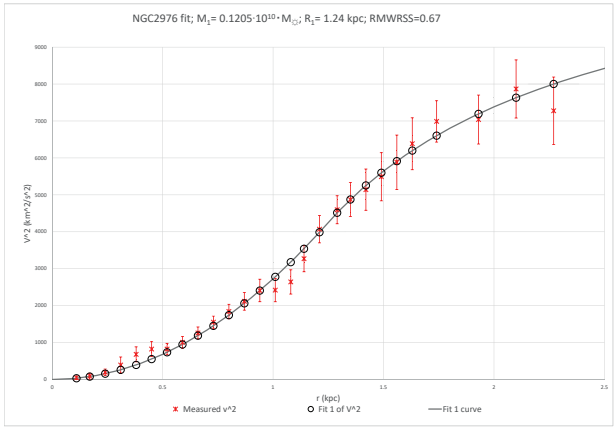

NGC2976

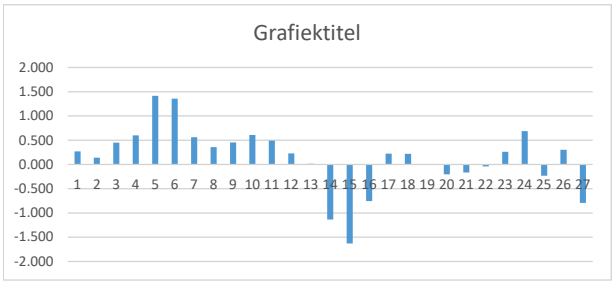

NGC2976-WR; RMWRSS = 0.67

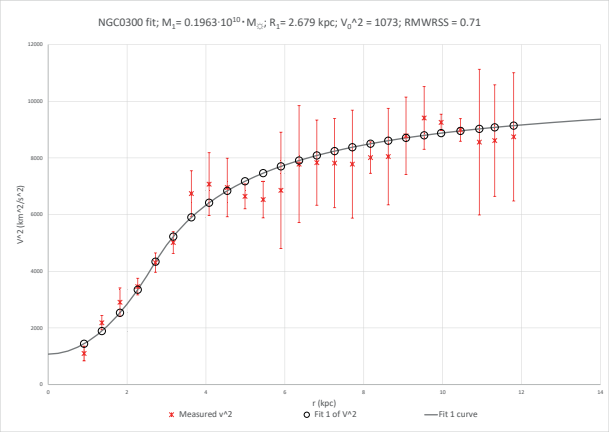

NGC0300

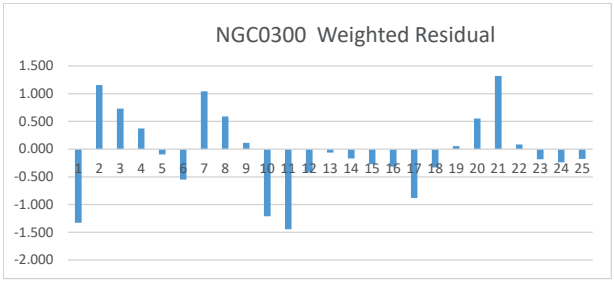

NGC0300-WR; RMWRSS = 0.71

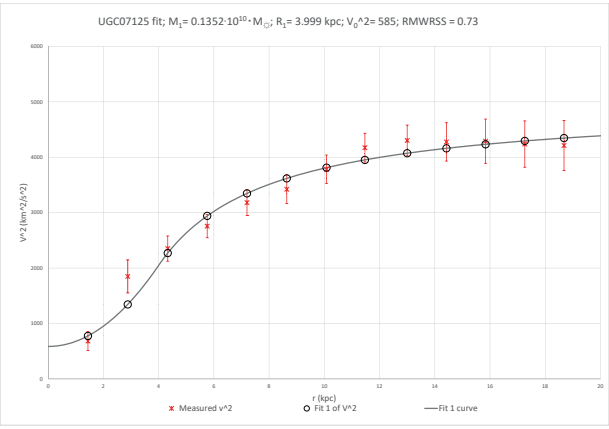

UGC07125

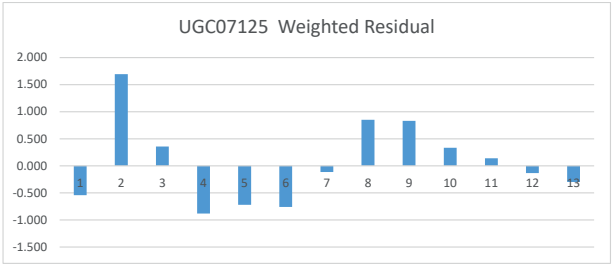

UGC07125-WR; RMWRSS = 0.73

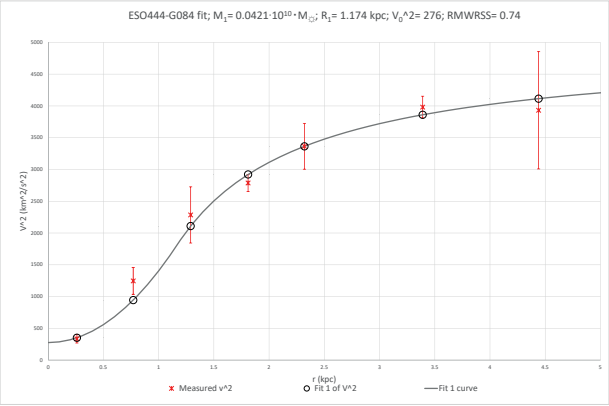

ESO444-G084

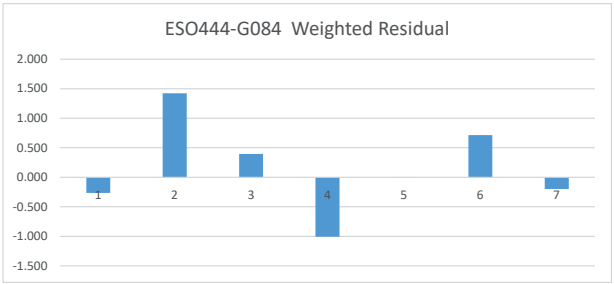

ESO444-G084-WR; RMWRSS = 0.74

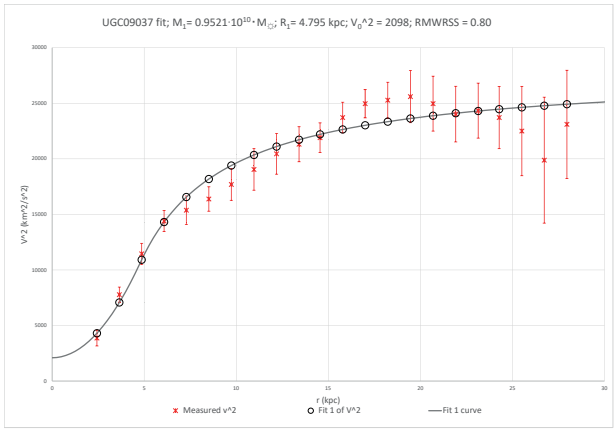

UGC09037

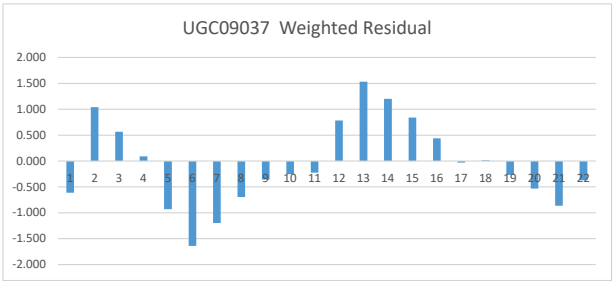

UGC09037-WR; RMWRSS = 0.80

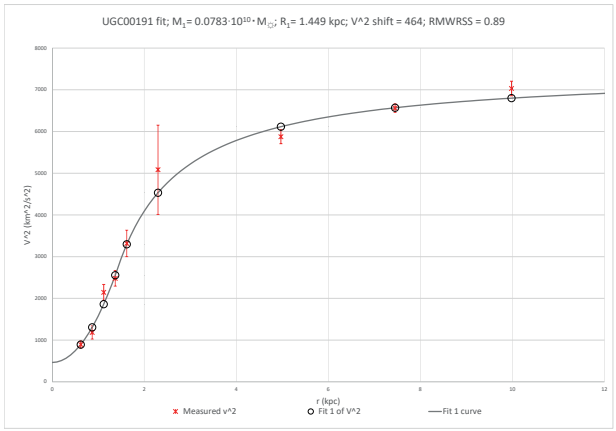

UGC00191

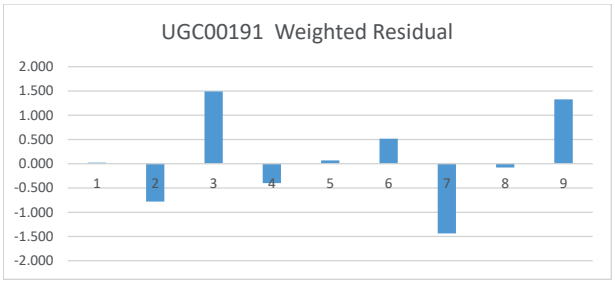

UGC00191-WR; RMWRSS = 0.89

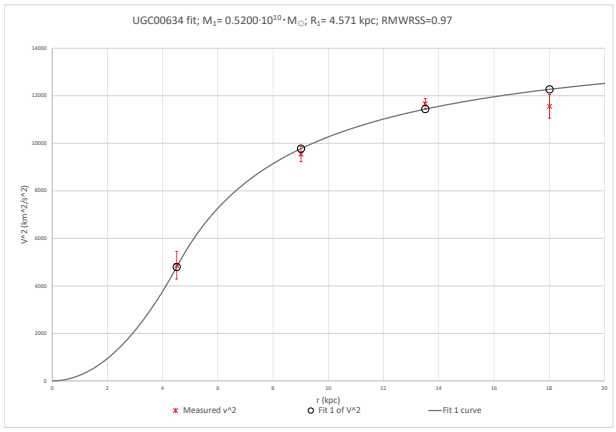

UGC00634

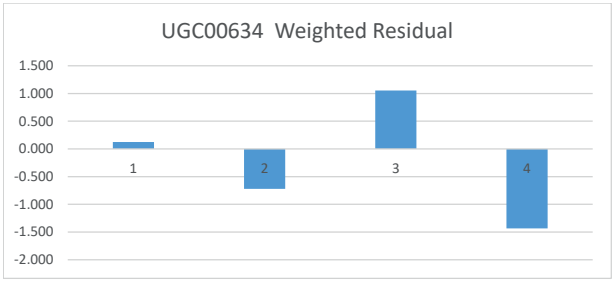

UGC00634-WR; RMWRSS = 0.97

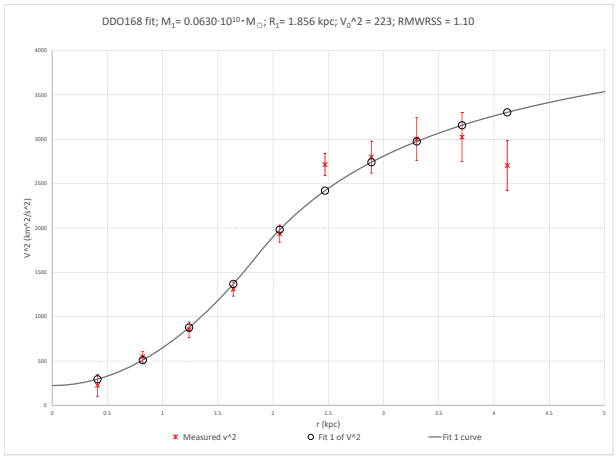

DDO168

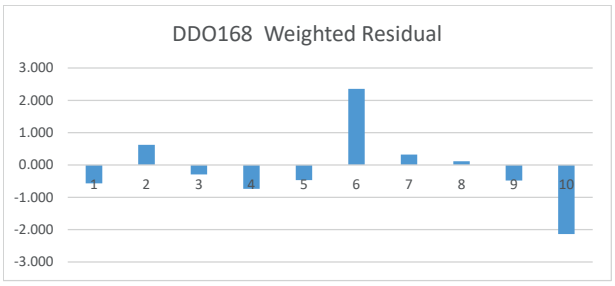

DDO168-WR; RMWRSS = 1.10

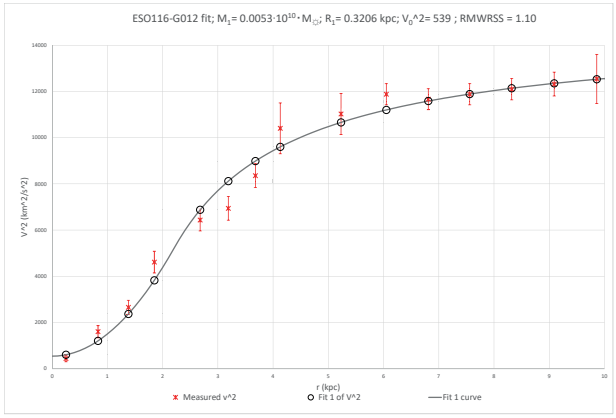

ESO116-G012

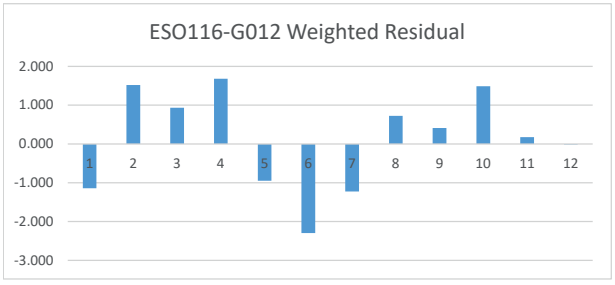

ESO116-G012-WR; RMWRSS = 1.10

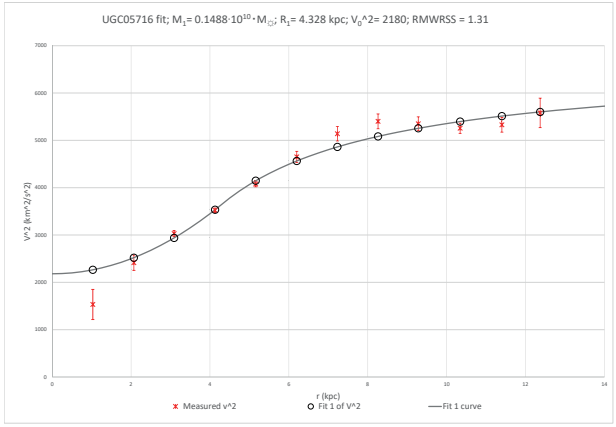

UGC05716

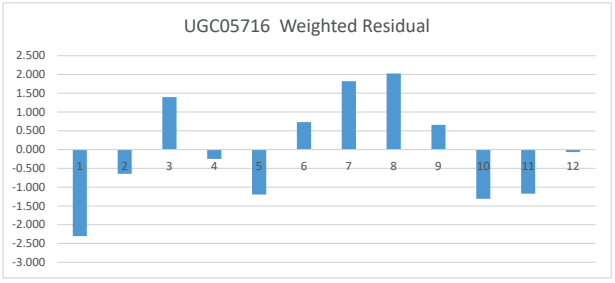

UGC05716-WR; RMWRSS = 1.31

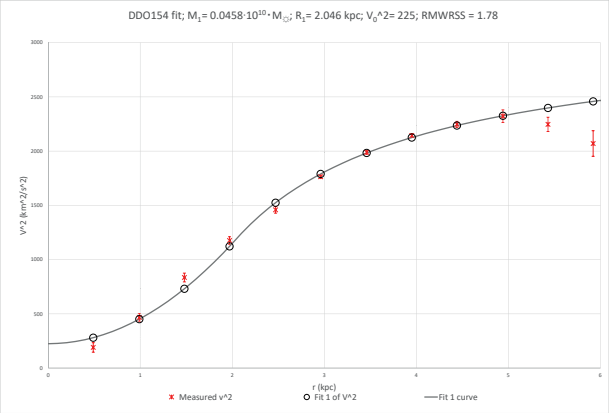

DDO154

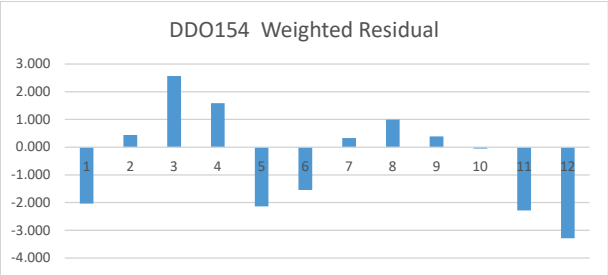

DDO154-WR; RMWRSS = 1.78

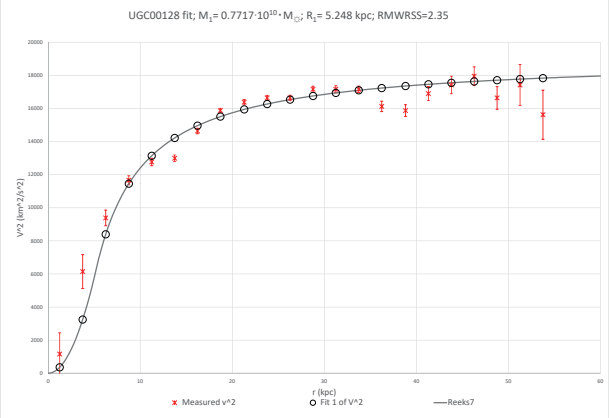

UGC00128

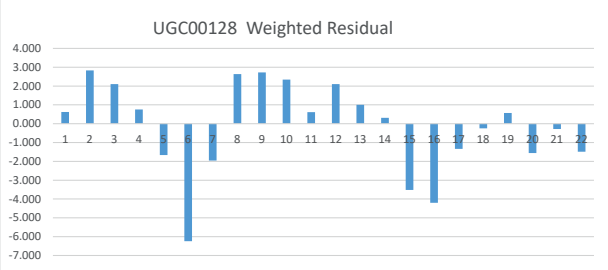

UGC00128-WR; RMWRSS = 2.35

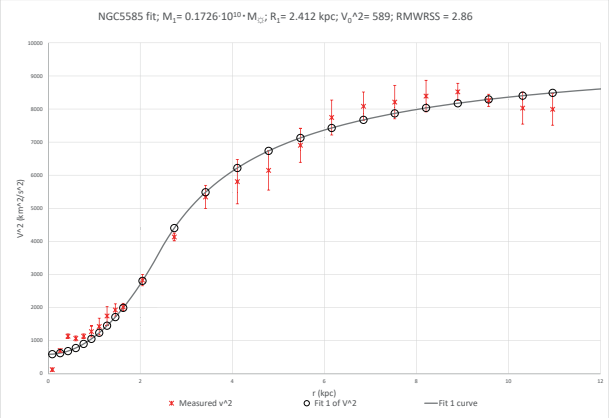

NGC5585

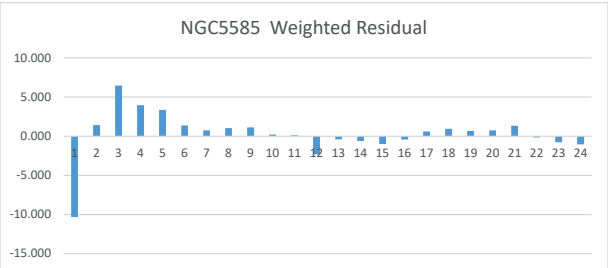

NGC5585-WR; RMWRSS = 2.86

C. ABRUPT LAGRANGIAN TRANSITION CROSSOVER DUAL FIT GALAXIES

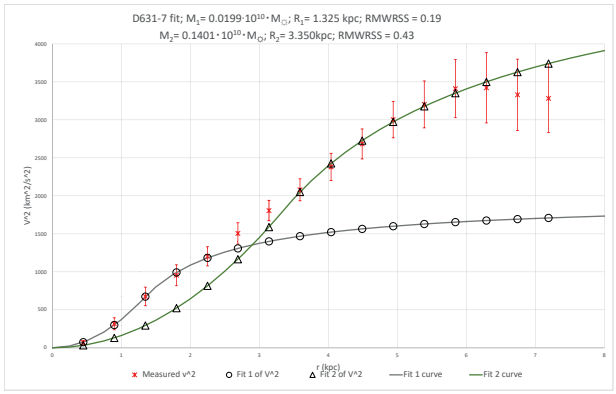

D631-7

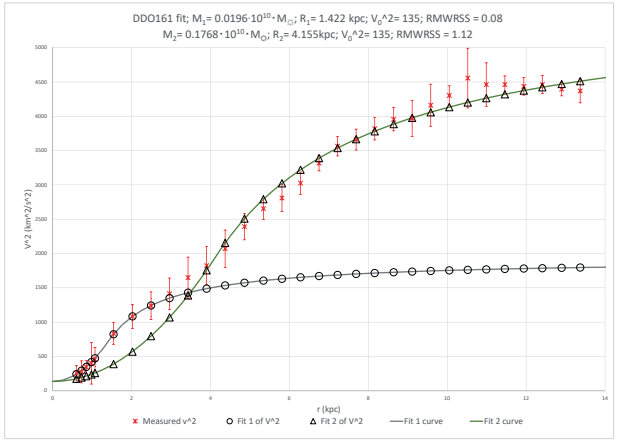

DDO161

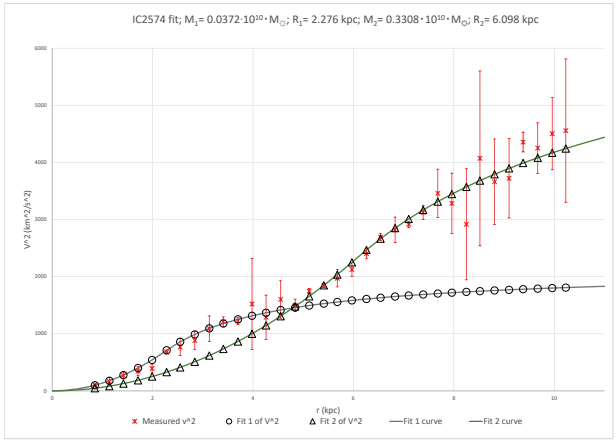

IC2574

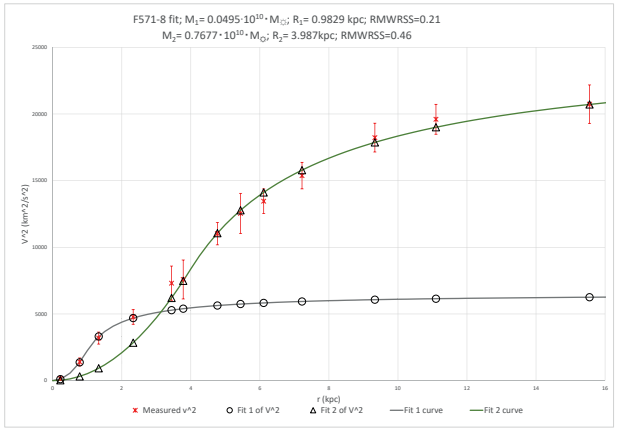

F571-8

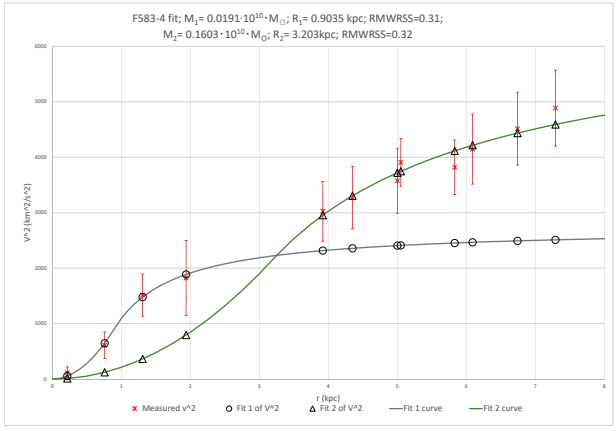

F583-4

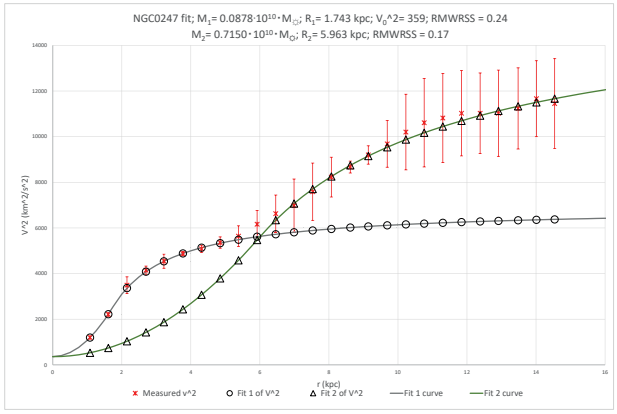

NGC0247

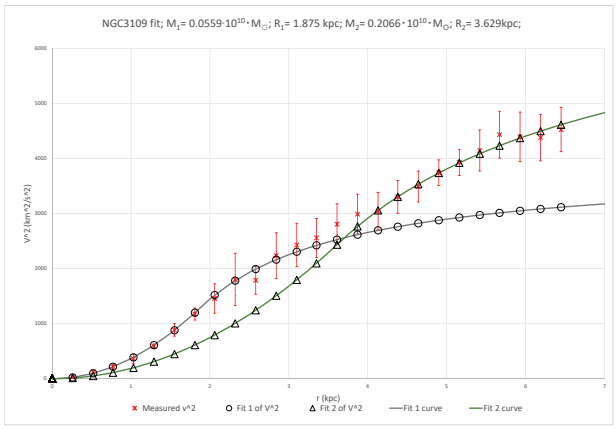

NGC3109

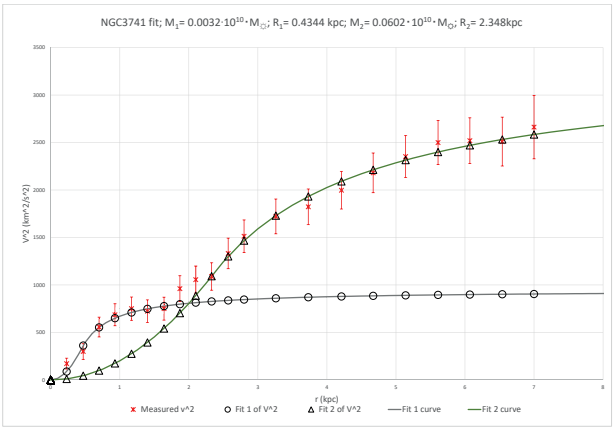

NGC3741

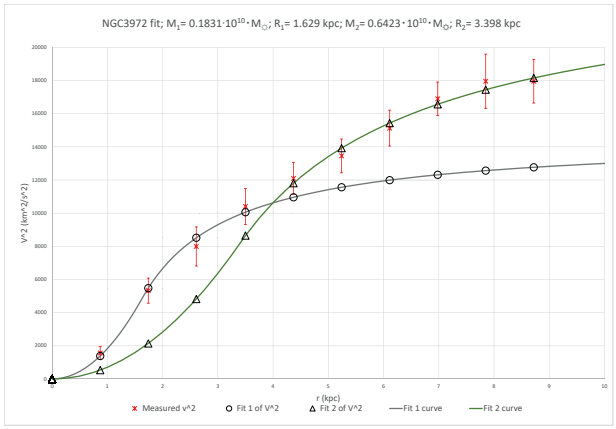

NGC3972

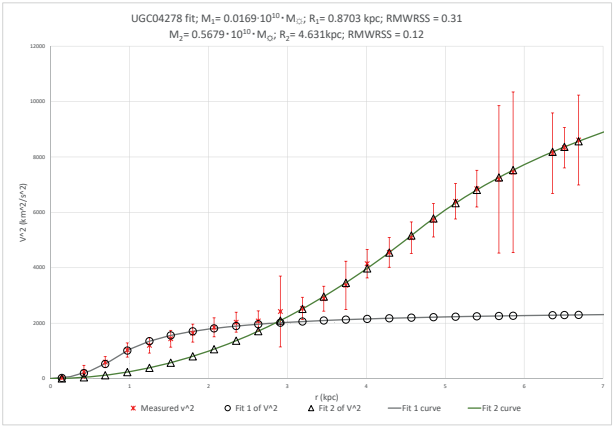

UGC04278

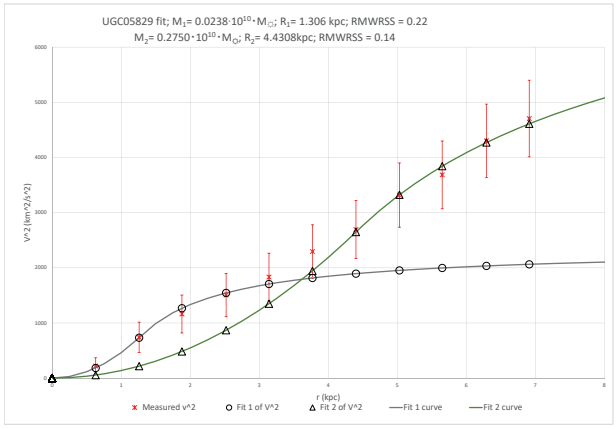

UGC05829

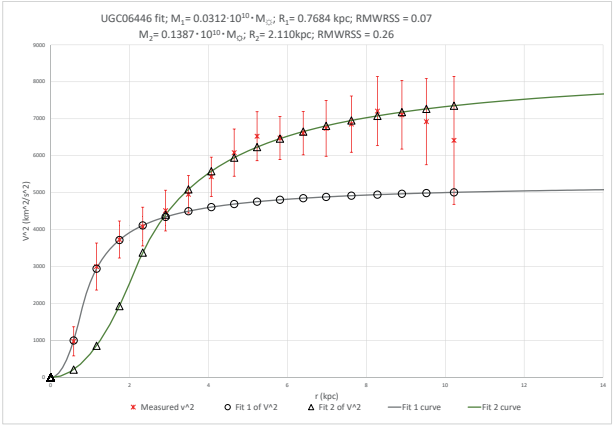

UGC06446

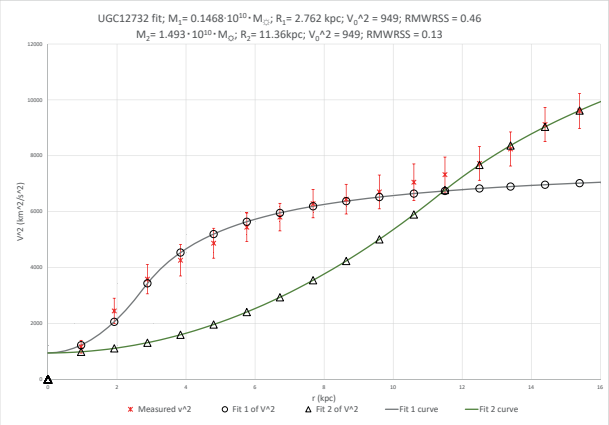
UGC12732 fit; M1= 0.1468·10^10·M☉; R1= 2.762 kpc; V0^2 = 949; RMWRSS = 0.46
M2= 1.493·10^10·M☉; R2= 11.36kpc; V0^2 = 949; RMWRSS = 0.13
V^2 (km^2/s^2)
r (kpc)
Measured v^2
Fit 1 of V^2
Fit 2 of V^2
Fit 1 curve
Fit 2 curve

UGC12732

D. RECEDING TO A FINAL ENERGY FIT GALAXIES

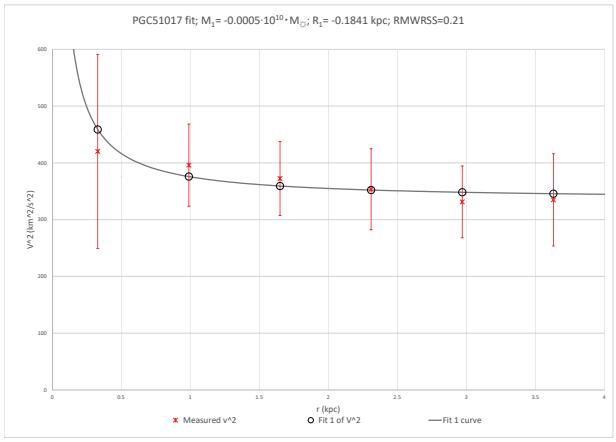

PGC51017

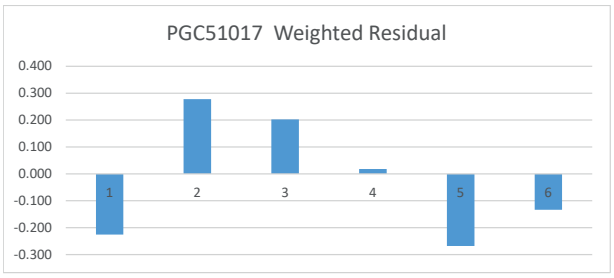

PGC51017 WR; RMWRSS = 0.21

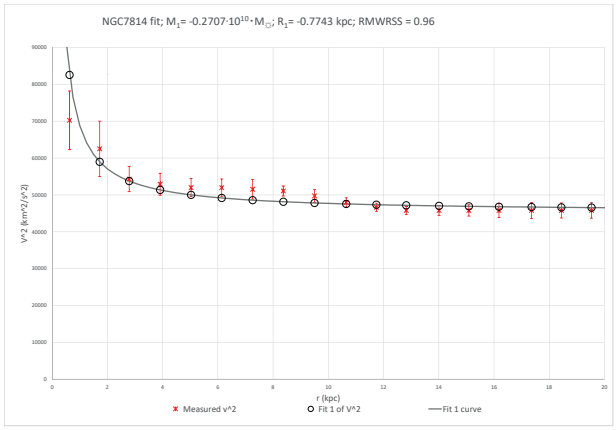

NGC7814

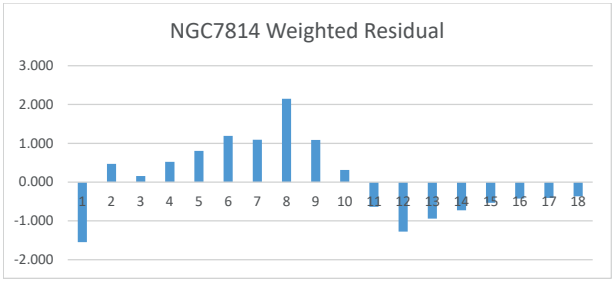

NGC7814 WR; RMWRSS = 0.96

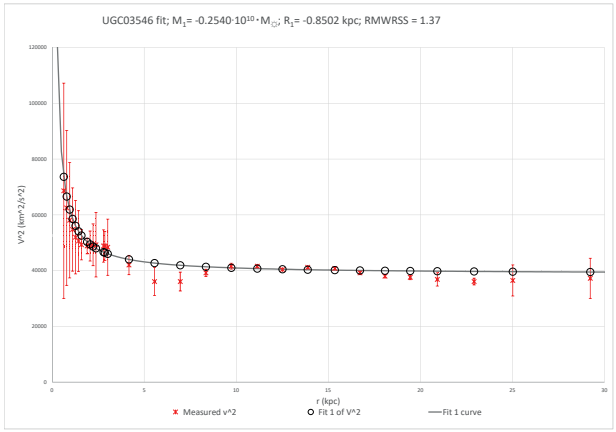

UGC03546

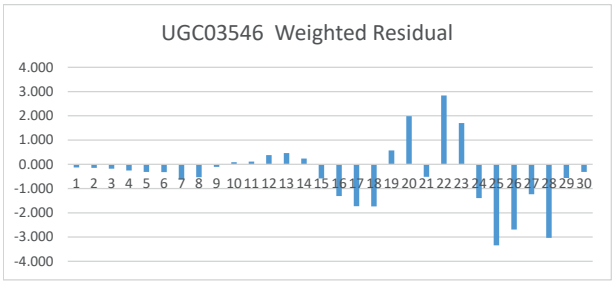

UGC03546 WR; RMWRSS = 1.37

E. LAGRANGIAN TO SEMI-NEWTONIAN TRANSITION

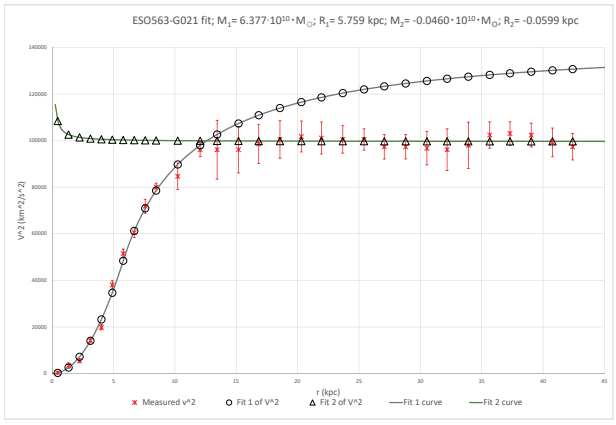

ESO563-G021

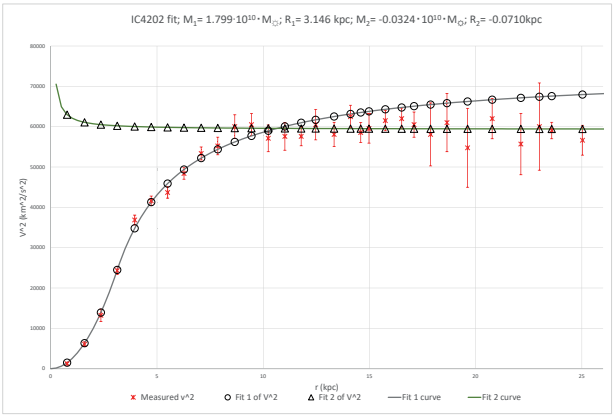

IC4202

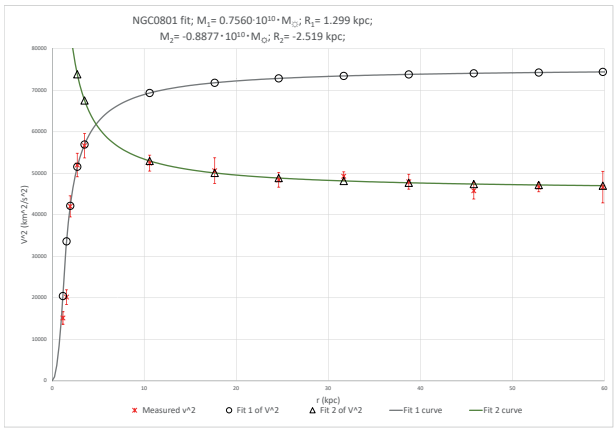

NGC0801

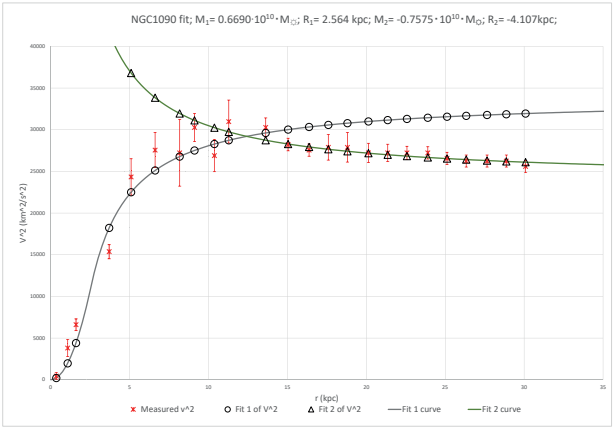

NGC1090

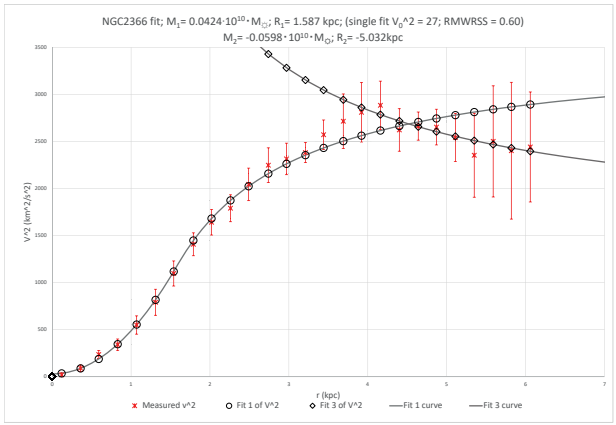

NGC2366

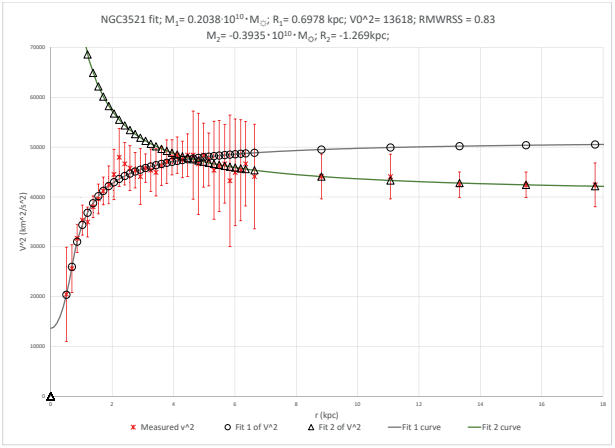

NGC3521

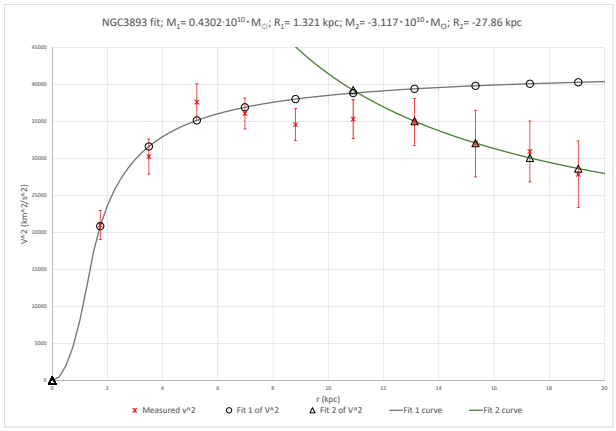

NGC3893

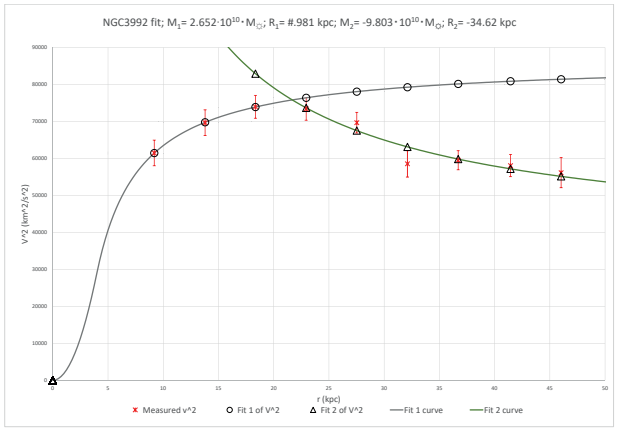

NGC3992

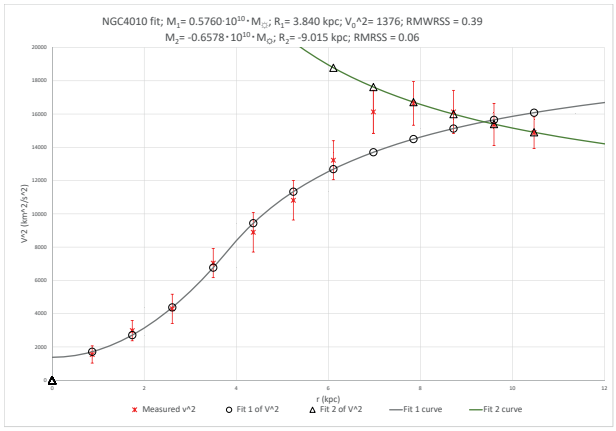

NGC4010

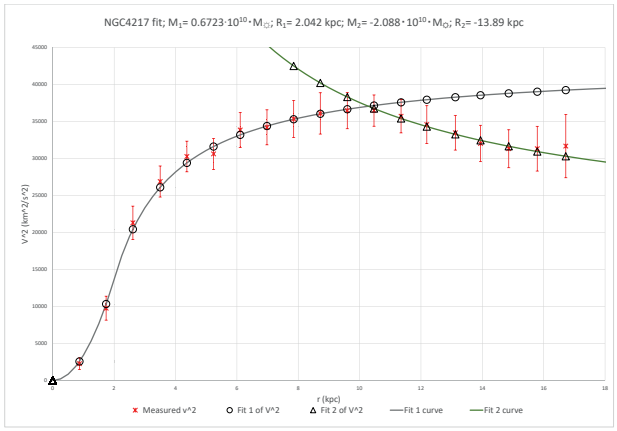

NGC4217

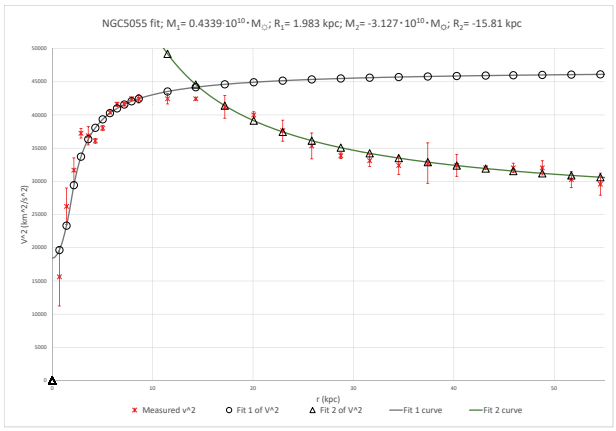

NGC5055

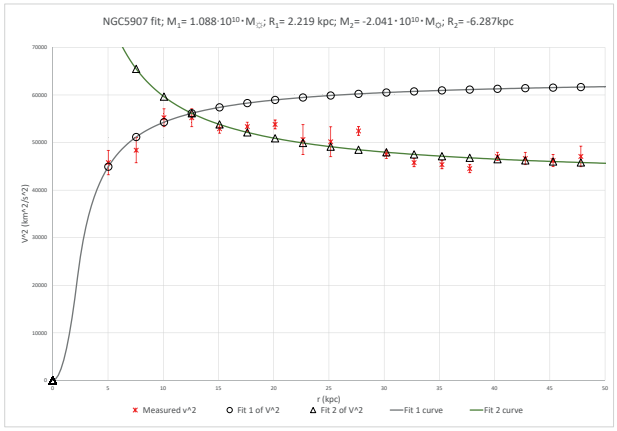

NGC5907

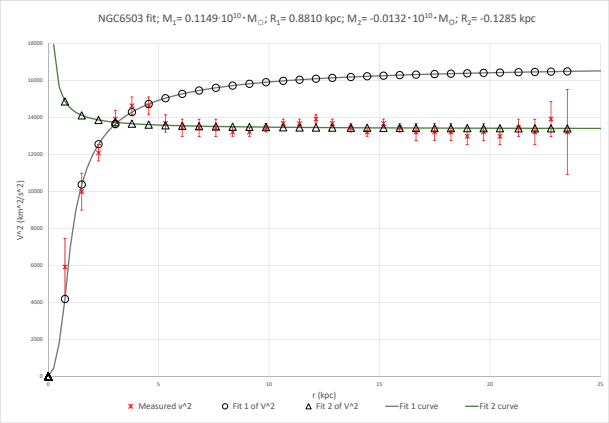

NGC6503

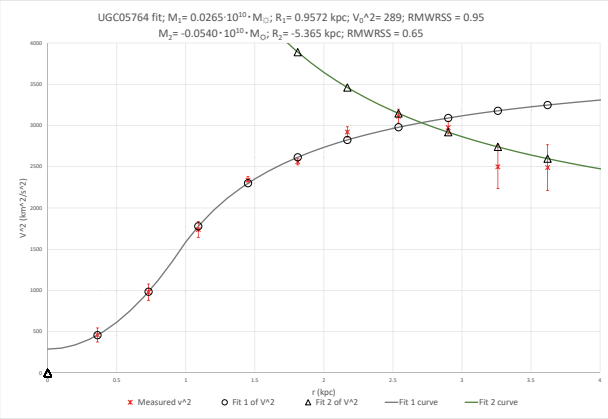

UGC05764

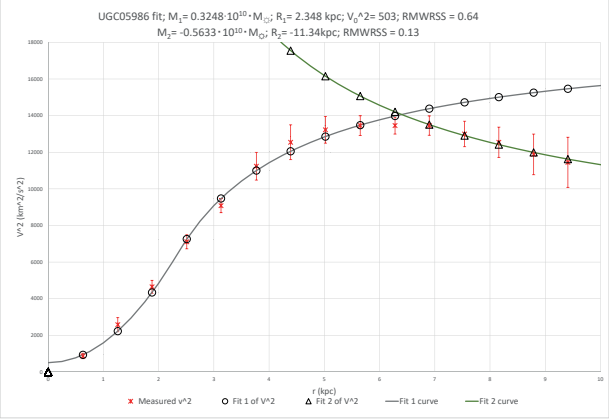

UGC05986

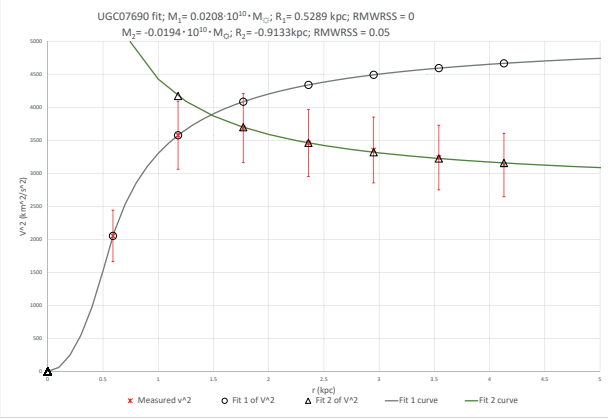

UGC07690

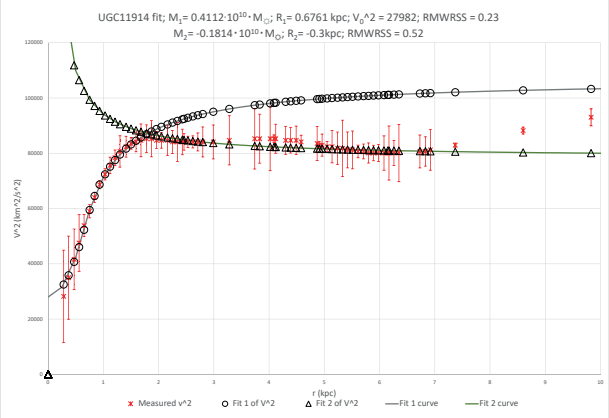

UGC11914

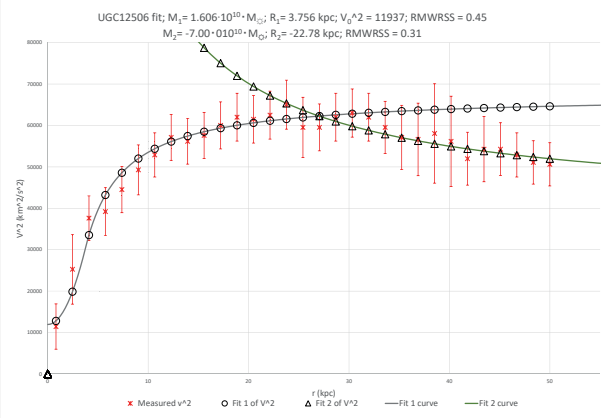

UGC12506

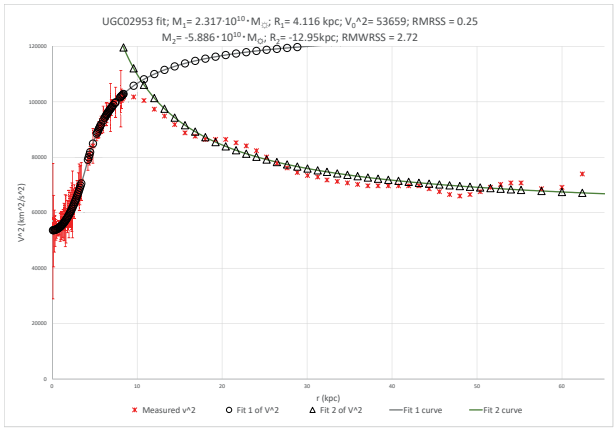

UGC02953

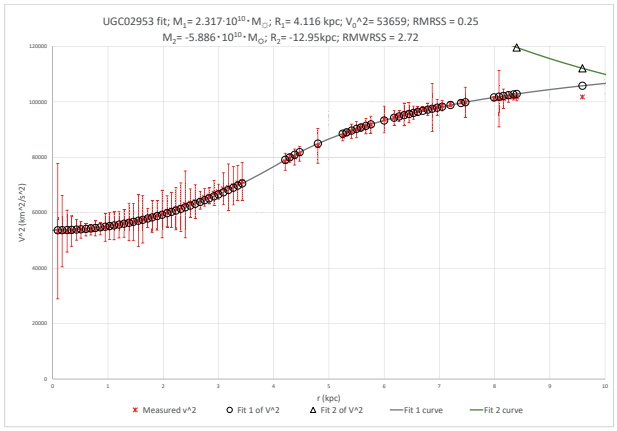

UGC02953 zoom

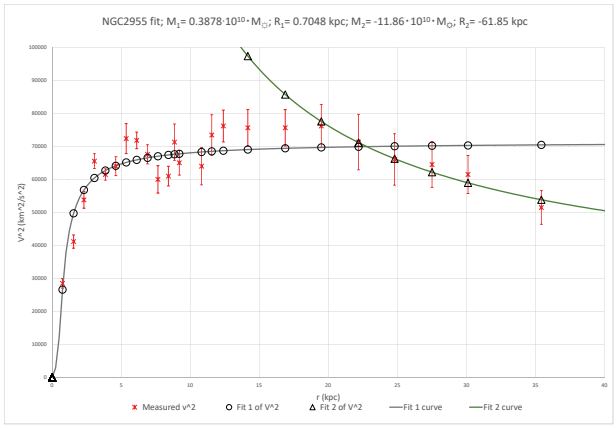

NGC2955

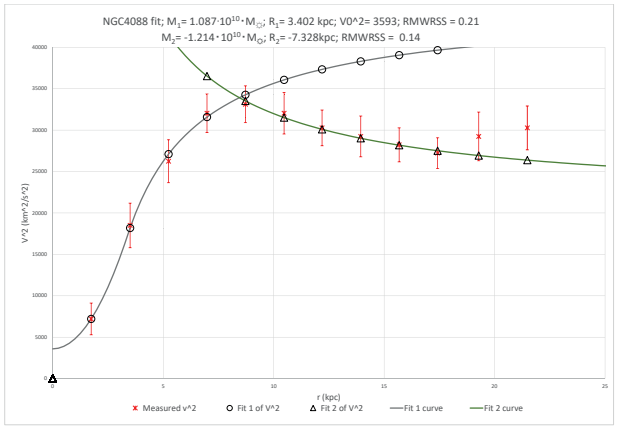

NGC4088

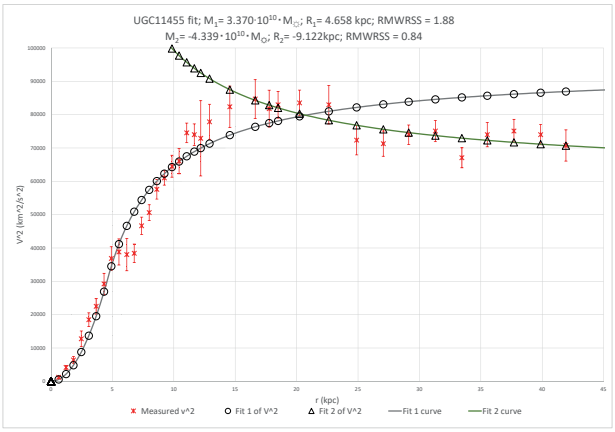

UGC11455

F. GALAXIES WITH THREE FITS

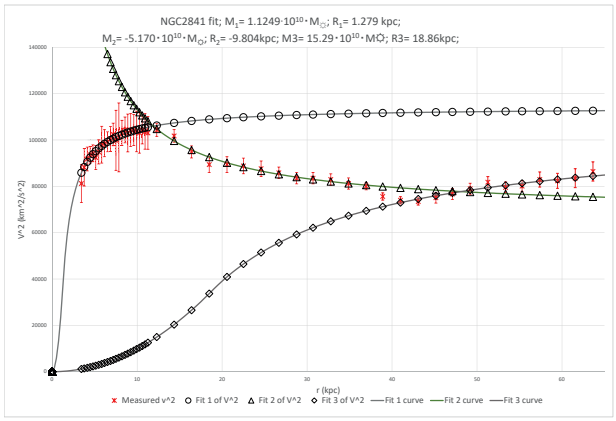

NGC2841

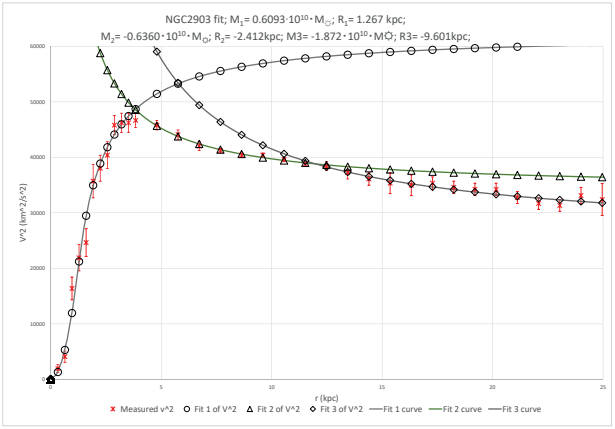

NGC2903

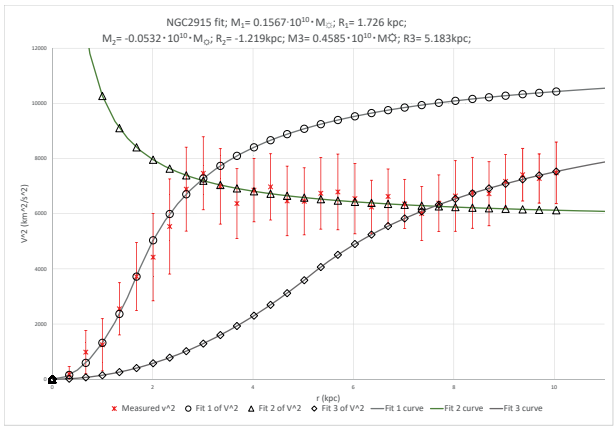

NGC2915

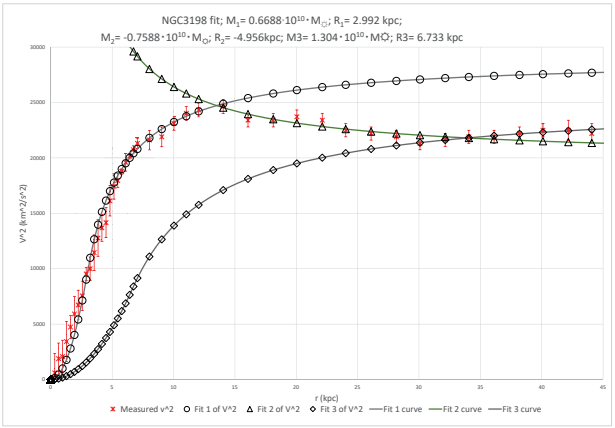

NGC3198

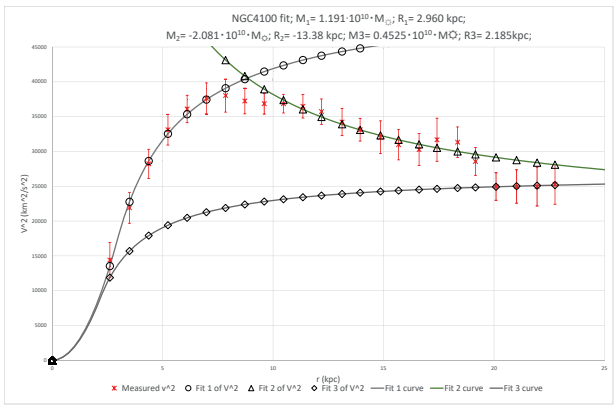

NGC4100

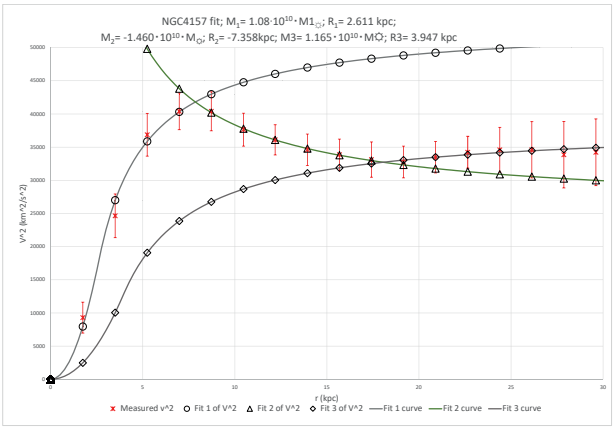

NGC4157

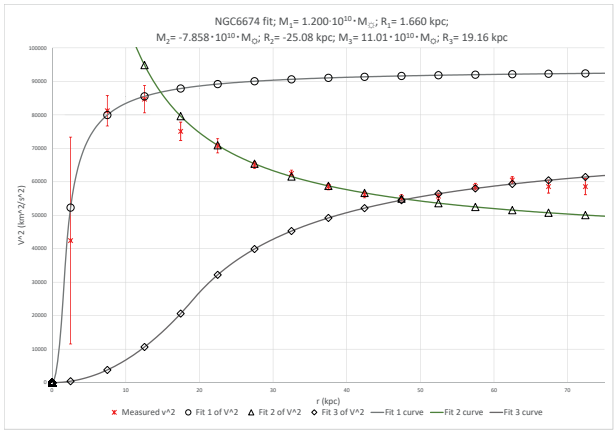

NGC6674

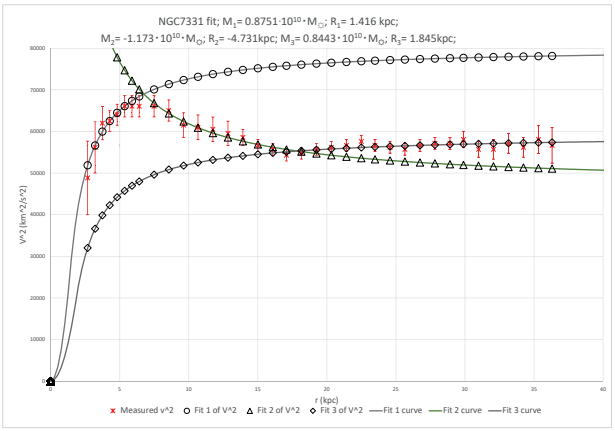

NGC7331

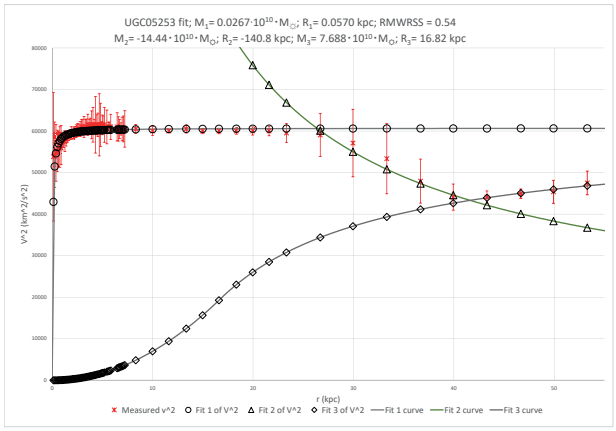

UGC05253

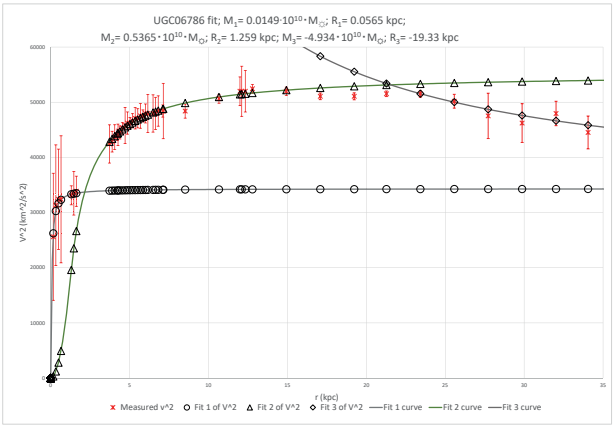

UGC06786

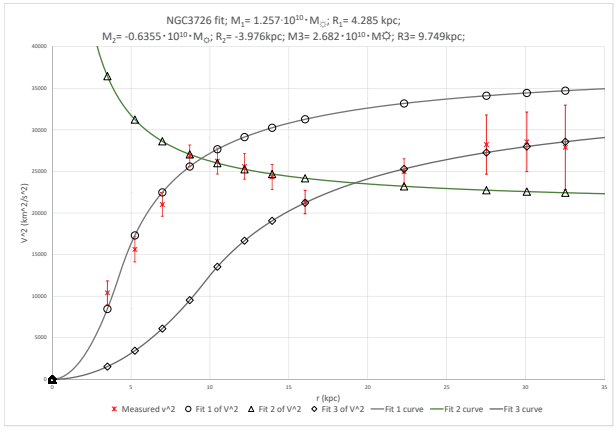

NGC3726

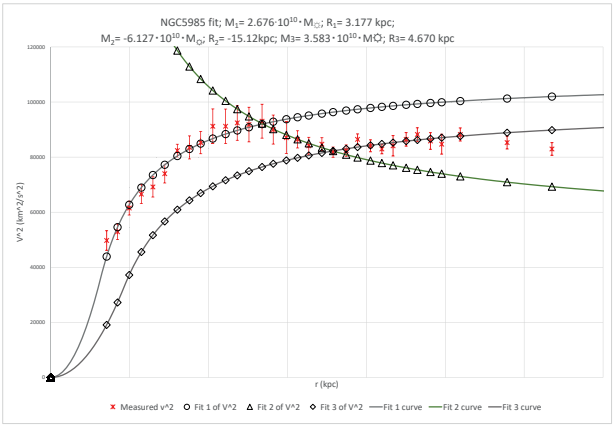

NGC5985

G. THE REST

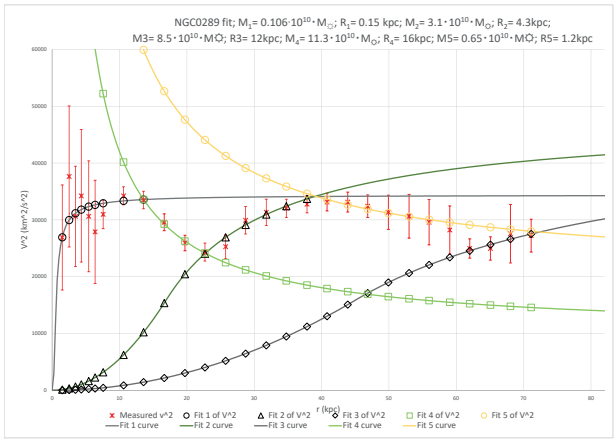

NGC0289

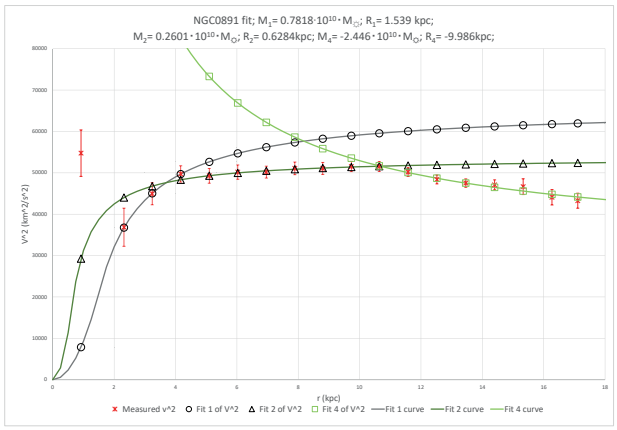

NGC0891

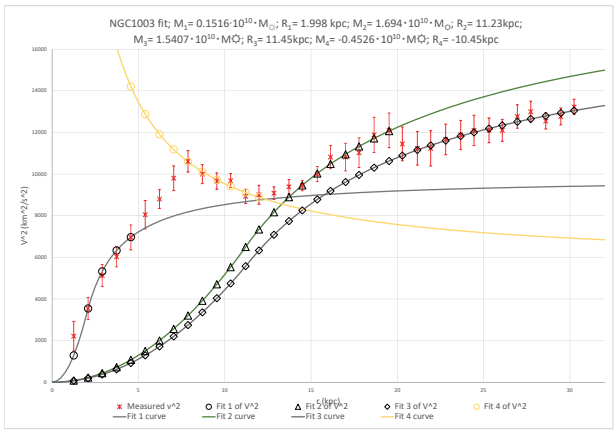

NGC1003

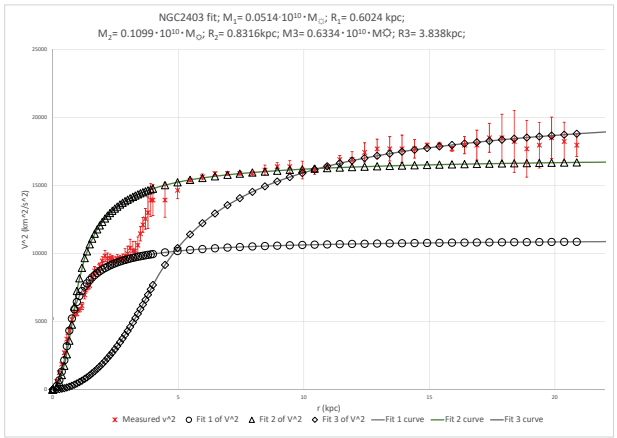

NGC2403

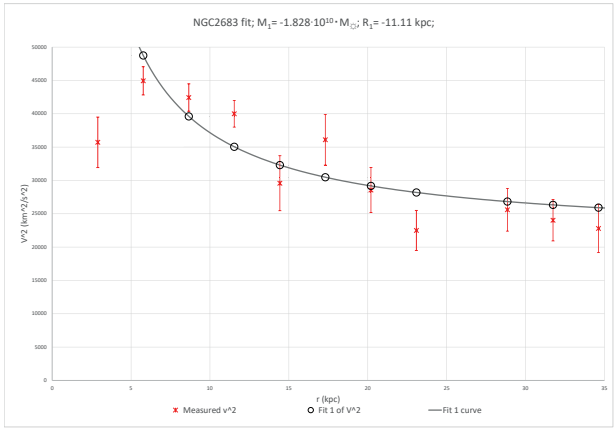

NGC2683

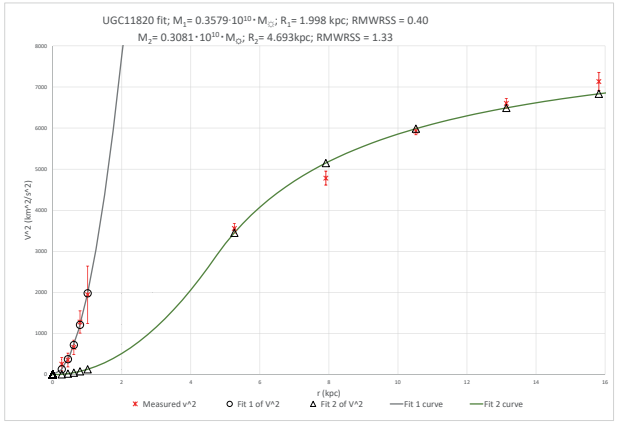

UGC11820

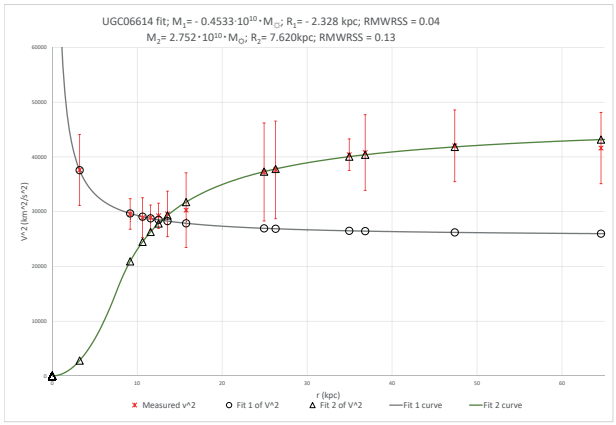

UGC06614

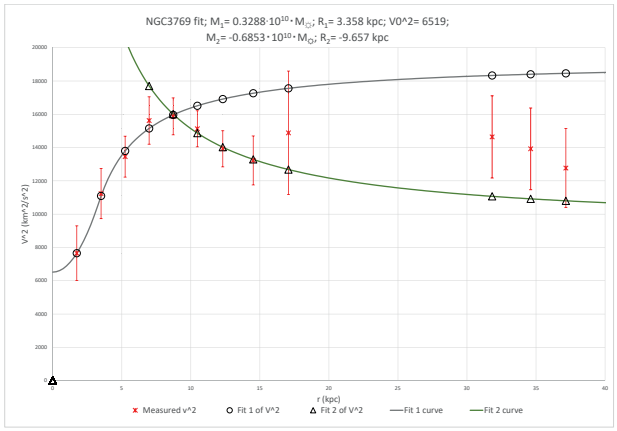

NGC3769

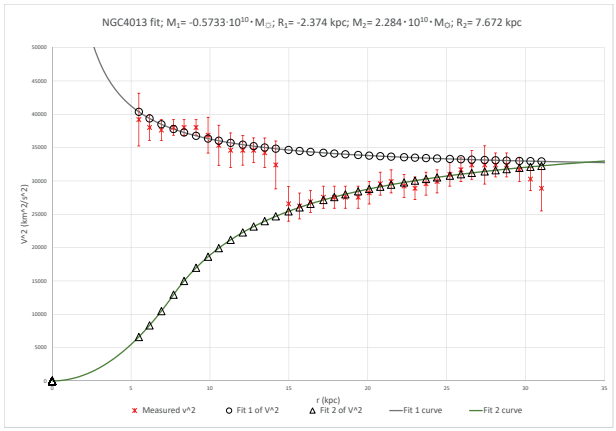

NGC4013

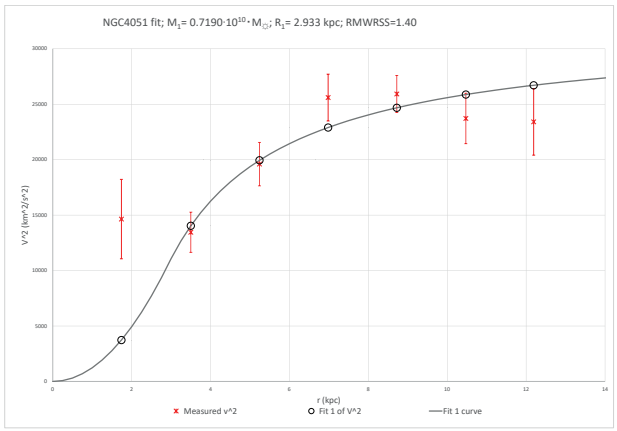

NGC4051

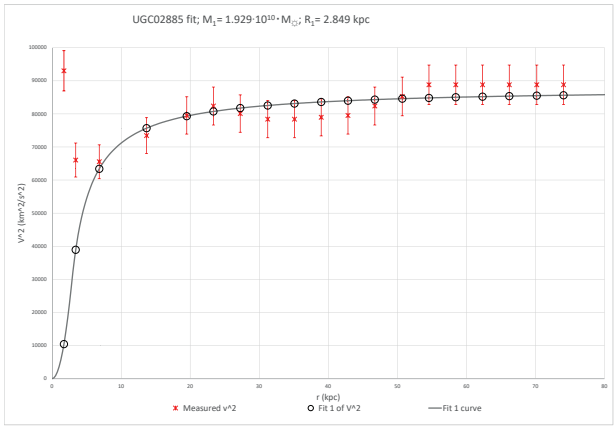

UGC02885

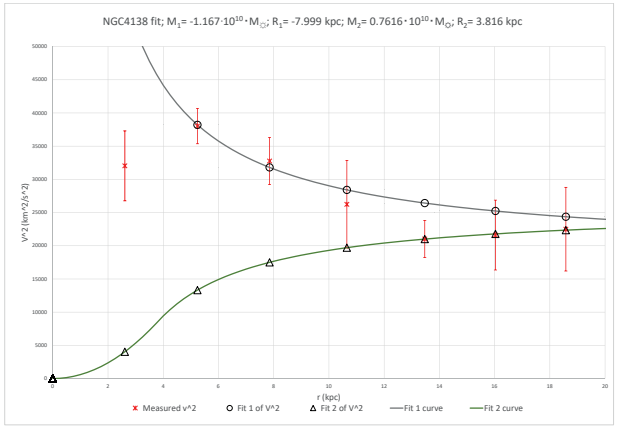

NGC4138

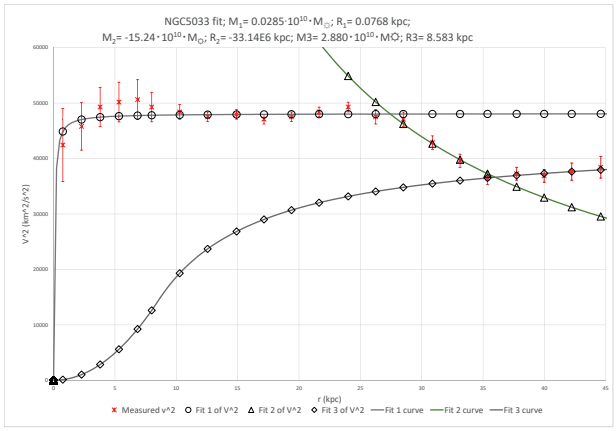

NGC5033

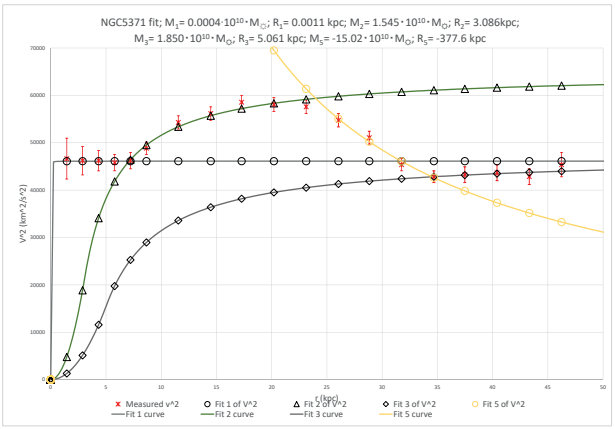

NGC5371

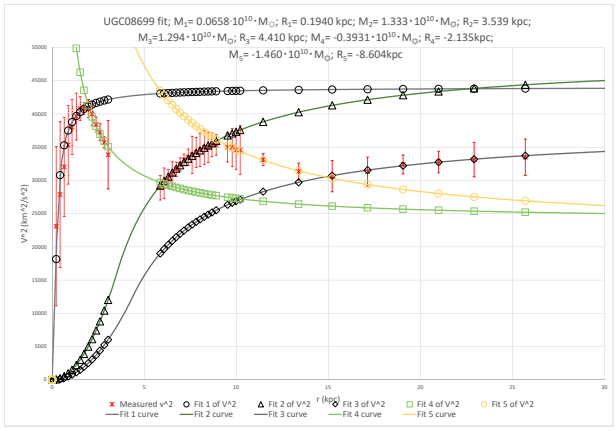

UGC08699

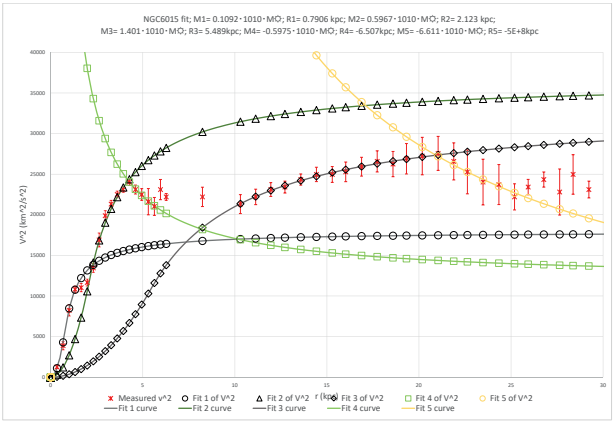

NGC6015

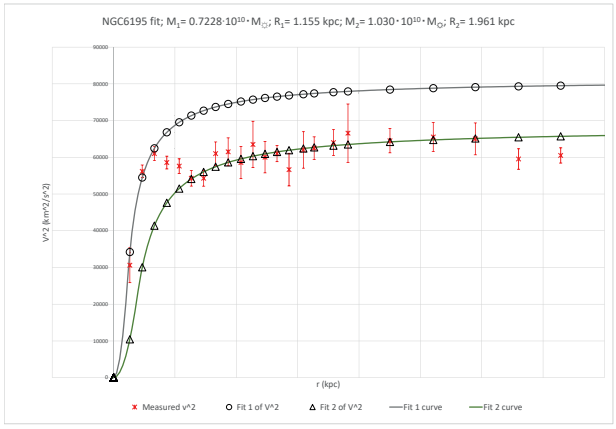

NGC6195

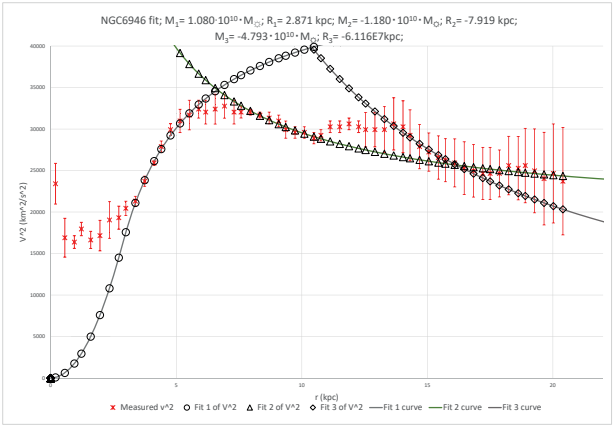

NGC6946

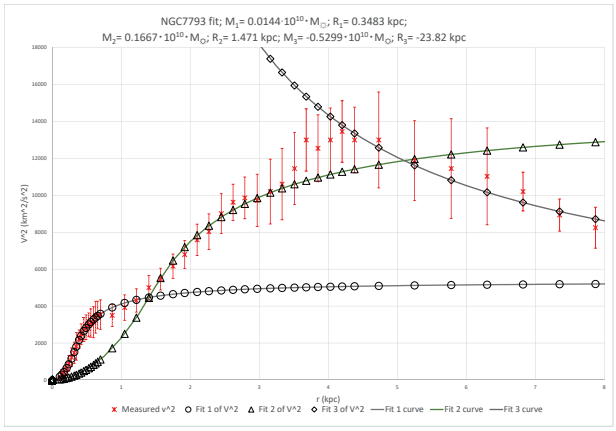

NGC7793

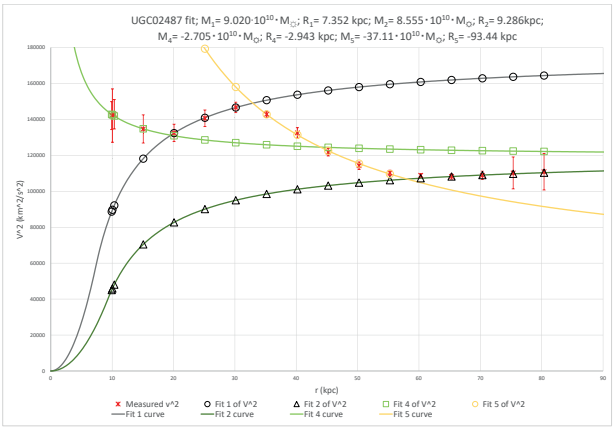

UGC02487

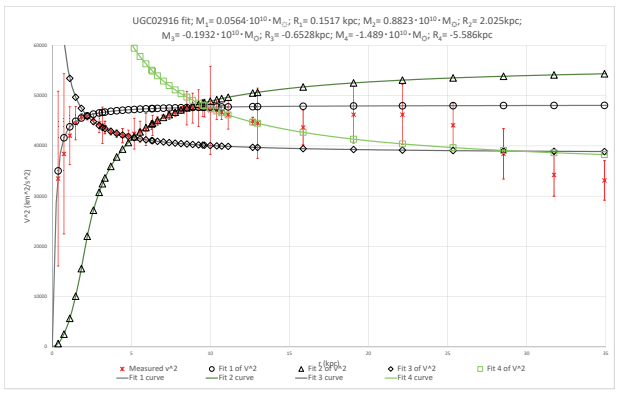

UGC02916

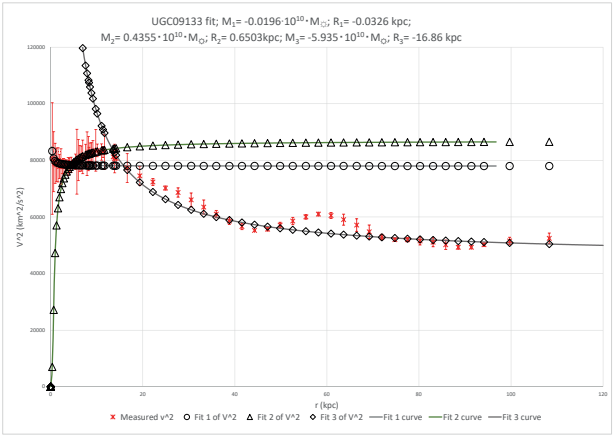

UGC09133

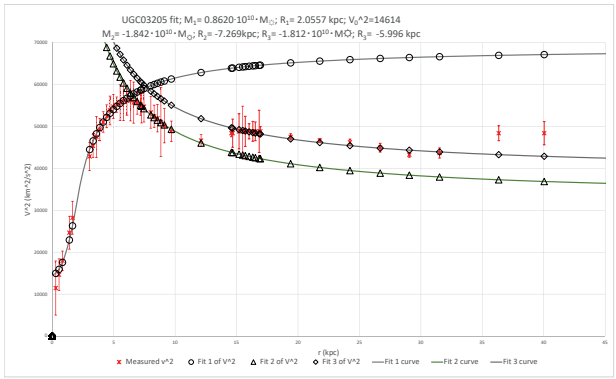

UGC03205

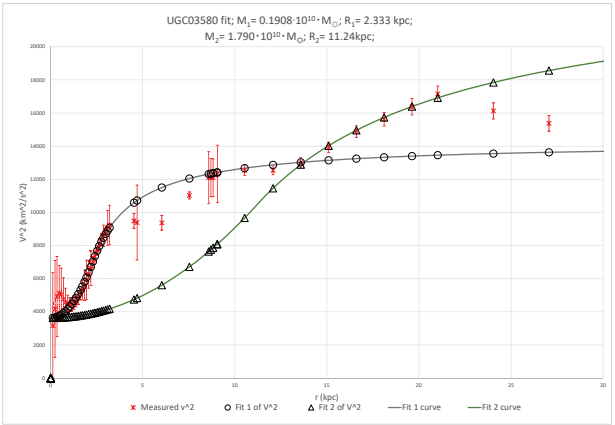

UGC03580

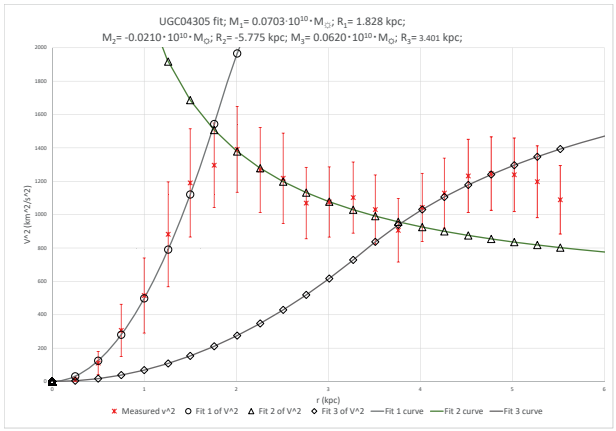

UGC04305

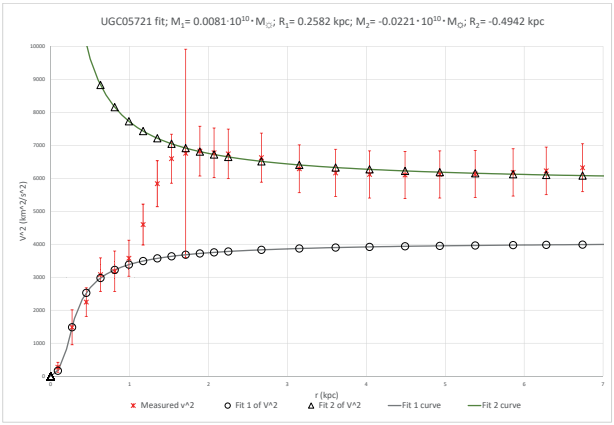

UGC05721

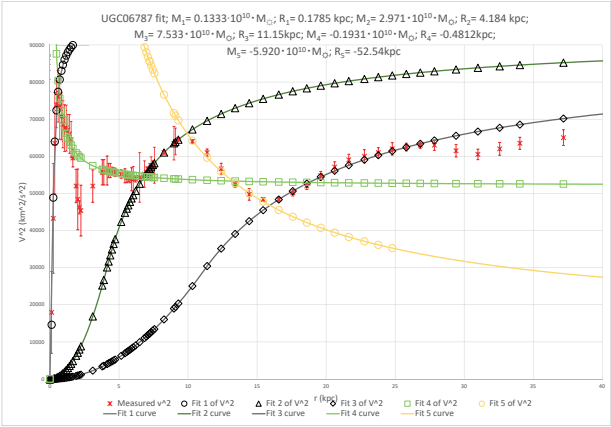

UGC06787